POLITECNICO DI TORINO

Department of Environment, Land and Infrastructure Engineering

Master of Science in Petroleum and Mining Engineering

Investigation of Solid Transport with Non-Newtonian Fluid Flow in an Inclined Annulus through Particle Image Velocimetry (PIV) Technique

Supervisor: Prof. Guido Sassi (Politecnico di Torino)

Co-Supervisor: Prof. Dr Azizur Rahman (Texas A&M University at Qatar)

Student: Muhammad Usman SIDDIQUI

March 2020

Thesis submitted in compliance with the requirements for the Master of Science degree

Abstract

In this thesis experimental and visual analysis are conducted to better understand the velocity behaviour by means of Particle Image Velocimetry (PIV) technique. The method was implied with multiphase flow system of 6.16 m long pipe having 2 ½ by 4 ½ inner pipe and outer pipe diameter respectively. The observation was carried out in an inclined annulus with the inclination degree of 2.5˚ and 5˚ in toe-up and 2.5˚ toe-down condition. The Newtonian fluids as a single-phase (liquid) flow and non-Newtonian fluid as a two-phase (liquid/solid) flow has been compared. The data for both single-phase (liquid), and dual-phase (liquid/solid) is analysed in inclined concentric and different eccentric conditions with respect to the horizontal annulus.

The past research keenly focused on the solid cuttings transport behaviour in vertical annulus while few in horizontal annulus. To my knowledge extent the solid cuttings behaviour in an inclined annulus has not been thoroughly studied. This thesis analysed both toe-up and toe-down conditions.

In the first part of this research thesis, turbulent behaviour of single-phase (liquid phase) water and non-Newtonian fluid (Flowzan) were observed and are reported on different parameters. In the second part of this research thesis, two-phase (liquid/solid) non-Newtonian fluid along with the addition of solids experiments flow were analysed. The solids (glass beads) were transported during the fluid flow and observations were studied using a turbulent flow of Water used as Newtonian fluid and Flowzan used as Non-Newtonian fluid. Different solid flow behaviour was observed and visualised, and the critical velocity and pressure losses required to form such a solid pattern were observed.

The combined effect of different values of flow rate at 500, 600 and 700 RPM, concentric and eccentric values of 0, 0.3 and 0.6 values are observed. The presence of solid glass beads reported the conclusive results. The data analysis for the Newtonian Fluid (Liquid phase) and the data generated for the Non-Newtonian Fluid (Solid/Liquid phase) reported that comparison on 2.5˚ and 5˚ in toe-up and 2.5˚ toe-down inclinations concerning horizontal affected the solid flow behaviour. The change in flow behaviour was also

reflected upon changing the eccentricity. Acquired velocity profile follows and depends on the universal law of the wall.

The achieved results comprehensively concluded the cutting transport behaviour and provided the result will help in making of appropriate drilling fluid. This can also be helpful for the industry using two-phase flows.

Keywords: Particle Image Velocimetry, PIV, multiphase, single-phase, dual-phase, cutting transport, Newtonian fluid, non-Newtonian fluid.

Acknowledgemet

In the beginning, I want to like to express my sincere gratefulness to God Almighty, without whom everything was impozxssible.

Special thanks to my family, mainly my parents for their affection, continuous provision, and firm faith in me. Without them, I would not be at the position today I am.

I want to express my truthful acknowledgements to my internal supervisor, Prof. Dr. Guido Sassi and external supervisor, Dr Mohammad Azizur Rahman, for his support, encouragement, commitment and supervision through this study. Their supervision assisted during my experimental research and compiling the thesis writeup.

I want to show gratitude to my lab colleagues Dr Muhammad Saad Khan, Abinash Barooah, Muhammad Yousuf Khan and Burak Celal, for the massive assistance and suggestions they provided me during the experiments. Without their enormous motivation and sharing of knowledge, this journey would have been much more challenging to accomplish. I appreciate their guidance and patience to answer my questions during my stay in Qatar.

Finally, I would like to thank Qatar Foundation and Texas A&M University at Qatar for supporting me to carry out the experiments during this research.

Table of Content

List of Figures

List of Tables

Chapter 1 Introduction

1.1 Overview

The fluid flow in an oil and gas exploration and production is a common mechanism. The first encounter of such fluid flow occurs during drilling operation when drilling mud is passed through the drill pipe to remove the cuttings and transport them to the surface. Typically, drilling fluid has a non-Newtonian nature, and a major share of the drilling expense is related to drilling muds and the additives. The core interest of this thesis is the examining of fluid flow performance with the cutting beds in the annulus exhibiting different velocities. The observation of critical velocity profiles, the distribution of shear stress around the boundaries of the annulus and turbulent intensities were carried out.

Horizontal and extended reach wells either toe-up or two-down have intensely increased over the past decades and are now the primary interest of exploration and production companies for the exploitation of unconventional hydrocarbon reserves. Drilling unconventional off-shore and onshore wells form stationery cutting beds. The formation of stationary cuttings beds is unavoidable when drilling such horizontal and extended reach wells. The solid cuttings produced during the drilling are not removed from the annulus in a timely manner and taken out efficiently by the drilling mud, a thick bed of solid cutting particles might accumulate on the bottom of the annulus [1]. This accumulation may anticipate different well drilling and well completion operational problems (i.e. pipe stuck, hole fill, excessive torque and drag, loss circulation, wellbore cleaning, additional drilling cost, etc.) [2-4]. Therefore, efforts are applied to mitigate near-wall turbulence which requires a comprehensive investigation of different near-wall turbulent factors.

To remove the cuttings efficiently in extended reach wells, fluid is pumped on a high flow rate [5]. This methodology is evident in short reach wells; however, in extended reach wells, due to certain limitations like dynamic pressure losses, slow drilling rates, high drag and force is not feasible.

.

Several experimental facilities have carried out investigations to improve the cutting bed problem associated with horizontal and extended reach wells. Many drilling parameters during drilling operations have been the interest of study including angle of inclination angle [6], rheology of fluids [7], drill pipe eccentricity [8], cutting size [1, 9, 10], flow rates [1], etc.

1.2 Problem Statement

The behaviour of the fluid flow within the round pipes is symmetric [11, 12] whereas the fluid flow in an annular area is non-symmetric. The presence of turbulent flow areas intensifies the problems as there no theoretical explanations exist. The near-wall turbulent behaviour can either be studied experimentally or through numerical simulation but the simulation bounds to the low value of Reynolds number. Therefore, investigation of near-wall turbulent behaviour with excellent facilities and accurate tools can be a great addition to the solution of the problem. The examining of a non-Newtonian fluid is very complex due to the rheological properties and not reported well in the past. However, the study of such behaviour through evolving Particle Image Velocimetry (PIV) technique has made a lot easier and accurate.

Severe problems, findings and limitations related to non-Newtonian flow in an inclined annulus reported in the past studies are mentioned briefly to make these uncertainties more clear.

1.3 Goals and Objectives of the Thesis

The vital objective of this research thesis title implies is to investigate near-wall turbulence of Solid Transport with non-Newtonian fluid flow in an inclined annulus through PIV technique. A medium-sized flow loop system from Texas A&M University at Qatar has been used. Overall, this research thesis depend upon the experimental study of solid cuttings transport in an inclined annulus considering real drilling case scenario. The non-Newtonian flow in the concentric condition when flowing in an annulus exhibits turbulent behaviour.

The aim is to carry out the study and find out at what conditions are responsible for initiating the movement of solid cuttings. The effect of flow rate, eccentric condition and the inclination angle is to be studied with turbulent flow.

The study follows the systematic path and divides the investigation into two main components. First, analysing the behaviour of turbulent behaviour of single-phase (liquid phase) water and non-Newtonian fluid (Flowzan) at a different flow rate and inner pipe RPM in the concentric and eccentric positions and during an inclined condition. Secondly, correlating the result obtained in the single-phase with two-phase (liquid/solid) non-Newtonian fluid flow with solid cutting transport. The solids (glass beads) were transported during the fluid flow and observations were studied using a turbulent flow of Newtonian fluid (Water) and non-Newtonian fluid (Flowzan).

All the behaviour will be analysed with the help of Particle Image Velocimetry technique. The difficulties mentioned in the statement of the problem related to the turbulent flow will be investigated.

The analysis of the two components is associated with the implementation of Particle Image Velocimetry on the flow loop system. The most challenging task for its setup is the calibration of the camera since it will visualise the behaviour.

Additionally, the most important step is to use the non-Newtonian fluid with certain properties that can exhibit as a real drilling fluid and it is transparent enough to visualise the solid cutting transport behaviour.

Moreover, the next step is to explain the limits of the experimental setup in terms of annulus diameter, pump power and eccentricity. Once after defining the limit, the next task is to select the appropriate polymer which fulfils the requirement of achieving turbulence and must exhibit non-Newtonian behaviour.

With the facts acquired from past research regarding the turbulent fluid flow in an annulus, the subsequent are the major objectives of the first stage of the experiments.

- To measure the velocity profile intended for Newtonian fluids for horizontal, toe-down and toe-up conditions with different drilling parameters.

- To measure the velocity profile intended for Non-Newtonian fluids for horizontal, toe-down and toe-up conditions with different drilling parameters..
- To compare the turbulent flow of Newtonian and non-Newtonian fluids.
- To compare the behaviour in toe-up and toe-down well with reference to horizontal.

To be precise, the ultimate aim of this thesis research was the comparative study of non-Newtonian fluids flow with Newtonian fluid flow in an inclined annulus in different degrees and their effect on solids cutting transport in inclined concentric and eccentric inner pipe.

1.4 Method and Approach

An experimental and visualisation method was the prime technique to accomplish the thesis research goal. The analysis of turbulent was vital for achieving velocity profiles and other near-wall turbulent behaviours. The visualisation was conducted with the help of Particle Image Velocimetry technique. The main tools used for such purpose were High Power Diode Laser and High-Resolution camera. The investigation, processing and generation of the image profiles were carried out and obtained through Davis software.

PIV technique requires the implementation of some factors such as the window of observation and the fluid used should be transparent. In our case, the Flowzan Non-Newtonian fluid was not 100% transparent. In order to coup with this problem, fluorescent particles were mixed with the fluid. Fluorescent particles, along with High Power Class IV laser illuminated the particles in the fluid, and the comprehensive visualization images were captured for the research.

Another important factor considered was the refractive index similarity. The matching of the refractive index was attained by using the RIM box and filling it with the fluid used in the annulus.

Moreover, the calculation of the percentage used for the solid cutting transport during annular flow was important. This was vital because more than 5% of cuttings are not desired during drilling as it causes pipe sticking problem.

The most considering factor was the rotation of agitator for 20 seconds every second, to make sure an equal amount of solid cuttings are transported into the annulus.

Furthermore, to make sure 200 images are processed in Davis software after every experiment.

1.5 Thesis Research Contribution

The current investigation targets the study of solid cutting transport behaviour through the concentric and eccentric annulus, considering the flow.

It also aims to predict the effect of turbulent fluid flow behaviour on different aspects such as velocity profiles and shear stress of Newtonian and non-Newtonian fluids in concentric, eccentric and different inclined annulus toe-up and toe-down condition with the application of PIV technique.

The outcomes from this study research thesis are beneficial for the interpretation and getting aware of the behaviour that happens during solid cutting transport experimentations. Moreover, these experiments are helpful in filling the research gap of solid cutting transport in concentric, eccentric and different inclination angles.

1.6 Structure of the Thesis

The thesis draft is the results of velocity profile investigation of solid cutting transport with Non-Newtonian Fluid Flow in an Inclined Annulus through Particle Image Velocimetry (PIV) Technique. In the section, a brief overview of the thesis is enlisted.

Chapter 2: This chapter discusses the background literature review. Also, mentioning the past research carried out. Overview of Newtonian, non-Newtonian fluids is also described in the chapter. This study of the behaviour of non-Newtonian fluids have been discussed in this chapter. An additive used with water and its preparation are reported in this chapter

Chapter 3: This chapter refers to the experimental facility and the working principle of the flow loop system. The system used to obtain anticipated results for the thesis. The comprehensive information about the PIV measurements, types of equipment and techniques are enlisted. Also, the detailed discussion of PIV (Particle Image Velocimetry) setup has been explained, including processing steps.

Chapter 4: Results, the most important aspect of the thesis has been discussed and reported. A thorough explanation of both Newtonian and Non-Newtonian fluids finding are discussed in the chapter.

Chapter 5: The last chapter of the thesis contains the significant conclusions of the experiments, as stated in the previous chapter. The recommendations for future aspects are also mentioned.

Chapter 2 Literature Background

This chapter explains the theory behind our area of research thesis interest. An outline explained related to the previous research carried out in our related field. A brief review of the fundamentals of the concept is defined. The study of fundamental is always helpful since the understanding part relies on it.

2.1 Extended Reach Wells

The drilling and development of extended reach wells or also known as multilateral wells has been the interest of oil and gas companies for maximizing the oil recovery. The long-reach wells are often adapted in offshore wells [13]. The Extended Reach Wells is commonly defined as that the ratio of measured depth (MD) and True Vertical Depth (TVD) is at least 2:1 [14].

Extended reach wells can be extremely long. The extremely long reach wells are typically drilled closed to the reservoirs to decrease the operational cost.be required to access the resource [14]. The operational cost of extended reach wells is expensive and also technically challenging. The challenges like pipe stucking, hole cleaning [15, 16], well-bore instability [17] and drill string vibrations [18] are occurred in such kind of wells.

2.1.1 Types of Extended Reach Wells

Extended Reach Wells can either be horizontal or inclined. When a drilling fluid flows through an inclined annulus, the fluid flow rate is influenced by fluid density, gravity and the inclination. The inclined extended reach wells further classify into toe-up and toe-down wells.

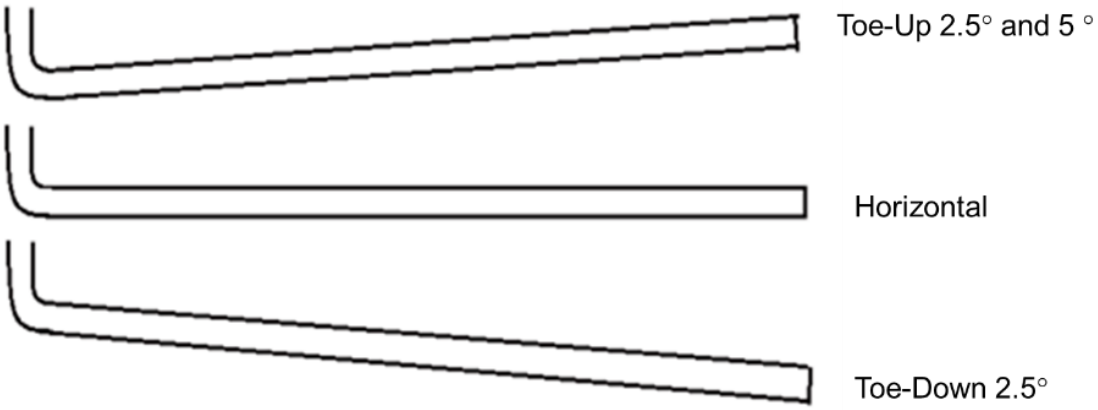

Figure 2.1: Graphical Representation of Horizontal & Inclined Trajectories

2.1.1.1 Toe-Up & Toe-Down Wells

Toe-up wells are defined as the horizontal well where the inclination angle is higher than a 0˚ degree concerning the horizontal wells [19, 20]. The shift towards the top is represented as negative. Whereas, toe-down wells are defined as the horizontal well where the inclination angle is less than the 0˚ degree concerning the horizontal wells. The shift towards the bottom is represented as positive.

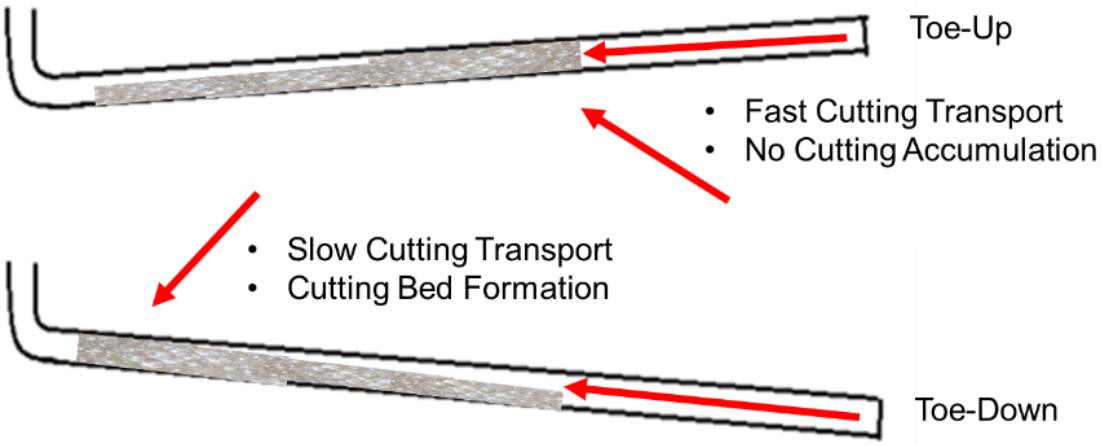

Figure 2-1: Cutting Transport Behaviour

Figure 2-1: Cutting Transport Behaviour represents when the inclination angle of the well changes from horizontal to toe-up or toe-down, the flow of the fluid, its holdup and flow behaviour changes [19]. Toe-up provides better cutting transport because of gravity and fluid flows fast. This gravity driving force the fluid and cuttings to towards the bend from the vertical and as a result, less reservoir pressure is expected [21]. Whereas, toe-down wells condition leads to liquid holding problems and cannot reach to critical velocity [21]. As a result, the toe-down state leads to more cutting bed formation.

2.1.1.2 Horizontal Wells

The wells which are drilled at a high angle approximately or nearly 90˚ demonstrate as a horizontal well. The drilling of horizontal wells takes place in specific conditions. It is drilled along a deviated well path just above the reservoir. Horizontal wells help to target narrow channels [22]. Similar to vertical wells, horizontal wells are more complex. The initial challenge is faced during the solid cutting transport, which leads to several other problems, mainly pipe sticking. Figure 2-2 is a generalized illustration of a horizontal well.

Figure 2-2: Horizontal Well

2.2 Concentric & Eccentric Annuli

The position of the inner pipe concerning the outer pipe has a significant impact on the solid cuttings transport and fluid flow. Analysis and studies have revealed that a long solid cutting bed starts to form with the increase in eccentricity [23].

The equivalent difference between inner and outer pipe diameter refers to the concentric annulus [24]. However, by another definition, the concentric annulus refers to the similarity in the fluid flow in concentric pipes. The flow can either be laminar or turbulent,

but similarity exists in the fluid flow [25]. Figure 2-3: Concentric Annulus shows a basic demonstration of concentric annuli.

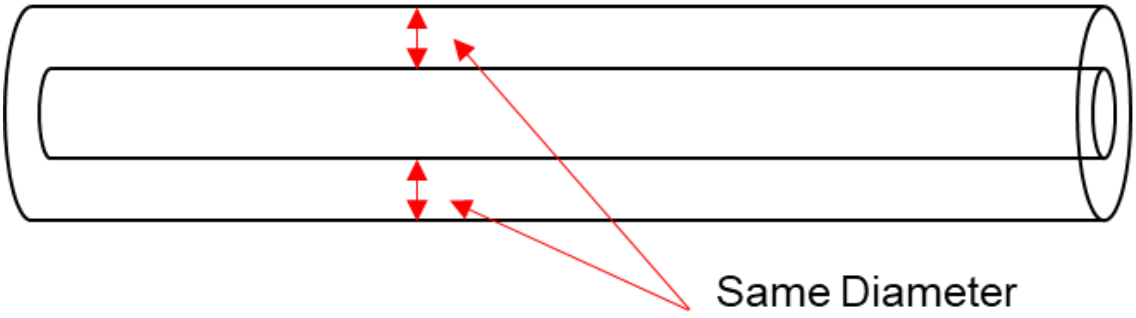

Figure 2-3: Concentric Annulus

Generally, the non-equivalent difference between inner and outer pipe diameter refers to the eccentric annulus. Eccentric value varies from 0-0.95 [24]. Figure 2-4: Eccentric Annuli is an illustration of eccentric annuli.

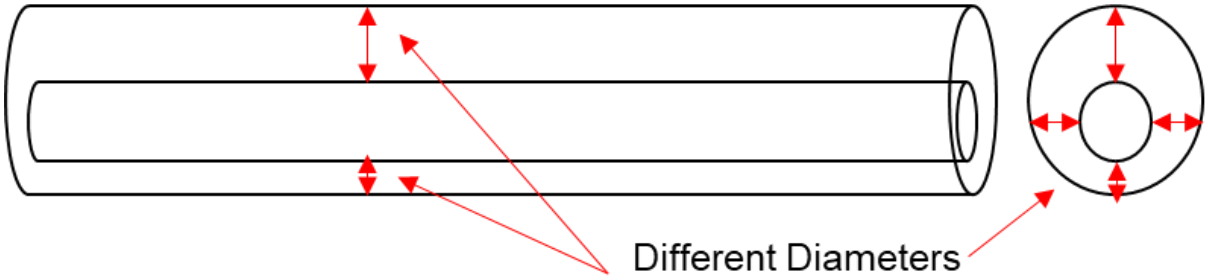

Figure 2-4: Eccentric Annuli

2.3 Laminar and Turbulent Flow

Laminar flow is defined as the flow where the fluid is smoothly flowing, and the shear layers are also parallel to each other. In a laminar flow, the fluid momentum starts due to molecular diffusion; also, no mass is transported among the shear layers [26]. Fluid flow having Reynold's number less than 2300 is considered as the Laminar.

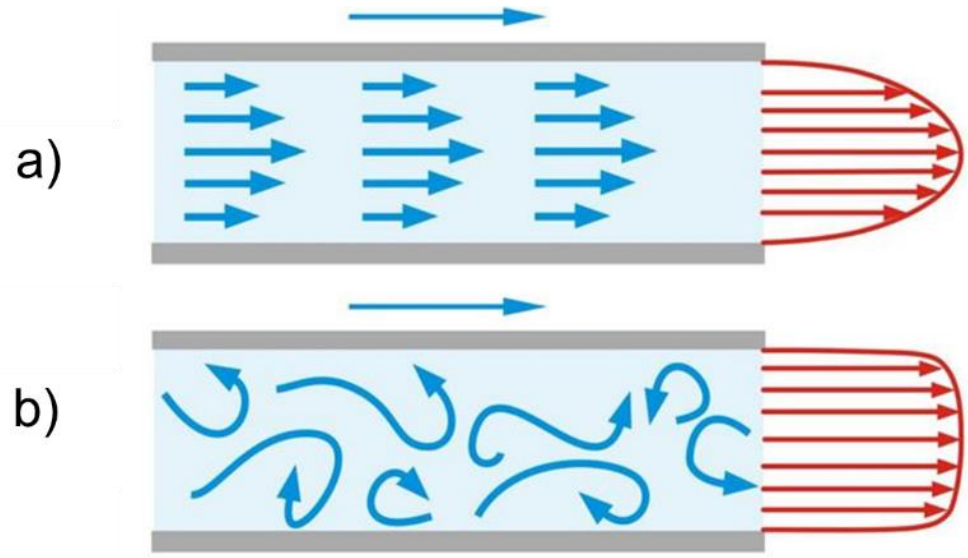

Figure 2-5: a) Laminar Flow b) Turbulent Flow

Alternatively, turbulence flow refers to the flow of the fluid where viscous forces are dominated by momentum effect. This domination occurs due to random unstable motions of the fluid. Fluid flow having Reynold's number greater than 4000 is considered as the Turbulent.

2.4 Reynolds number (Re)

Reynolds Number (Re) is stated as the relation of the inertial and viscous forces. If the Reynolds number increases then the flow is considered by areas having the fast velocity differences [27]. For a normal flow in a circular tube, the 'Re' is denoted by:

$$Re = \frac{\rho \mathrm{u} \mathrm{D}}{\mu} \qquad \text{Eq 1}$$

Where 'ρ' represent the density of the fluid, 'u' is velocity in the inlet flow, 'D' represents the diameter of the pipe and 'μ' is the fluid viscosity [28].

For the identification of Reynold's number in an annulus hydraulic diameter, D_H will be used.

$$Re = \frac{\rho \mathrm{u} D_H}{\mu} \qquad \text{Eq 2}$$

Where, D_H is the difference between the inner diameter of the outer pipe and outer diameter of the inner pipe.

2.5 Newtonian Fluids

The fluids having a linear relationship concerning the applied shear stress, τ and the shear rate, dv/dy termed as Newtonian fluids. In Newtonian fluids, the viscosity simply depends on temperature and pressure. Basic terminology for Newtonian fluids is the fluid with simple molecular formula and small molecular weight. The particular example of Newtonian fluid is water and is analysed in this research thesis.

Rothfus et al. 1966 proposed an eddy viscosity model. This model analysed the turbulent flow and proposed the calculation of velocity profiles in the concentric annulus. At high Reynolds numbers in turbulent fluid flows, the region where velocity is maximum is supposed to be nearer to the inner wall. Therefore, relating the flow in annuls with the flow in pipe would need a far more complex method [29].

Brighton et al. 1964 stated an asymmetry in the velocity profile. He published the results by explaining that area, where velocity is maximum, entirely turbulent flow, occurs close to the boundary of the annulus. Regardless of the statement on their observation and statement related to stress distribution, they did not mention the radius of zero shear stress. Therefore, to calculate wall shear stress, they took the radius of maximum velocity. Obtained velocity results for the outer wall displays decent relation with the law. [30].

2.6 Non-Newtonian Fluids

The fluids having with a non-linear relationship concerning the applied shear stress, τ and the shear rate, dv/dy termed as non-Newtonian fluids. In non-Newtonian fluids, the viscosity depends on temperature, pressure, shear stress and shear rate. The particular example of non-Newtonian fluid is Flowzan and is analysed in this research thesis.

The three kinds of non-Newtonian fluids exist; shear thickening, sear thinning and Bingham plastic fluids. Figure 2-6 displays the relation of a Newtonian fluid with the sorts of non-Newtonian fluids, wherein the graph the x-axis and y-axis represent the shear stress and shear rate, respectively. Likewise, for the research, Flowzan has been used,

which is the Shear Thinning Fluid. Since shear-thinning fluid helps in reducing both film thickness and friction.

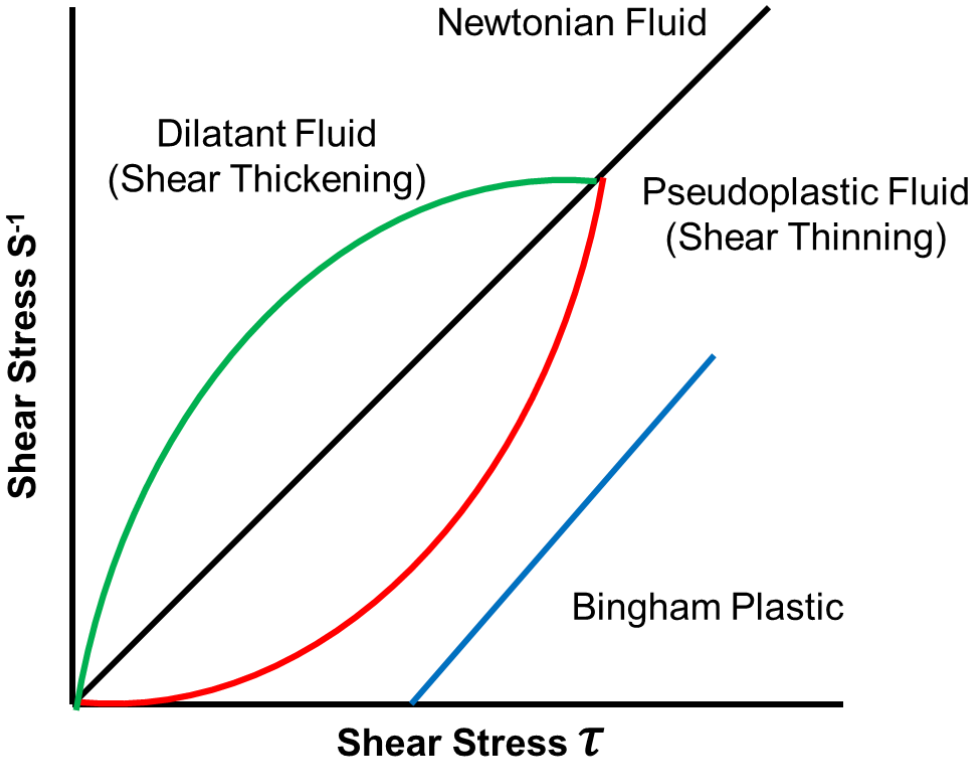

Figure 2-6: Comparison of Newtonian and non-Newtonian fluid

Dodge et al. 1959 reported analytical study on non–Newtonian fluids. The concluded analysis also helped to calculate the turbulent velocity profile. The eventually anticipated relationships are an improved sort of Reynolds number that combined both the behaviour index of the flow and velocity profile equation. The suggested model was then matched with experimental data. The model obtained satisfactory results [31].

2.7 Annular Velocity

Annular velocity is the velocity of the fluid with which it moves in inside the annular area. The unit of annular velocity is feet per minute (ft/min) or meters per minute (m/min) or

meters per second (m/sec). AV denotes annular velocity. Mathematically, it is expressed as;

$$\mathrm{AV} = \frac{24.5(\mathrm{Pump\ RPM_{gpm}})}{\mathrm{ID}^2 - \mathrm{OD}^2} \quad \text{Eq 3}$$

Where 'ID' is the inner diameter of the outside pipe whereas 'OD' is the outer diameter of the inside pipe. '24.5' is the ft/min conversion factor, while Pump RPM is taken in gallons per minute (gpm).

2.8 Friction Velocity

Friction velocity, also known as shear velocity, is defined as the shear stress of wall termed with the same unit as of velocity. The explanation of the wall shear stress will enable to derive non-dimensional sets in the additional investigation as it exhibits a dimension of velocity. Similarly, it is acknowledged that turbulent fluctuations around the wall of the boundary increase with this velocity [32].

$$u^* = \sqrt{\frac{\tau_w}{\rho}} \quad \text{Eq 4}$$

Where u^*represents shear velocity, ρ is the density of the fluid and τ represents shear stress of the wall.

The equation of viscous sublayer thickness defined with respect to friction velocity is written as;

$$\delta_s = \frac{5v}{u^*} \quad \text{Eq 5}$$

The velocity relates to the fluid density near to the wall area also to the fluid kinematic viscosity, and distance from the smooth surface to the shear stress wall.

$$U = U(\rho, \tau_w, v, y) \quad \text{Eq 6}$$

By means of the friction velocity and dimensional analysis the equation becomes;

$$U = U(u^*, v, y) \quad \text{Eq 7}$$

Additional analysis rendering to the pi law: There must be two non-dimensional law which are associated in some kind of universal relation [32].

$$\frac{U}{u^*} = f\left(\frac{yu^*}{v}\right) = f(y^+) \quad \text{Eq 8}$$

Near to the solid (cuttings) surface, the viscosity dominates the momentum transport. In this region, turbulence is repressed due to viscosity, and the believe that flow in this region is laminar. However, later on, this was proved wrong due to the presence of sporadic actions that intrudes the viscous sublayer [33]. Although, with the presence of strong fluctuations in the viscous sublayer, Reynolds stress is still negligible and hence the equation mentioned below can be considered as velocity gradient in this thin layer area [32].

$$\tau_w = u\frac{du}{dy} \quad \text{Eq 9}$$

$$\frac{U}{u^*} = \frac{yv}{u^*} \quad \text{Eq 10}$$

The dimensionless velocity can be reported as;

$$u^+ = \frac{U}{u^*} \quad \text{Eq 11}$$

Hence, for the smooth surface, the universal law of the wall is reported as;

$$u^+ = y^+ \quad \text{Eq 12}$$

2.9 Turbulent Intensities

The strength of the turbulent flow is defined as Turbulent Intensity. Turbulent Intensity is associated with the intensity of variations in the flow of the fluid. The greater the differences, the greater is the turbulence and vice versa. For variation velocities, the time

average is zero during a certain period of time. To average the time Root Mean Square (RMS) is used for the variation velocities. The RMS of axial fluctuation velocity is stated as:

$$u_{RMS} = \sqrt{\overline{(u'^2)}} \quad \text{Eq 13}$$

Indeed turbulent intensity relates with RMS of fluctuation velocities, but for the comparison of the turbulence intensity which is a dimensionless intensity is desired for different kind of flows.

Hence, frictional velocity is considered for keeping the similarity in the outcome results and also relating those results for different kinds of fluids.

$$TI = \frac{u_{RMS}}{u^*} \quad \text{Eq 14}$$

$$TI_{radial} = \frac{v_{RMS}}{u^*} \quad \text{Eq 15}$$

2.10 Turbulent Flow Stresses

2.10.1 Normal Stresses

Stress tensor in Cartesian coordinates has a total of nine components. It includes three normal stresses and six shear stresses.

$$\tau = \begin{bmatrix} \tau_{xx} & \tau_{xy} & \tau_{xz} \\ \tau_{yx} & \tau_{yy} & \tau_{yz} \\ \tau_{zx} & \tau_{zy} & \tau_{zz} \end{bmatrix} \quad \text{Eq 16}$$

2.10.2 Viscous Shear Stress

The viscous stress is a kind of shear stress formed due to viscosity. It is anticipated that this stress has large values where the velocity gradient is high. High-velocity gradient occurs in the vicinity of the solid surface [34].

2.11 Flowzan

Flowzan is biopolymer xanthum-gum with high viscous properties. Flowzan helps in shear-thinning fluid for optimal flow rate, reduces formation damage, reduce pressure loss and makes the transport of solid cuttings easy [35].

The main reason to use Flowzan as a drilling fluid during our experiment was it's shear thinning behaviour and good solution for the easy transport of solid cuttings.

Table 2-1: Flowzan Characteristics

Apperance	**Properties**
Form	Powder
Colour	Cream to light yellow
Odour	Slight
Relative density	From 1.4 to 1.6
Specific Gravity	0.995
pH	From 5.5 to 8.5

Figure 2-7: Flowzan

2.12 Solid Glass Beads

The beads used during the experiments which represents the drill solid cuttings are spherical borosilicate solid glass beads. The significant properties of solid glass beads are mentioned in

Table 2-2: Glass Beads Properties

Apperance	**Properties**
Material	Borosilicate
Diameter	2-3 mm
Shape	Sphere
Chemical Compostion	Silicon oxide (SiO_2) and Boron oxide (B_2O_3)
Refractive Index	1.48

Figure 2-8: “2 mm” Solid Glass Beads

2.13 Flow Patterns

The flow patterns are characterised into five main with additional sub classifications. Figure 2-9 express different flow patterens obtained in the annulus with increase in the velocity [36, 37].

- **Homogenous flow:** The solid cutting slurries are homogeneously suspended in the flow due to the turbulence of the fluid. Homogenous flow arises at high flow rate.
- **Heterogeneous flow:** When particles flows without settling refers to heterogenous flow. The lifting force which is greater than the gravitational force does not all the settling of the slurries. No solid beds occur at high flow rates.
- **Saltating flow:** When slurries stars to settle at the bottom of annulus causes saltating flow. This occurs with the decrease in flow rate. The particles on the top have relatively high velocity as compared to the particles accumulating at the bottom.
- **Moving bed:** The more we decrease the flow rate, the slurries on the top rolls and slides on the top of the accumulated beds.
    - Continuing Moving Bed (CMB): Due to the low flow rate, the slurry beds starts to make long length beds due to sliding. The slurry cutting particles on the top of the dunes is transported forward by drag and lift forces.
    - Separated Moving Bed (SMB): The dunes having a small distance between them are referred to SMB. This happens due to the inside particles of the dunes that remains stationary due to the flow while the top particle keeps on moving forward.
- **Stationary flow:** At the minimum flow rate, the particles accumulate at the bottom due to not enough velocity to move them forward. However, in stationery flow, the top particles move, but the velocity is very low.

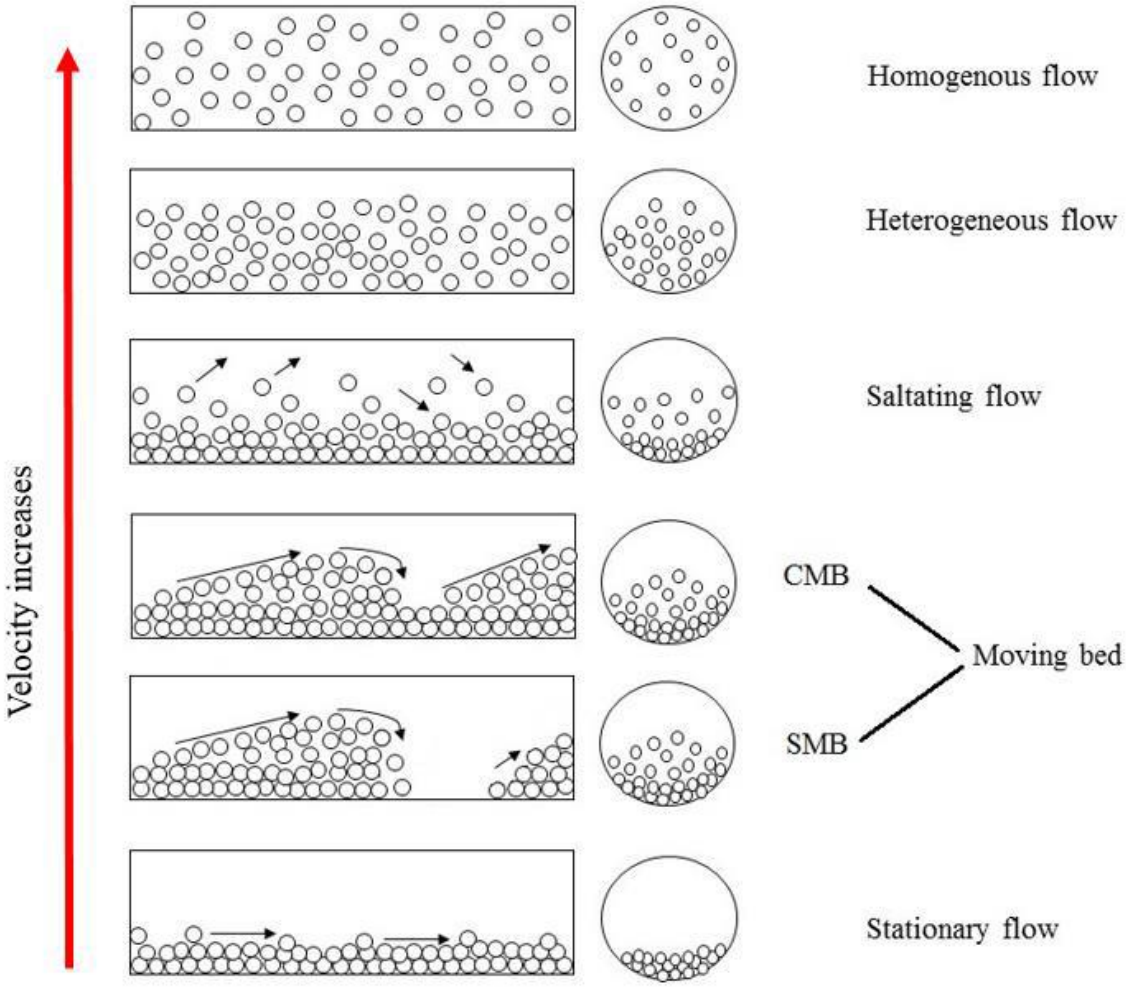

Figure 2-9: Flow Patterns

Chapter 3 Experimental Facility

The chapter explains the thorough information of the experimental setups and methods applied for the measurements and calculations are described in two subsections. The first section of the chapter describes the complete structure of the horizontal flow loop transformable into an inclined flow loop system along with the essential parts of the flow loop system are well defined. Also, the significant accuracy and requirement of all devices attached to the flow loop system are stated. From the functional control of the flow loop facility to the data acquisition procedure are also explained. The novel PIV method, which has been used for the the velocity profile measurements, is also described thoroughly in the next chapter. The second part of this section is dedicated to the experimental phase in which a thorough procedure is discussed. It also includes comprehensive measurement methods and investigation of the data.

3.1 Flow Loop System

Figure 3-1 is the simple horizontal (transformable into inclined position) illustration of the flow loop system and the assembled apparatus installed in Texas A&M University at Qatar.

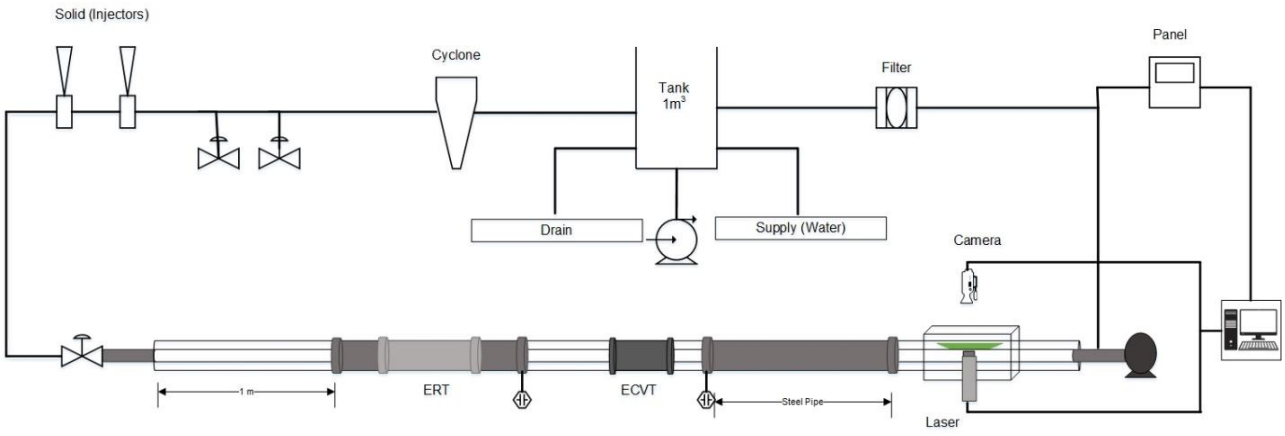

Figure 3-1: Illustration of the Flow Loop Facility

The flow loop system - Figure 3-2 comprises of a 6.16m long pipe having 6.4 cm x 11.4cm (2 ½ by 4 ½ in.) inner pipe diameter and outer pipe diameter which is treated as the annulus. The annulus area of the flow loops system is 70.9 cm^2. The flow loop depicts an

actual wellbore scenario. First, the outer pipe which acts like as an annulus is composed of acrylic pipe and an inner rotating pipe which behaves like a drill pipe is made up of PTFE pipe. The outer pipe consists of three 1m sections made of transparent acrylic material for ease of visualisation and two 1m of steel pipe connected with aluminium flanges of 180 x 2000 mm dimensions.

All sections have an inner diameter of 4.5 inches. The inner pipe is made of five 1 m PTFE pipes with an outer diameter of 2.5 inches. The inner rotating pipe, which acts as like a drill string, can be rotated and positioned into concentric or eccentric conditions.

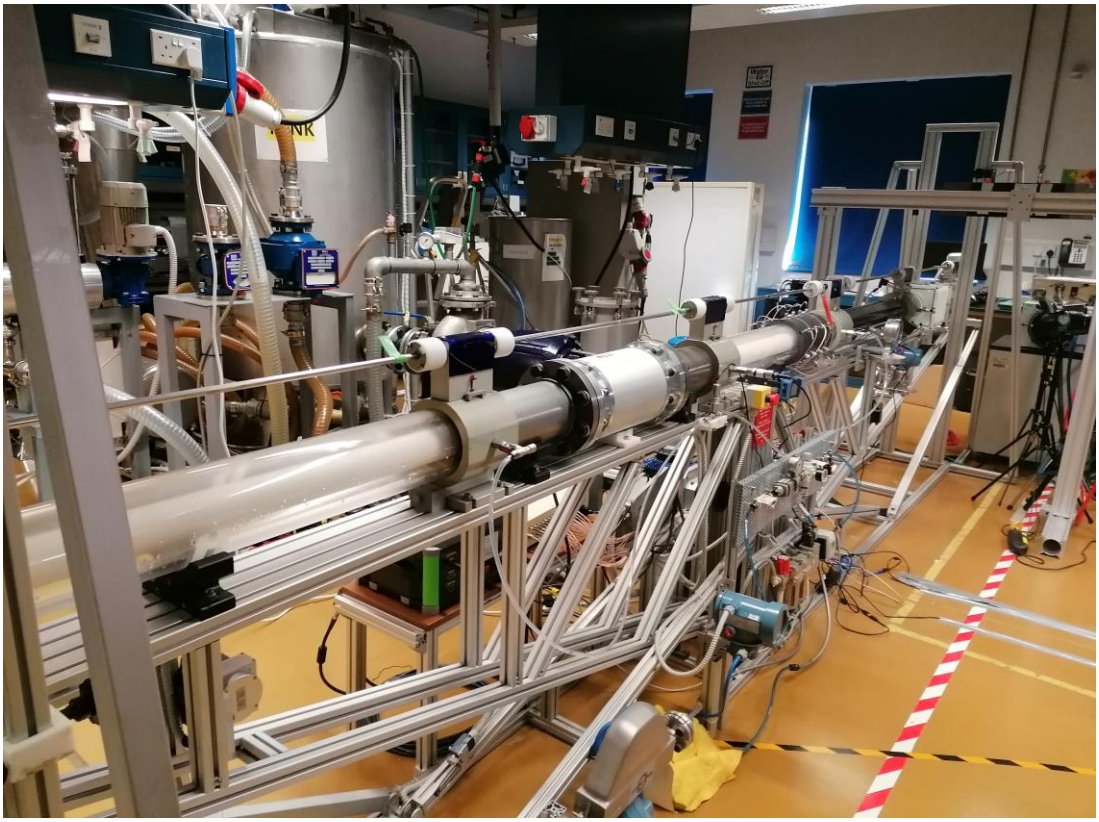

Figure 3-2: Real Image of Flow Loop Facility at TAMUQ in Horizontal Position

The entire unit is built on an aluminium structure which capable of inclination. The inclination angle can 15^0 from the horizontal, and is built to study the effects of inclination as illustrated in Figure 3-3. The specially designed fasteners are used to secure the frame in position and also allow the system to move in one axis to position it manually eccentric or concentric.

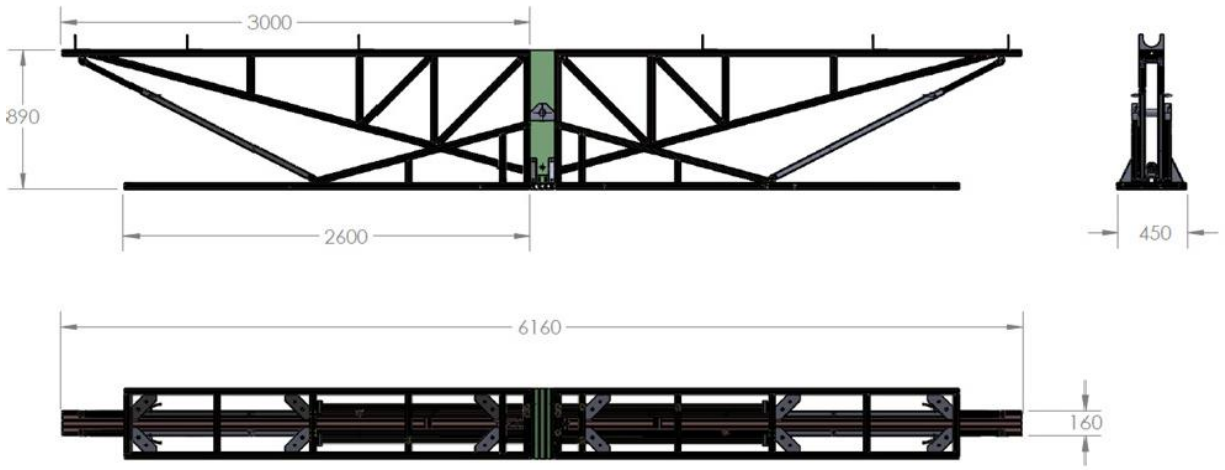

Figure 3-3: Frame that allows the movement of flow loops facility to make it inclined (Units are in mm)

The system includes a flow tank of 1000L capacity (265 gallons) fitted with an agitator Figure 3-4. The storage tank is a multipurpose tank which can be used as a storage of the fluid and agitator inside the tank is used for mixing the fluid. The storage tank is an open tank, and the RPM of the agitator is adjustable from (150 – 250 RPM). The tank has a sensor which notifies about the volumetric flow rate.

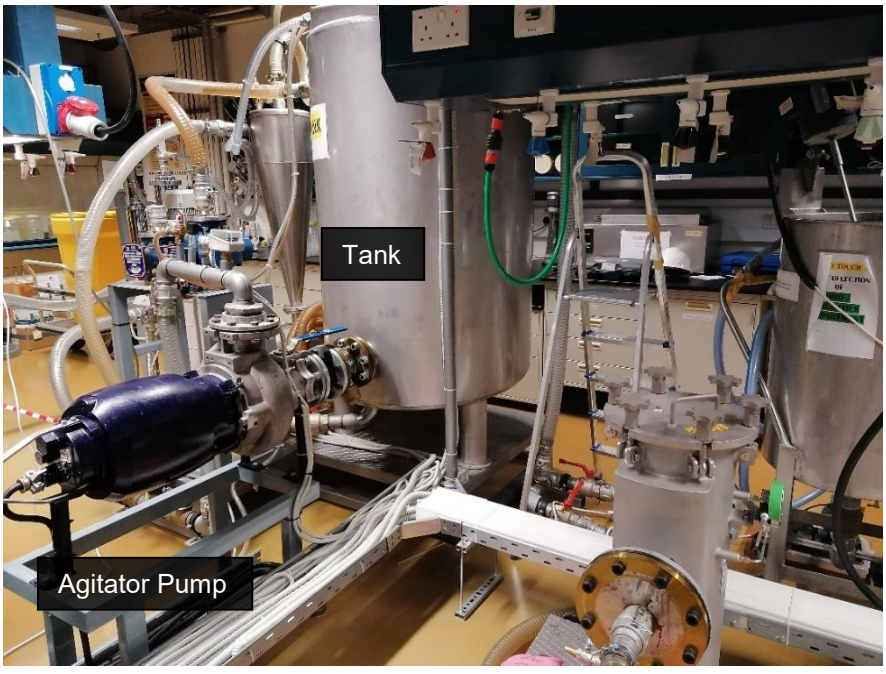

Figure 3-4: Flow Loop Tank and Agitator Pump

A rotor can rotate the inner tube between 0-150 RPM. Figure 3-5 and Figure 3-6 is a high speed and high quality camera which was used to capture the movement of solids along with the High Power Diode Lasers.

Figure 3-5: LaVision High-Speed Camera

Figure 3-6: High Power Diode Lasers

Figure 3-7 illustrates the Refractive Index Matching (RIM) is a plexiglas box, which is rectangular in shape fitted around the outer pipe of the glass section to monitor solid cutting behaviour and calculate velocity. The main reason to use this RIM box was to reduce the consequence of pipe curvature. The empty space concerning the outer pipe and the rectangular box was filled with the same fluid as in the annulus.

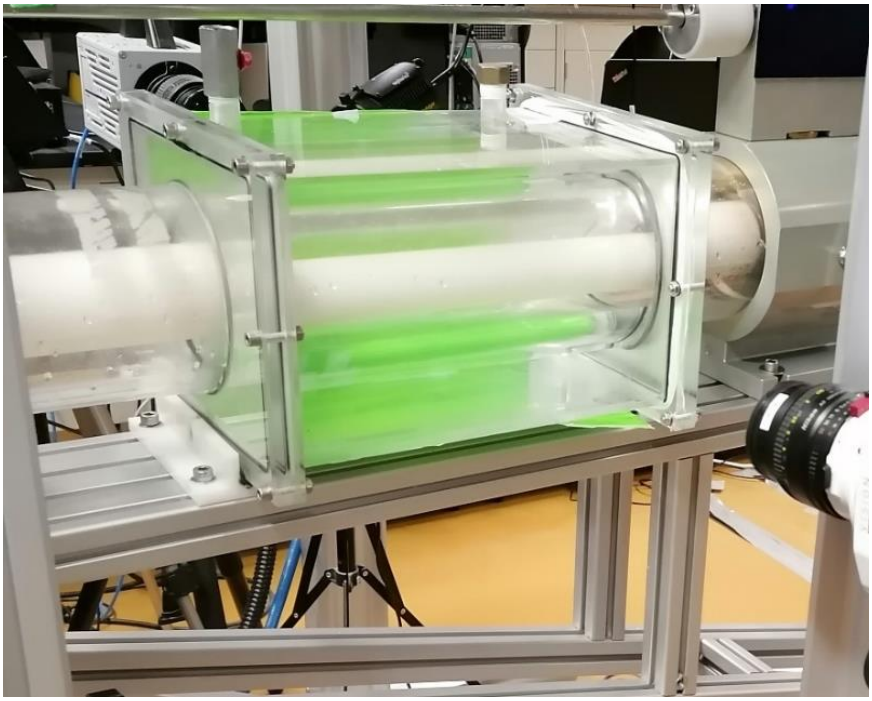

Figure 3-7: Refractive Index Matching (RIM) Box

The system can be functioned with maximum pressure in the annulus of 1.0 barg (15psig) when having air-liquid (two-phase) flowing in the annulus and 2.0 barg (30 psig) when having only liquid flowing.

A manual mechanism Figure 3-8 using locking devices for achieving its eccentric and concentric position is placed on the upper part of the tubes.

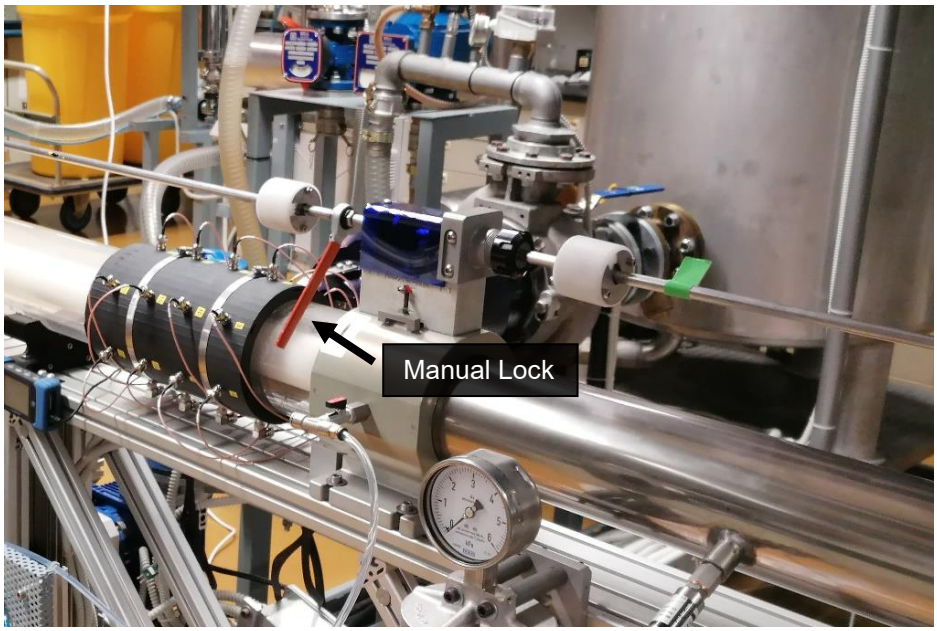

Figure 3-8: Mechanism to achieve eccentric/concentric position

The flow loop system is operated by a separate touch panel Figure 3-9 or through a laptop with the ability to control the followings parameters:

- RPM of the pump and liquid flow rate
- RPM of the agitator
- RPM for the rotation of the inner tube
- The Inclination of the frame
- Airflow rate on/off and airflow rate
- Emergency shut-off button

Figure 3-9: Control Panel of Flow Loop System

3.1.1 Flow Loop System Working Principle

The prime objective to conduct these experiments was to find the velocity of the solid particles passing from the annulus. This experiment exhibits the hole cleaning procedure in real case scenario during drilling processes, where cuttings solid beds initiate to develop on the bottom of the annulus.

This section provides the detailed experimental procedure carried out with non-Newtonian fluid water and water mixed with flowzan on to find out the cutting bed procedure through the glass beads. Quantitative and qualitative, along with tools and techniques, are described in the later section. Also, the method applied for the acquisition of data, its processing and the output results has been explained.

Initially, by default, the Flow Loop System is on horizontal position. However, the inclination can be applied in both direction (upward and bottom), but in this thesis, the annulus was uplifted, as shown in Figure 3-10 to 5˚ and 10˚ from the horizontal. Every control of the Flow Loop System was controlled through the laptop.

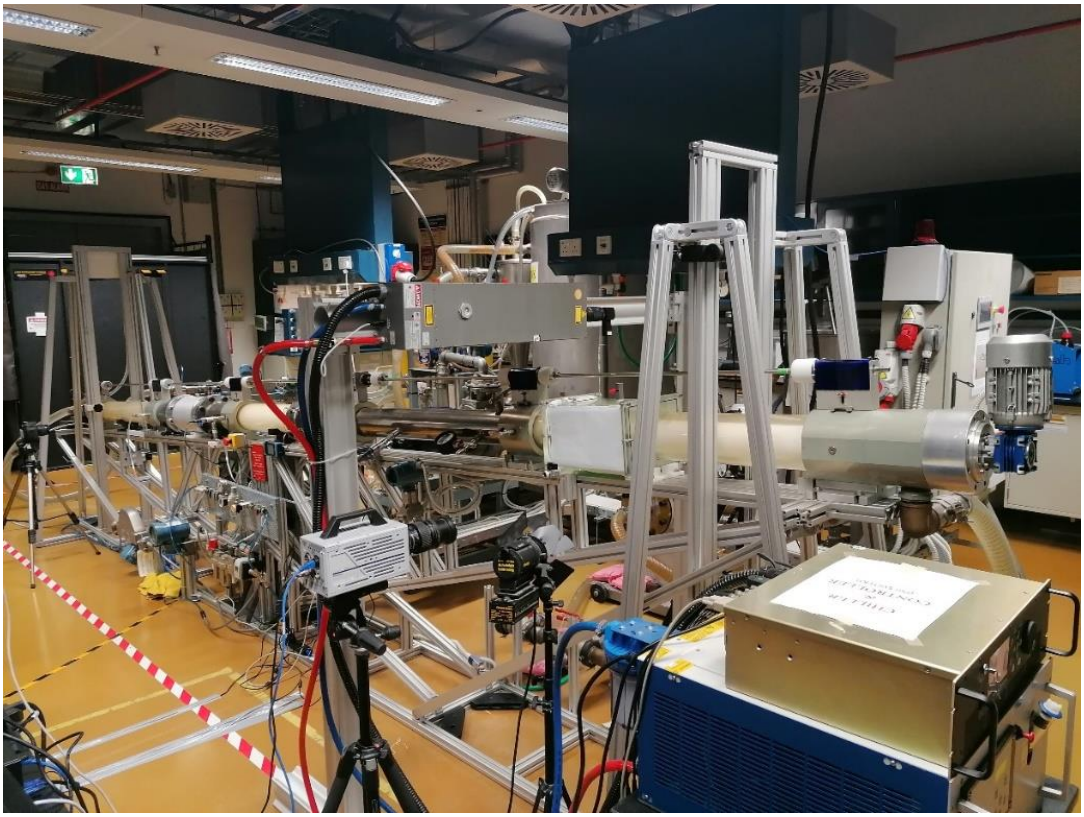

Figure 3-10: Flow Loop System in Inclined Position - 5˚

During drilling scenario, to avoidm ainly pipe sticking problem, it is anticipated to keep the cuttings concentrations below 5%. A concentration of 4% of the liquid has been used during the experimentations phase. Solid glass beads with a density of 2600 kg/m3 the type of cuttings used in these experiments. Each experiment would require about 12 kg of glass beads, as illustrated in Figure 3-11: Solid Glass Beads. A small quantity of fluorescent particles Figure 3-12 are added to the tank with Flowzan to get the illumination effect of particles during the experiment.

Figure 3-11: Solid Glass Beads

Figure 3-12: Fluorescent Particles

The experimental pattern for Newtonian and non-Newtonian is described below:

3.1.1.1 Running Newtonian Fluid

The Newtonian fluid used for this experiment was water and a mixture of flowzan. The procedure pattern is described below:

1. To make sure the operation is carried out within the prescribed safety procedures.
2. Make sure the “fill tank” valve is open and the “drain tank” valve is closed.

3. Fill the tank with 300 litres of water and then start the circulation of water with our desired flow rate. In the case of flowzan mixture, add 125g for 0.05% concentration of flowzan.
4. With the help of inclination motor, take the flow loop annulus from 0˚ to 2.5˚ and 5˚ (toe-up) and 2.5˚ (toe-down).
5. Observe and take all the images on all flow rates with the help of PIV software.
6. Take PIV images on the concentric condition and then on an eccentric condition.
7. The annulus needs to be cleaned carefully after the experiments.

3.1.1.2 Running Non-Newtonian Fluid

The non-Newtonian fluid used for this experiment was water and the mixture of flowzan along with solid glass beads to make the system. The procedure pattern is described below:

1. To make sure the research is carried out within the prescribed safety procedures.
2. Make sure the “fill tank” valve is open and the “drain tank” valve is closed.
3. Fill the tank with 300 litres of water and then start the circulation of water with our desired flow rate. In the case of flowzan mixture, 150g of 0.05% concentration of flowzan is added with water.
4. 12 Kg of solid glass beads is added to the solid injection system.
5. With the help of inclination motor, take the flow loop annulus from 0˚ to 2.5˚ and 5˚ (toe-up) and 2.5˚ (toe-down).
6. Observe and take all the images on all flow rates with the help of PIV instrument.
7. Take PIV images on the concentric condition and then on an eccentric condition.
8. The annulus needs to be cleaned carefully after the experiments.
9. Let the fluid to remain in the tank to solid to settle down.

3.1.2 Flow Loop System Measurement Tools and Techniques

The key purpose of glass beads experimentations is to obtain the velocity data at which cuttings start to flow. Flow recording and the particle visualisation tool is of great help to analyse the flow changes and visualise the bed transportation. A camera with high-

resolution and a high-diode laser were used to capture solid beads movement in a bed. Figure 3-13 represents a typical imaging technique carried out during the experiment.

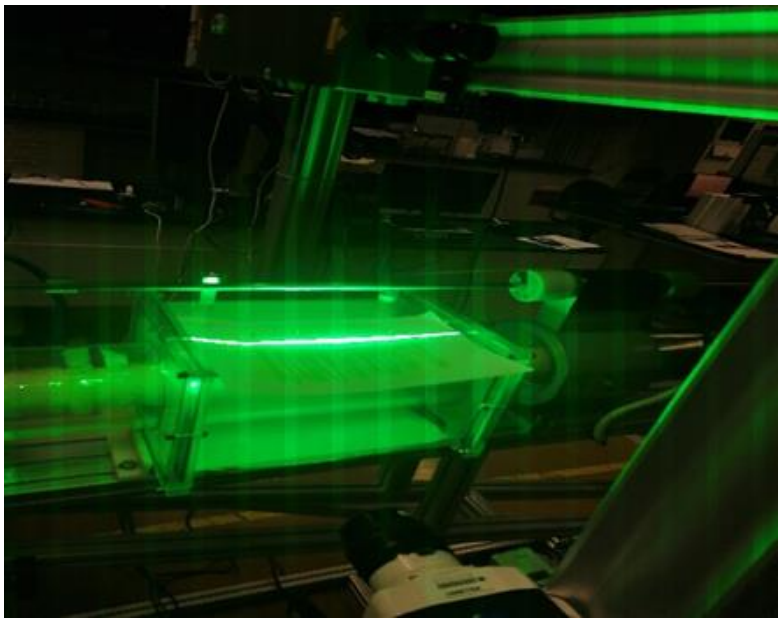

Figure 3-13: Laser Emission during the Experiment

The experiments conducted were tried to make as real as promising to the real drilling situation. One crucial factor was to avoid the backflow of the solid cutting bed once they were removed from the annulus. During drilling processes, the solid cuttings from slurries are separated from the drilling fluid on the shale shaker. The flow loop system is an open system, every time the same fluid flowed during the experiment. Therefore, to remove the solid glass beads introduced to the system is removed through the filter. The filter later catches the particles and send the fluid back to the system. Moreover, with the bypass, the glass beads can also be transported directly to the system.

The camera and high diode laser are placed at a distance to make sure the focus is enough to the point of observation. The experiments start with the lease flow rate as in our case; the first flow occurs at 500 RPM to stabilize the bed. This is important to confirm that the annular velocity is less than the critical velocity of particle movement. Then the flow rate is steadily increased by varying the pump RPM before the critical velocity is attained.

3.2 Particle Image Velocimetry System

This part discusses the essential concepts of Particle Imaging Velocimetry (PIV) technique. Starting from the configuration of the PIV equipment to the tuning of the camera and laser will be discussed. Pre-processing of images and then post-processingof vector profiles and the results obtained will be thoroughly discussed.

3.2.1 PIV Method: Theories and Fundamental

The PIV method, with the help of tracer particles, observes the velocity profile of particles in the flow with the help of capturing images through the camera. The concept to calculate velocity is to track the displacement of a particle during the flow with respect to time. The idea to obtain velocity by these methods looks easy, but getting the movement of a tracer particle needs observation at multiple times. This can be achieved with the help of capturing various images. The first picture works as the reference of that tracer particle and then concerning time and its displacement will aid in calculating the velocity.

Though the idea of capturing images seems comparatively easy upon the application of such theory in micron size is not an easy task. The main requirement to operate the PIV technique is to have a transparent environment. The velocity profile of the tracer particles were obtained in a transparent environment. To capture images through the camera, the visualisation ultimately needs transparent flow pipes.

A typical PIV equipment involves a light emitter and a camera for capturing images. The light emitter used is a High Diode Laser which smoothly emits the light. A camera was the primary source of capturing images during the flow. The vital factor to run the PIV system is the coherency between the laser emission and the image takes. For this purpose, a special trigger option helps in emitting laser light and capturing images simultaneously. This helped in the proper processing of vector profiles.

Another major factor before running the PIV experiment is the orientation of the camera and laser. They must be perpendicular to each other and correctly aligned. After accurate alignment and laser emitting light illuminating the tracer particles, the PIV apparatus is ready to operate. Figure 3-14: Typical PIV Setup [38] Displays the typical PIV setup.

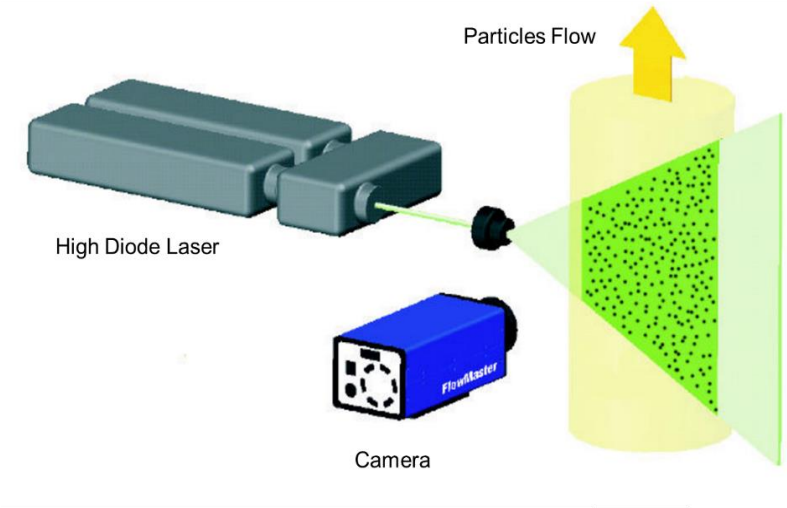

Figure 3-14: Typical PIV Setup [38]

Figure 3-14 discusses a typical PIV setup, and a trace of flowing particles is illustrated. The ray of light from Class IV High Diode Laser emits into the fluid flow and illuminates the fluorescent particles. Once the particles in the flow illuminate, couple of images could be recorded during the flow with the help of the camera. A number of pictures are captured with duing a period of time. Throughout our experiment, we obtained 200 images for 10 seconds. As soon as the displacement is known during the operation, the instantaneous velocity vector field can be generated. Further in this part, the capturing of images, pre-processing and post-processing have been discussed.

3.2.2 FFT-Based Cross-Correlation

This section discusses the method and technique to understand by what means instantaneous velocity vector field can be attained by the investigation of the images captured. The main software to process PIV images used was DAVIS 8.4.0.

To obtain the velocity field from the several images, the number of processing steps are followed. Firstly, chose an interrogating frame having size N×N pixels from the first captured image. To find comparisons, Direct Cross-Correlation Method (DCM) will be used. After identifying the illuminated points Figure 3-15, which are actually the peak points will be selected [39].

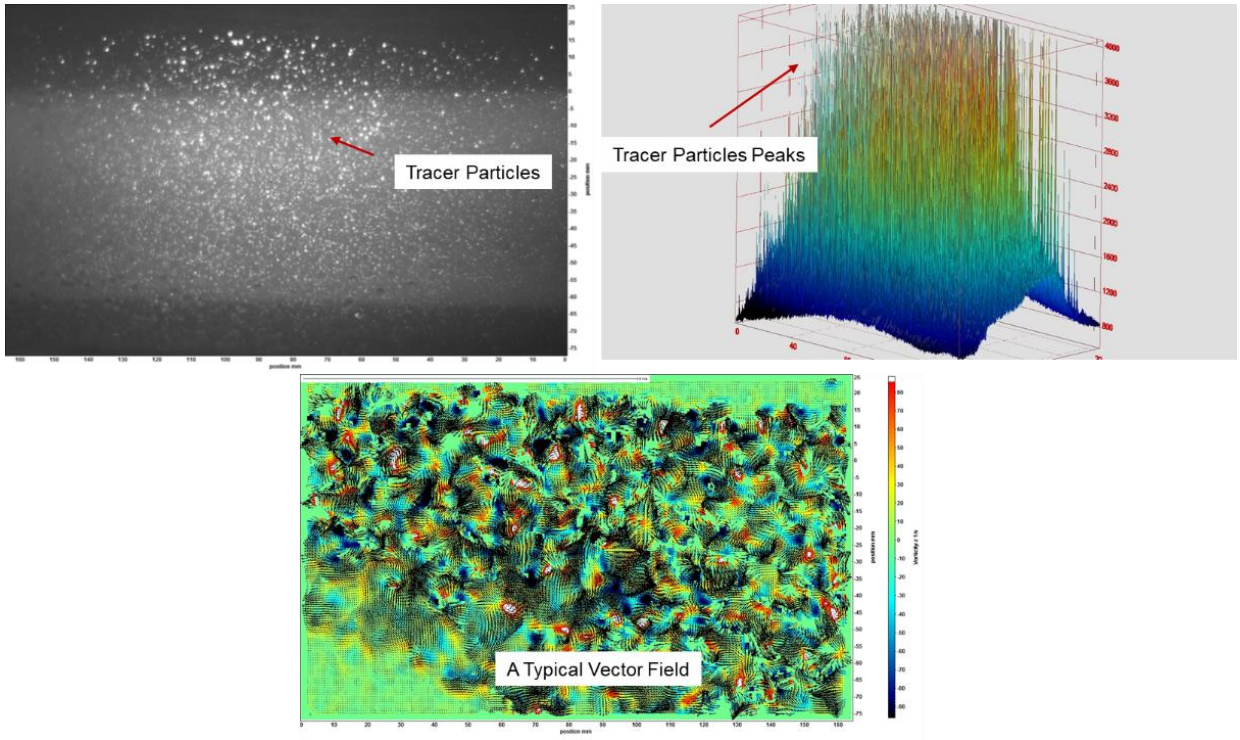

Figure 3-15: Pre-Processing PIV Images

To calculate the displacement of tracer particle the camera needs calibration or the number of images to be observed. The instantaneous velocity field can be acquired from;

$$\begin{cases} U = \dfrac{\Delta x}{\Delta t} \\ V = \dfrac{\Delta y}{\Delta t} \end{cases}$$

Another critical step is to choose an interrogation window again of $\frac{N}{2}\times\frac{N}{2}$ by applying Fourier Transformation (FFT). FFT is applied to several images that are captured through the camera. In our experimental case, we took 200 sets of images. They were then converted into vector field and then further processed to obtain the results. Two hundred images were gathered within 10 seconds.

The next step begins with the analysis of the images captured. Among 200 images, 50 images were processed with an increment of 4 images. Therefore, 50 images were further processed through the Davis software to get the desired value and the results obtained were also in agreement. Those images processed created a vector field showing the

movement of particles. Further, the vital step is to take the average of those 50 pictures in order to remove the noise. Taking average helps to obtain more accurate results.

3.2.3 PIV System Components:

The primary PIV system at TAMUQ comprises of the following three main equipment:

1. Class IV Laser
2. Chiller
3. High-Speed Camera

3.2.3.1 Class IV Laser

A class IV LASER Figure 3-16 has been installed to perform the PIV analysis. The Particle Image Velocimetry (PIV) requires the LASER to illuminate the flow field inside the RIM box. Then the premixed particles with the flow are being tracked by the PIV system to evaluate the velocity field for the respective interested area. The LASER can produce a maximum of 30 mJ of energy per pulse. The wavelength of the radiation is 527 nm. The diode current range is 16-30 amp, but in this experiment 20 amp has been used. A controller is also set to control the laser parameters.

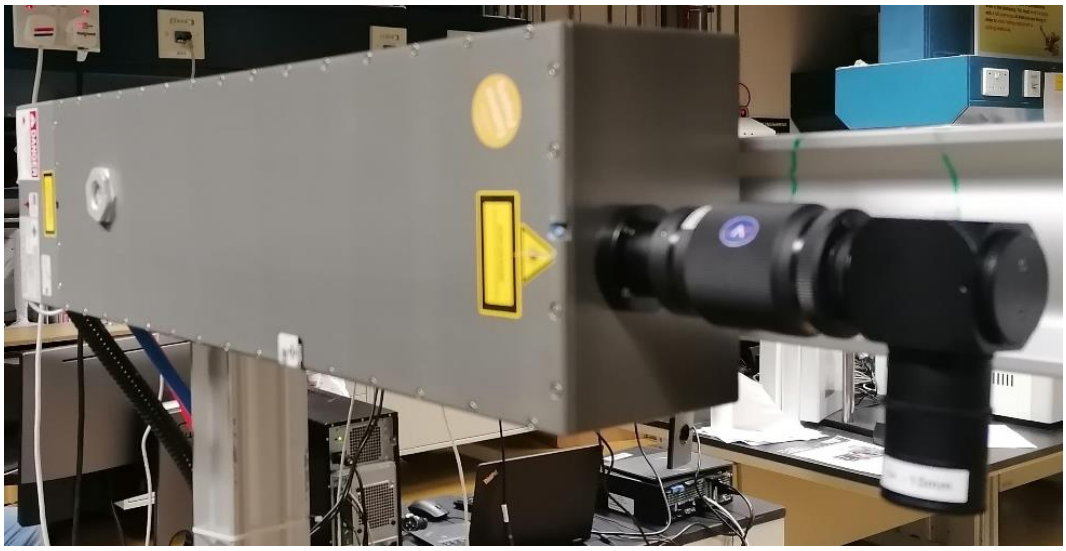

Figure 3-16: Class IV PIV Laser

3.2.3.2 Chiller Unit for Laser

The chiller Figure 3-17 is filled with a mixture of distilled water and the OptiShield Plus (around 10%) solution. The chiller pump outlet hose is connected to the laser-head IN hose connector, and the chiller inlet hose is connected to the Laser-head OUT hose connector.

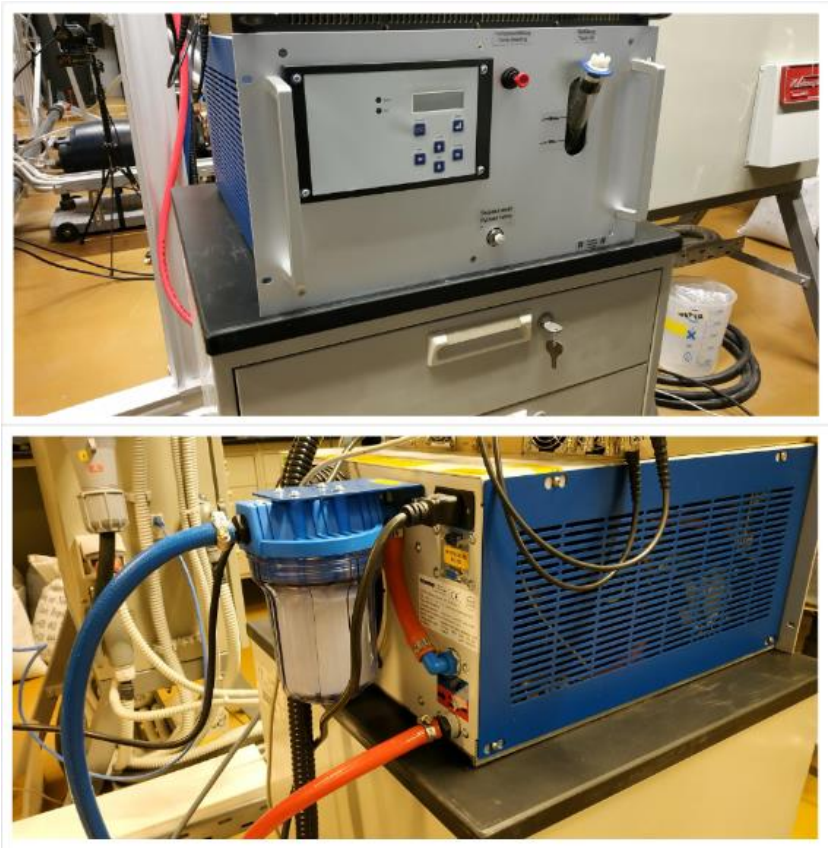

Figure 3-17: Chiller Unit for Laser

3.2.3.3 High Speed Camera

The high-speed camera Figure 3-18 used for PIV analysis is a 2-megapixel camera with 3.2 Gigapixels/second (Gpx/s) throughput. So, at 1380 frames per second at 1920 x 1200 pixels, or over 1500 frame per seconds at 1920 x 1080 pixels. Frame rates up to 325,000 fps are available at reduced resolutions. The camera helps in developing accurate timing and camera synchronisation with laser, easy triggering and excellent sensitivity to the light.

Figure 3-18: High-speed Camera

3.2.4 PIV Imaging Steps

Make sure PIV equipment is in the proper visualising zone. The imaging for both Newtonian and Non-Newtonian fluids, the following pattern is followed:

1. Calibrate the high-speed camera and make sure it focuses the RIM box
2. Scaling of the imaging area is set to on default since it covers the RIM box.
3. Calibrate the inner pipe area through PIV – Davis software.
4. Setting the laser's diode Current to 20 Ampere and turn it to on "On" mode.
5. Make sure, Cycle rate and Cycling Image rate is set to 1 Hz and 1 kHz.
6. Set number of images to 200 images.
7. Record the images when solid glass beads enter the RIM box area.

3.2.4.1 Adjusting Camera Focus

The adjustment of camera focus is necessary for the observation of transportation of solid cuttings during the experiment. The camera is tuned with the help of built-in fine-tuning options available in the camera.

3.2.4.2 Scaling and Calibrating the Image Window

Another essential step before capturing the images is to set the interrogating window. This interrogating window is necessary for the generation of graphs in post-processing steps. This can be achieved with the help of Davis software.

3.2.4.3 Turning on the Laser

The Class IV Laser possesses a safety hazard for the human eye. Due to this reason turning on laser comprises of four steps:

1. Turn on the Button
2. Turn on the Safety key
3. Set diode current to 20 amp.
4. Finally, click turn on the laser

3.2.4.4 Capturing Images

When Laser is turned on set the number of images to capture to 200 and the Cycle rate, and Cycling Image rate is set to 1 Hz and 1 kHz respectively. However, it is not necessary to set these values every time.

3.3 Experimental Matrix

This parts discusses all the experiments carried out mentioning different ranges of the different parameters. A total of 144 experiments were carried out with an additional repeat experiments in order to confirm the obtained result coherency. The different drilling parameter range used is described in Table 3-1: .

Table 3-1: Different set of of drilling parameters investigated during experiment

Parameters	Ranges
Fluids	Newtonian Fluid (Water) Non-Newtonian Fluid (Flowzan – 0.05% conc.)
Inclination Degrees	Horizontal (0°), Toe-up (2.5°, 5°), Toe-down (2.5°)
Pump RPM	800-1000
Mass Flow Rates (Kg/min)	225, 255, 285
Inner Pipe Positions	Concentric (0) , Eccentric (0.3,0.6)
Solid Cuttings	Glass beads (2-3 mm)

Chapter 4 Results and Discussions

This section contains the results obtained from the PIV experiments for both fluids flow Newtonian and Non-Newtonian fluids. This chapters reports the Newtonain Flow, Non-Newtonain Flow and a comprarision separately.

As discussed earlier in previous chapters about the experimental ranges so for every pump RPM the obtained flow rate and annular velocity is mentioned in Table 4-1.

Note: The values of flow rates is the average flow rate value through the experiment while annular velocity is rounded of to three scientific notations.

Table 4-1: Flow rates and annular velocities for water

Pump RPM	**Mass Flow Rate (Kg/min)**	**Volumetric Flow Rate (L/min)**	**Annular Velocity (m/sec)**
800	225	225	0.528
900	265	265	0.599
1000	285	285	0.669

The density used for the Flowzan was 995 Kg/m^3 and values were obtained for every pump RPM and the acquired flow rate and annular velocity is mentioned in Table 4-2.

Table 4-2: Flow rates and annular velocities for Flowzan (0.05% conc.)

Pump RPM	**Mass Flow Rate (Kg/min)**	**Volumetric Flow Rate (L/min)**	**Annular Velocity (m/s)**
800	225	226.131	0.531
900	265	256.281	0.602
1000	285	286.432	0.673

4.1 Flow Evaluation

The core interest of the thesis was velocity profiles. Therefore, to make sure if the obtained result identifies the turbulent flow regime or not, the Reynolds number value was achieved for both water and flowzan from Eq 2.

Table 4-3: Reynolds Numbers Obtained from Experiments with Water

Flow Rate Q (L/min)	N_{Re}
225	26843
255	30422
285	34001

Table 4-4: Reynolds Numbers Obtained from Experiments with Flowzan

Flow Rate Q (L/min)	N_{Re}
226	26978
256	30575
286	34172

In both Table 4-3: Reynolds Numbers Obtained from Experiments with Water and Table 4-4: Reynolds Numbers Obtained from Experiments with Flowzan, the minimum Reynolds number for different flow rates is 26843 for a flow rate value of 225 L/min. The minimum requirement for any fluid to come in turbulence category is to have maximum value than 2100.

4.2 Velocity Profiles of Water in the Annulus

The most important interest and goal of the thesis were to measure the velocity profile intended for Newtonian fluids and Non-newtonian fluids for horizontal, toe-down and toe-up conditions with different drilling parameters and their comparisons. This section of the chapter will thoroughly discuss the velocity profile with varying parameters of drilling results with an illustration. The PIV techniques helped to obtain velocity profile in both

single and dual phase fluid flow. The velocity profiles reported in this section are obtained in the the direction of the flow. The PIV method was used to calculate the velocity profiles on different inclination angles 2.5˚ and 5˚ toe-up while 2.5˚ in toe-down condition. 5˚ toe-down was not observed in this thesis due to the limitation of the bars on which laser was hanging. All single-phase flow of water and Flowzan has been reported along with their comparision. The solid cuttings behaviour on different pump RPM applied on horizontal, 2.5˚, 5˚ toe-up and 5˚ toe-down multiphase system.

4.2.1 Newtonian Fluid Velocity Profiles

All Newtonian fluid velocity profiles are observed in the direction of the flow from the top to bottom that is Vx component. The observation window has been illustrated in :

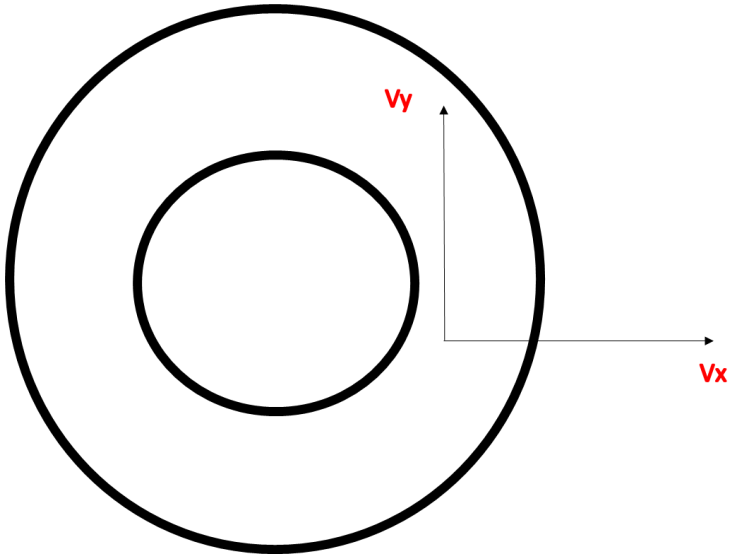

Figure 4-1: Calculation Window

4.2.1.1 Horizontal Annulus with Concentric Condition

The graph reported in Figure 4-2 illustrates the velocity profile of a Newtonian fluid measured utilizing the PIV technique on different pump RPMs from 800-1000. The velocity profile reported is for horizontal annulus in concentric condition and no solid was introduced. The plot shows the asymmetric flow. The fluorescent particles were suspended in the middle; behaviour on the outer boundary was challenging to observe. The pump RPM shows a very low impact on the fluid velocity. Moreover, we see the inner pipe effect on the graph.

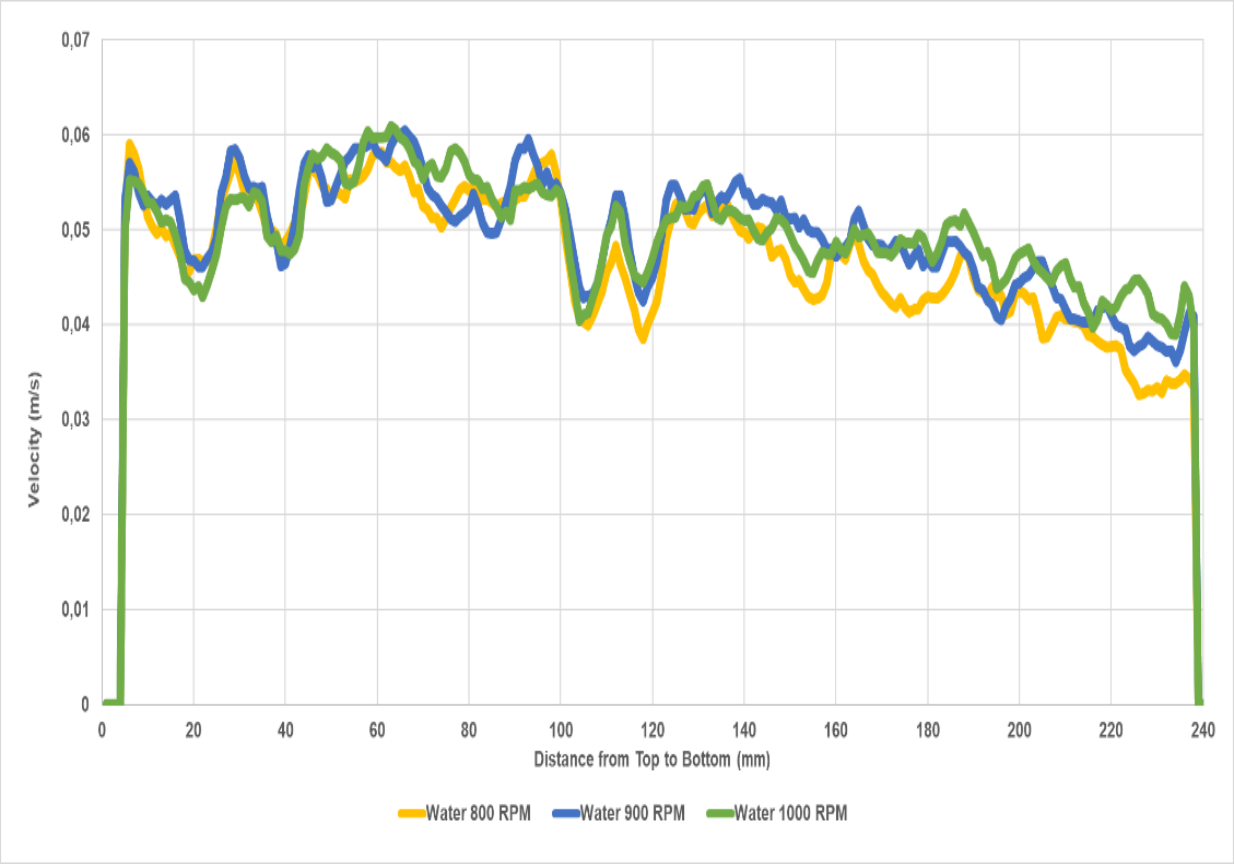

Figure 4-2: Newtonian (Water) fluid velocity profile with different RPM in concentric horizontal annulus

4.2.1.2 Horizontal Annulus with 30% Eccentric Condition

The graph reported in Figure 4-2 illustrates the velocity profile of a Newtonian fluid measured utilizing the PIV technique on different pump RPMs from 800-1000RPM. The velocity profile reported is for horizontal annulus in 30% eccentric, condition and no solids were injected. The plot shows the asymmetric flow. However, the pump RPM shows a very low impact on fluid velocity. However, the eccentricity effect on velocity can be observed.

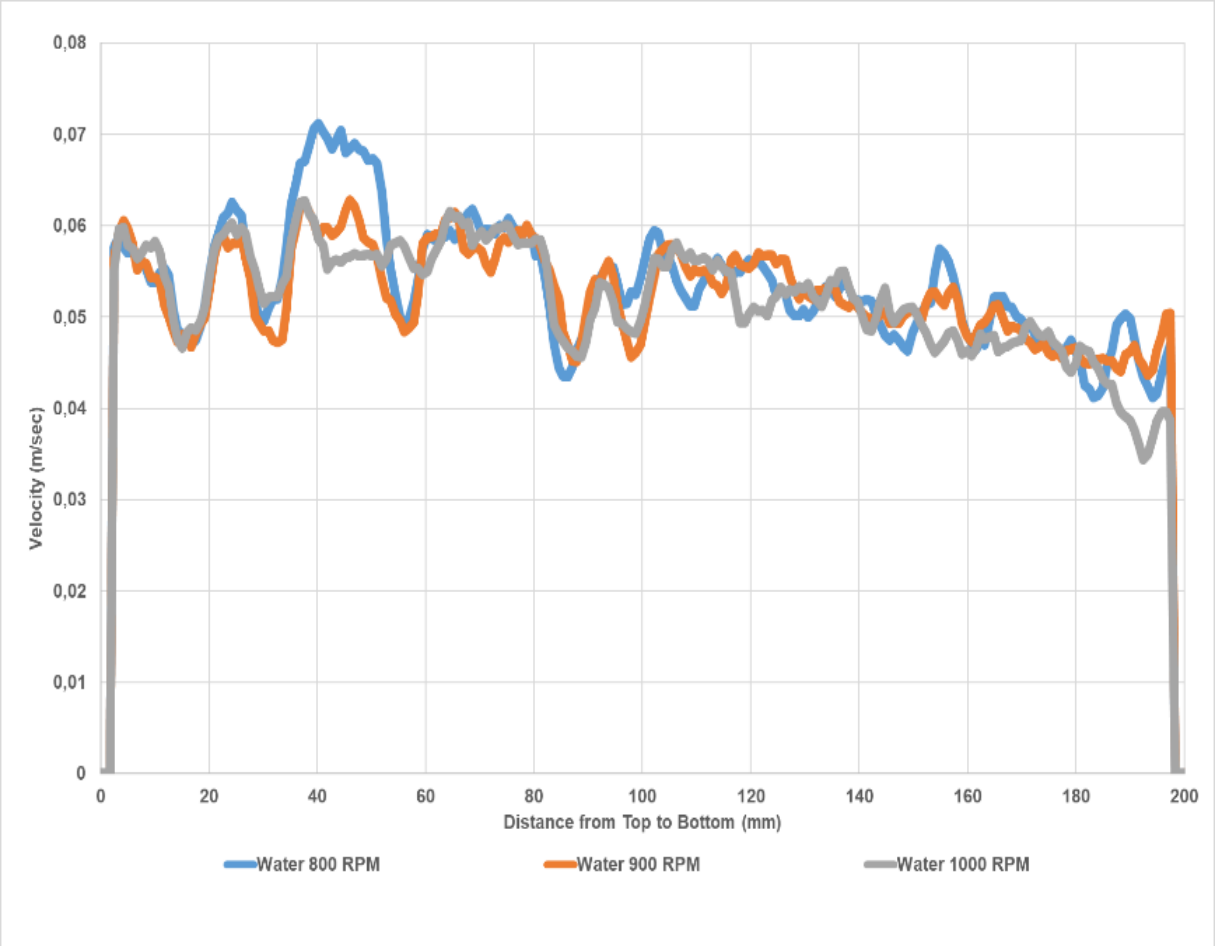

Figure 4-3: Newtonian (Water) fluid velocity profile with different RPM in horizontal annulus with 30% eccentricity

4.2.1.3 Horizontal Annulus with 60% Eccentric Condition

The graph reported in Figure 4-4 illustrates the velocity profile of a Newtonian fluid measured utilizing the PIV technique on different pump RPMs from 800-1000RPM. The velocity profile reported is for horizontal annulus in 60% eccentric, condition and no solids were injected. The plot shows the asymmetric flow. Still, the inner pipe effect can be observed in all previous velocity profiles mentioned. However, the pump RPM shows a very low impact on fluid velocity. However, the eccentricity effect on velocity can be observed.

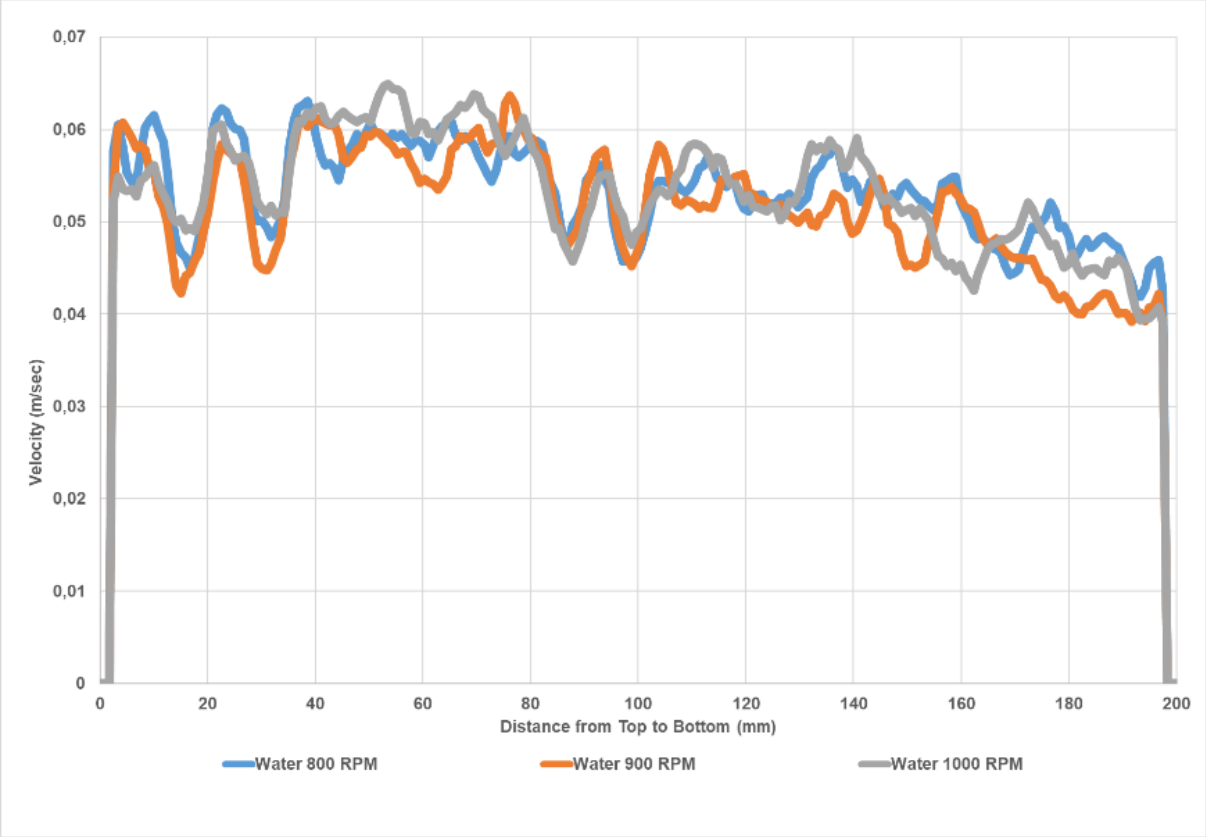

Figure 4-4: Newtonian (Water) fluid velocity profile with different RPM in a horizontal annulus with 30% eccentricity

4.2.1.4 Toe-up 2.5˚ Annulus with Concentric Condition

The graph reported in Figure 4-4 illustrates the velocity profile of a Newtonian fluid measured utilizing the PIV technique on different pump RPMs from 800-1000RPM. The velocity profile reported is for 2.5˚ toe-up annulus in concentric condition, and no solids were injected. The plot shows the asymmetric flow.

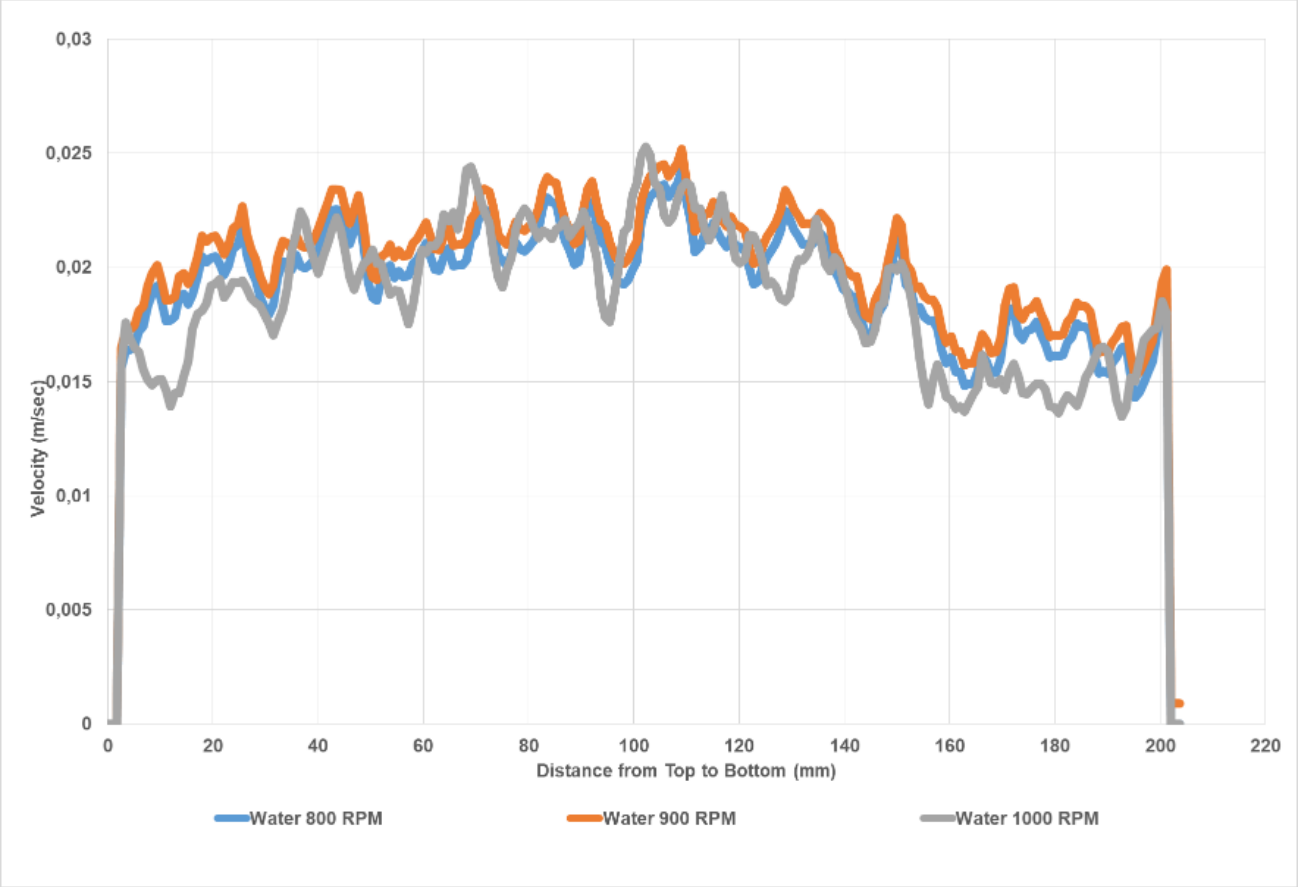

Figure 4-5: Newtonian (Water) fluid velocity profile with different RPM in a toe-up 2.5˚ annulus in Concentric Condition

4.2.1.5 Toe-up 2.5˚ Annulus with 30% Eccentric Condition

The graph reported in Figure 4-6 illustrates the velocity profile of a Newtonian fluid measured utilizing the PIV technique on different pump RPMs from 800-1000RPM. The velocity profile reported is for horizontal annulus in 30% eccentric, condition and no solids were injected. The plot shows the asymmetric flow. Still, the inner pipe effect can be observed in all previous velocity profiles mentioned. However, the pump RPM shows a very low impact on fluid velocity. However, the eccentricity effect on velocity can be observed on the right side of the graph. Velocity tends to low as it moves on the right.

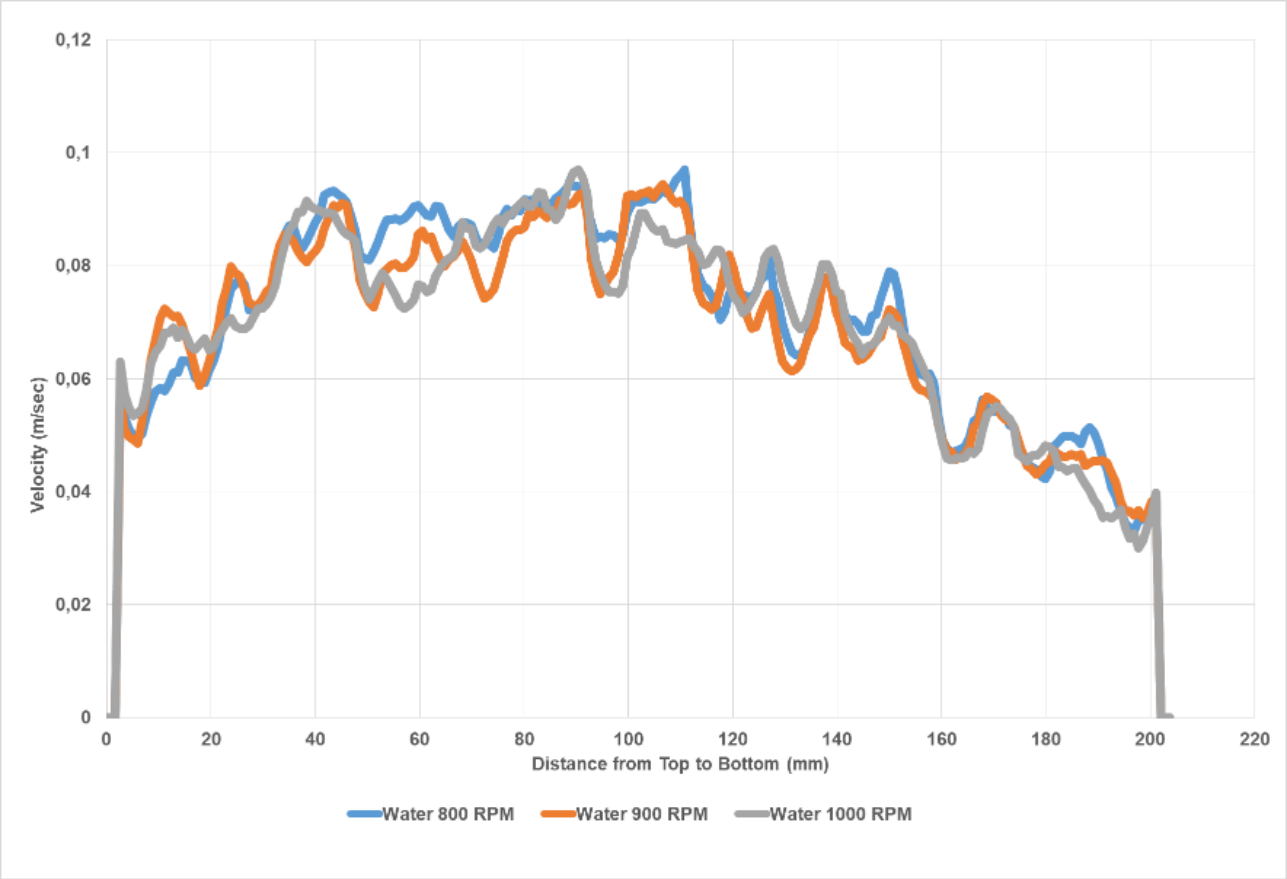

Figure 4-6: Newtonian (Water) fluid velocity profile with different RPM in a toe-up 2.5˚ annulus in 30% Eccentric Condition

4.2.1.6 Toe-up 2.5˚ Annulus with 60% Eccentric Condition

The variation in pump flow rates also shows a decent velocity profile in Figure 4-7. Due to high eccentric value, the radius of high velocity is found on the top of the inner pipe.

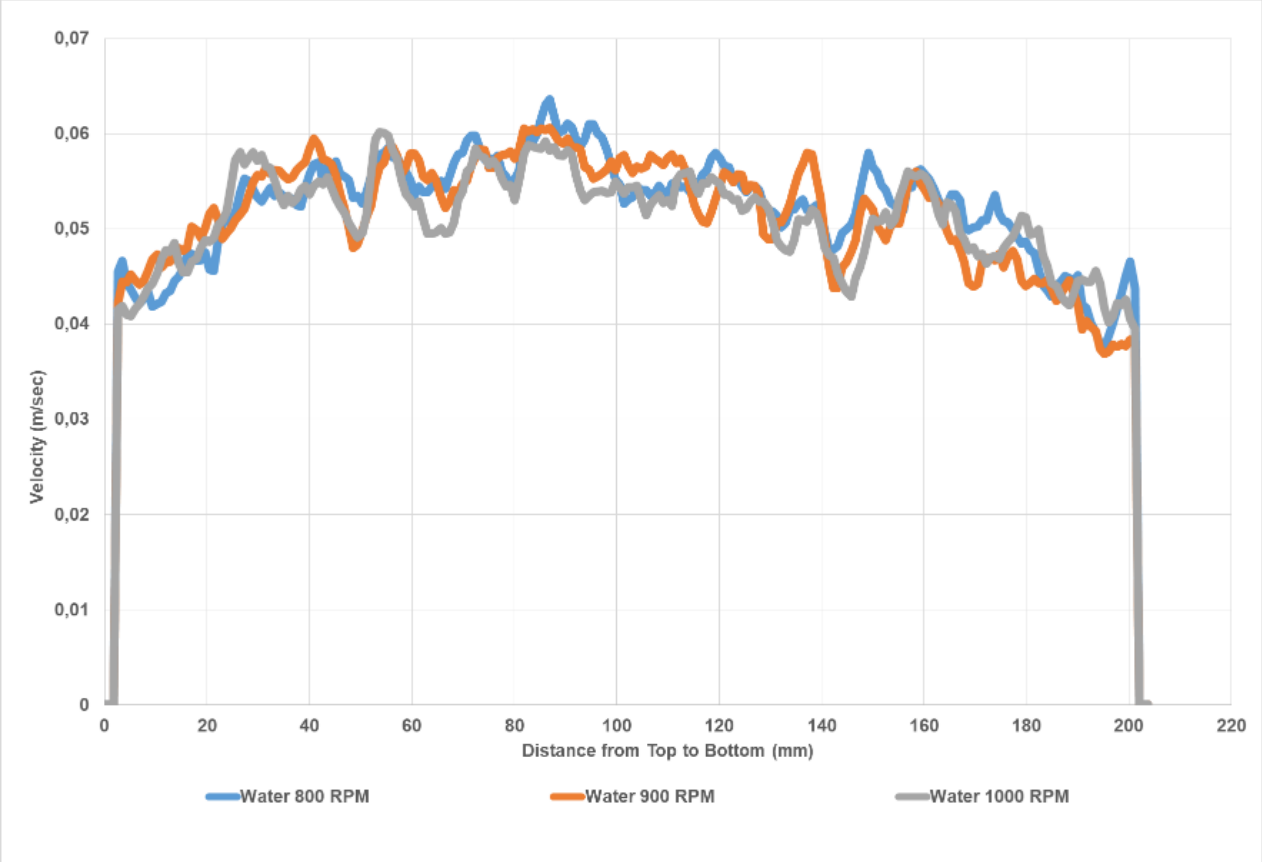

Figure 4-7: Newtonian (Water) fluid velocity profile with different RPM in a toe-up 2.5˚ annulus in 60% Eccentric Condition

4.2.1.7 Toe-down 2.5˚ Annulus with Concentric Condition

Toe-down shows smooth velocity profile due to the action of gravitational force. As the liquid tends to move forward more quickly, Figure 4-8 exhibits the same pattern in different RPMs.

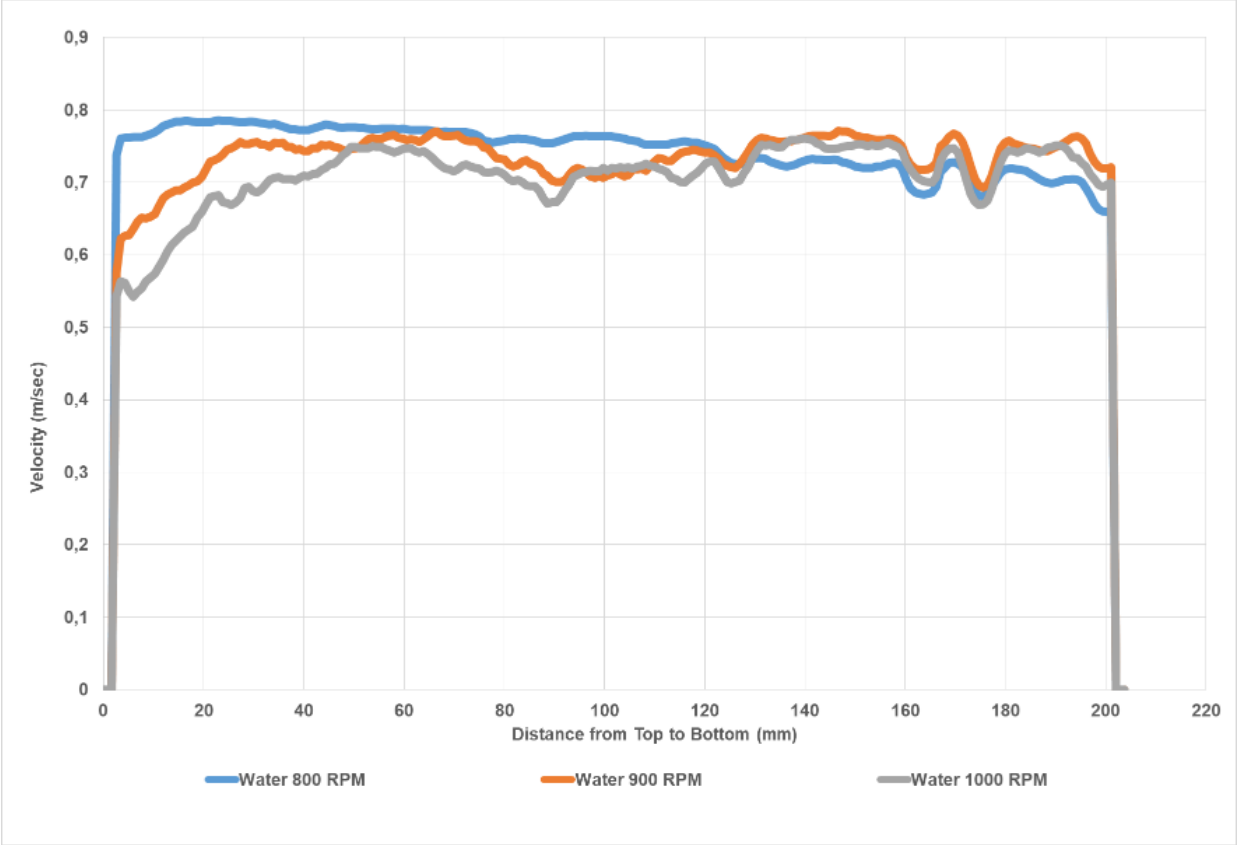

Figure 4-8: Newtonian (Water) fluid velocity profile with different RPM in a toe-down 2.5˚ annulus in 30% Eccentric Condition

4.2.1.8 Toe-down 2.5˚ Annulus with 30% Eccentric Condition

Toe-down condition and increasing the eccentricity shows the velocity drop near the drill pipe Figure 4-9, as seen in previous results as well. In Toe-down scenario, the fluorescent particle moves quickly, so the top position have less fluctuated profile.

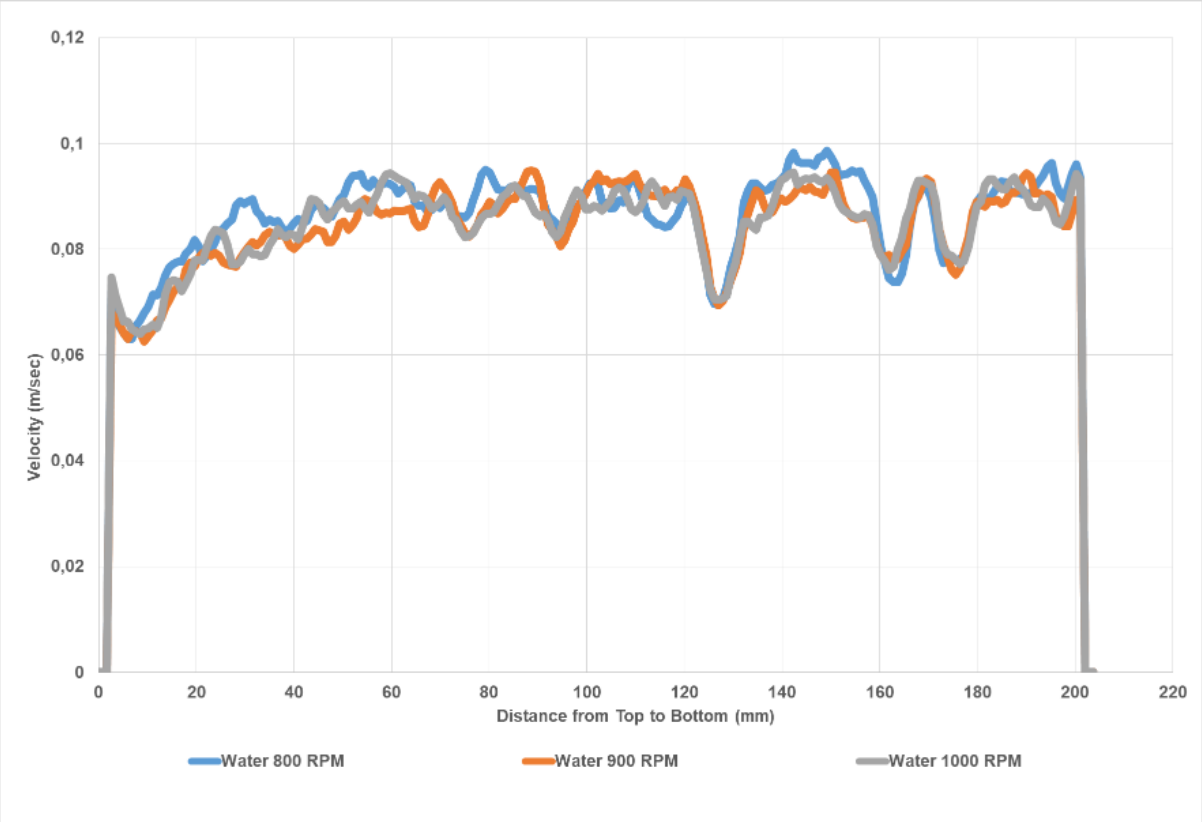

Figure 4-9: Newtonian (Water) fluid velocity profile with different RPM in a toe-down 2.5˚ annulus in 30% Eccentric Condition

4.2.1.9 Toe-down 2.5˚ Annulus with 60% Eccentric Condition

Toe-down increasing the eccentricity to 0.06 shows the velocity drop near the drill pipe Figure 4-10, as seen in previous results as well. In Toe-down scenario, the fluorescent particle moves quickly, so the top position have less fluctuated profile. We can also see the high velocity drop at the top of our inner pipe.

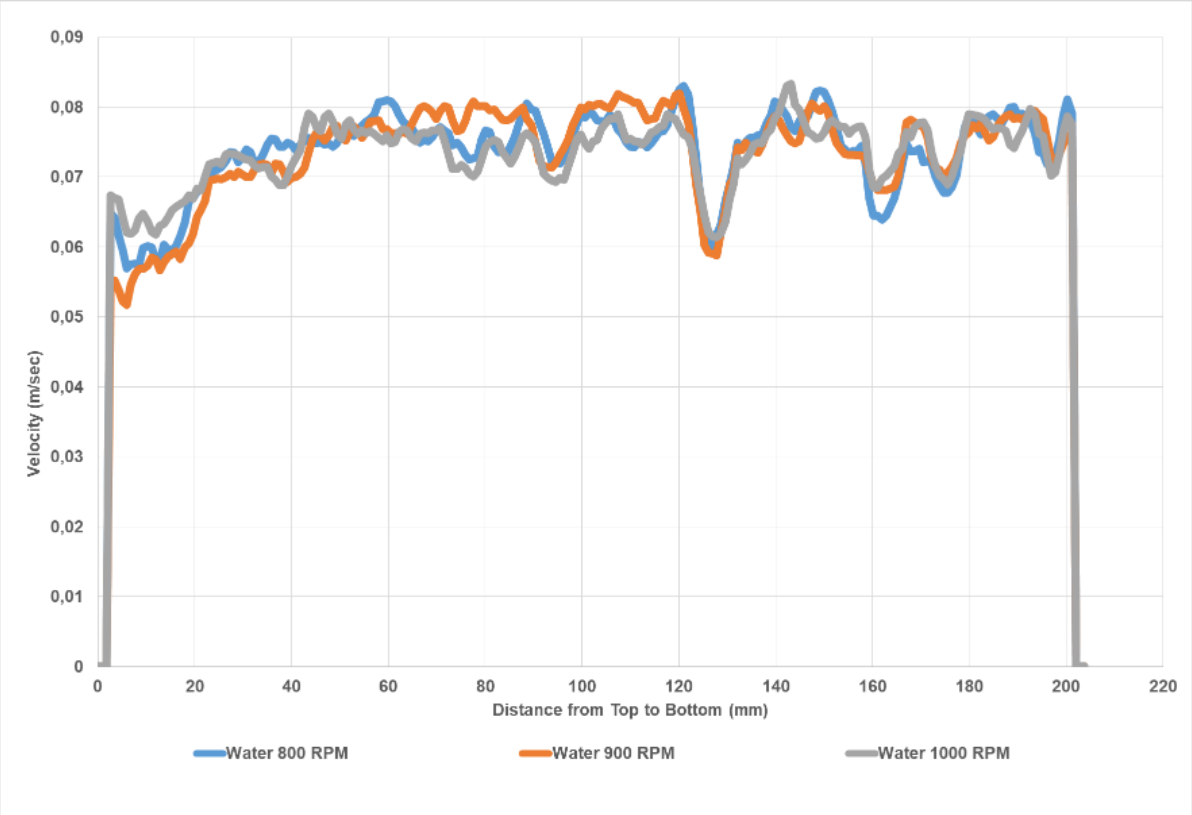

Figure 4-10: Newtonian (Water) fluid velocity profile with different RPM in a toe-down 2.5˚ annulus in 60% Eccentric Condition

4.2.2 Non-Newtonian Fluid Velocity Profiles

All non-Newtonian fluid velocity profiles have been investigated in the direction of the flow from the top to bottom that is Vx component. The same direction which we chose for Newtonian fluids. The observation window has been illustrated in :

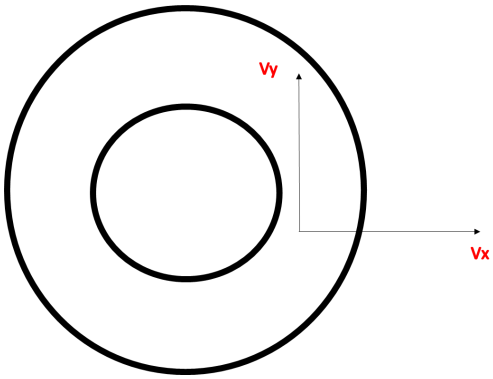

Figure 4-11: Calculation Window

4.2.2.1 Horizontal Annulus with Concentric Condition

The graph reported in Figure 4-12 displayes the velocity profile of a non-Newtonian fluid measured with the help of the PIV technique on different pump RPMs from 800-1000. The velocity profile reported is for horizontal annulus in concentric condition, and no solids were introduced. The plot shows the asymmetric flow. The fluorescent particles were suspended in the middle; behaviour on the outer boundary was challenging to observe. The pump RPM shows a very low impact on the fluid velocity. Moreover, we see the less inner pipe effect on the graph due tp the high-viscous property of Flowzan.

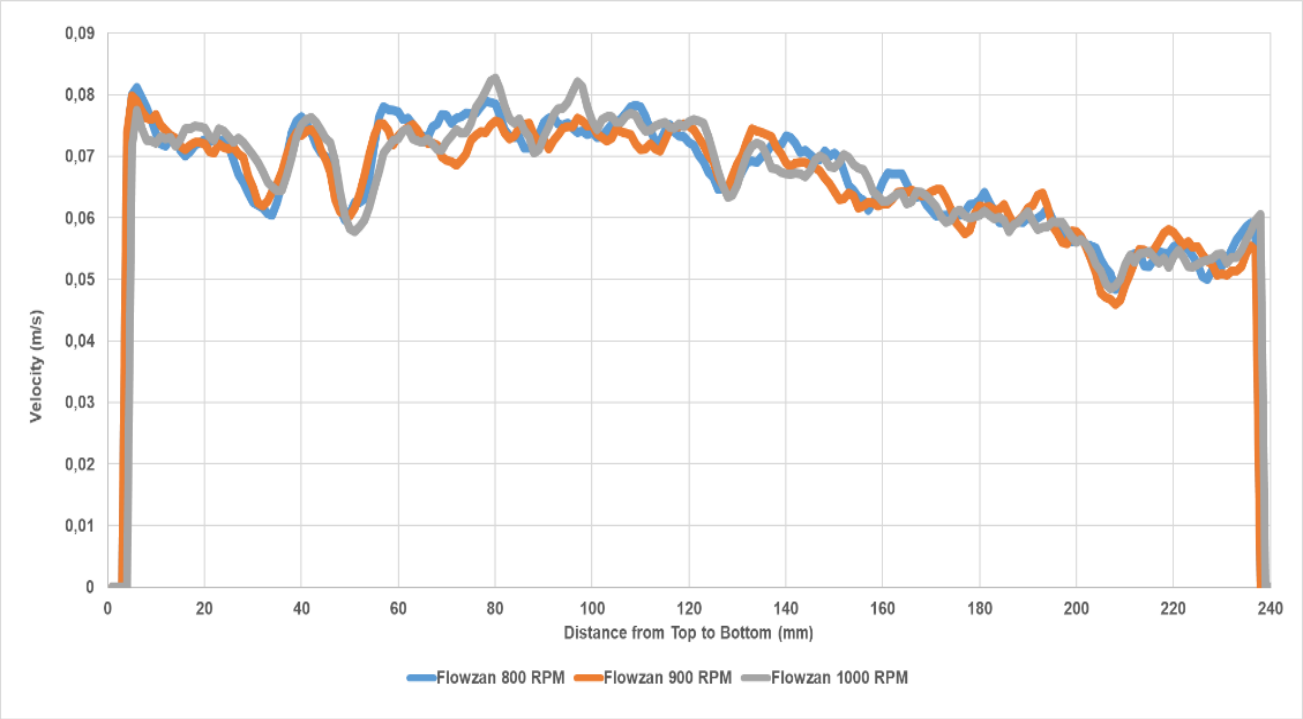

Figure 4-12: Non-Newtonian (Flowzan) fluid velocity profile on different RPMs in concentric condition

4.2.2.2 Horizontal Annulus with 30% Eccentric Condition

The graph reported in Figure 4-13 demonstrates the velocity profile of a non-Newtonian fluid measured utilizing the PIV technique on different pump RPMs from 800-1000RPM. The velocity profile reported is for horizontal annulus in 30% eccentric condition and no solids were injected. The plot shows the asymmetric flow. However, the pump RPM

shows a very low impact on fluid velocity. However, decreasing velocity due to the eccentricity effect on velocity can be observed.

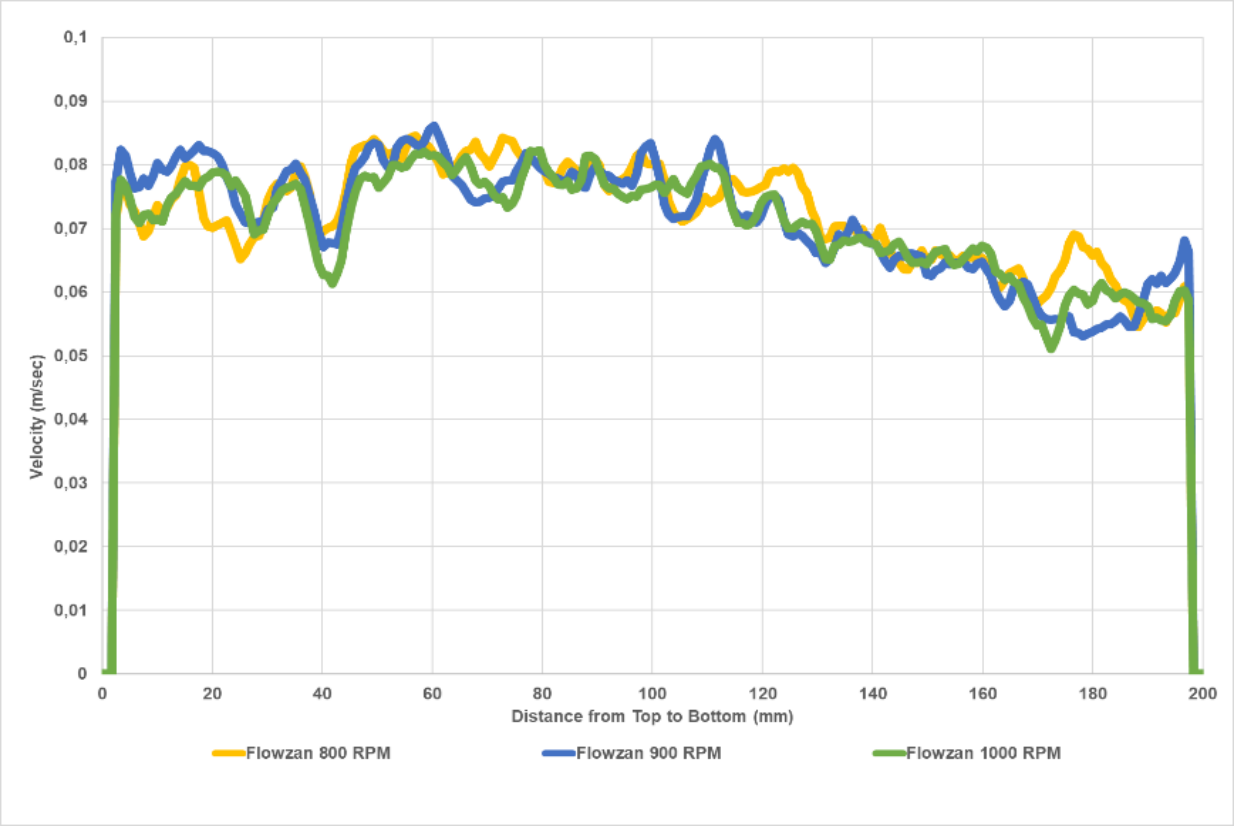

Figure 4-13: Non-Newtonian (Flowzan) fluid velocity profile on different RPMs in the horizontal annulus with 30% eccentric condition

4.2.2.3 Horizontal Annulus with 60% Eccentric Condition

The graph reported in Figure 4-14 explains the velocity profile of a non-Newtonian fluid measured utilizing the PIV technique on different pump RPMs from 800-1000RPM. The velocity profile reported is for horizontal annulus in 60% eccentric condition and no solids were injected. The plot shows the asymmetric flow. Still, the inner pipe effect can be observed in all previous velocity profiles mentioned. However, the pump RPM shows a very low impact on fluid velocity. However, the decreasing velocity due to eccentricity effect can be observed.

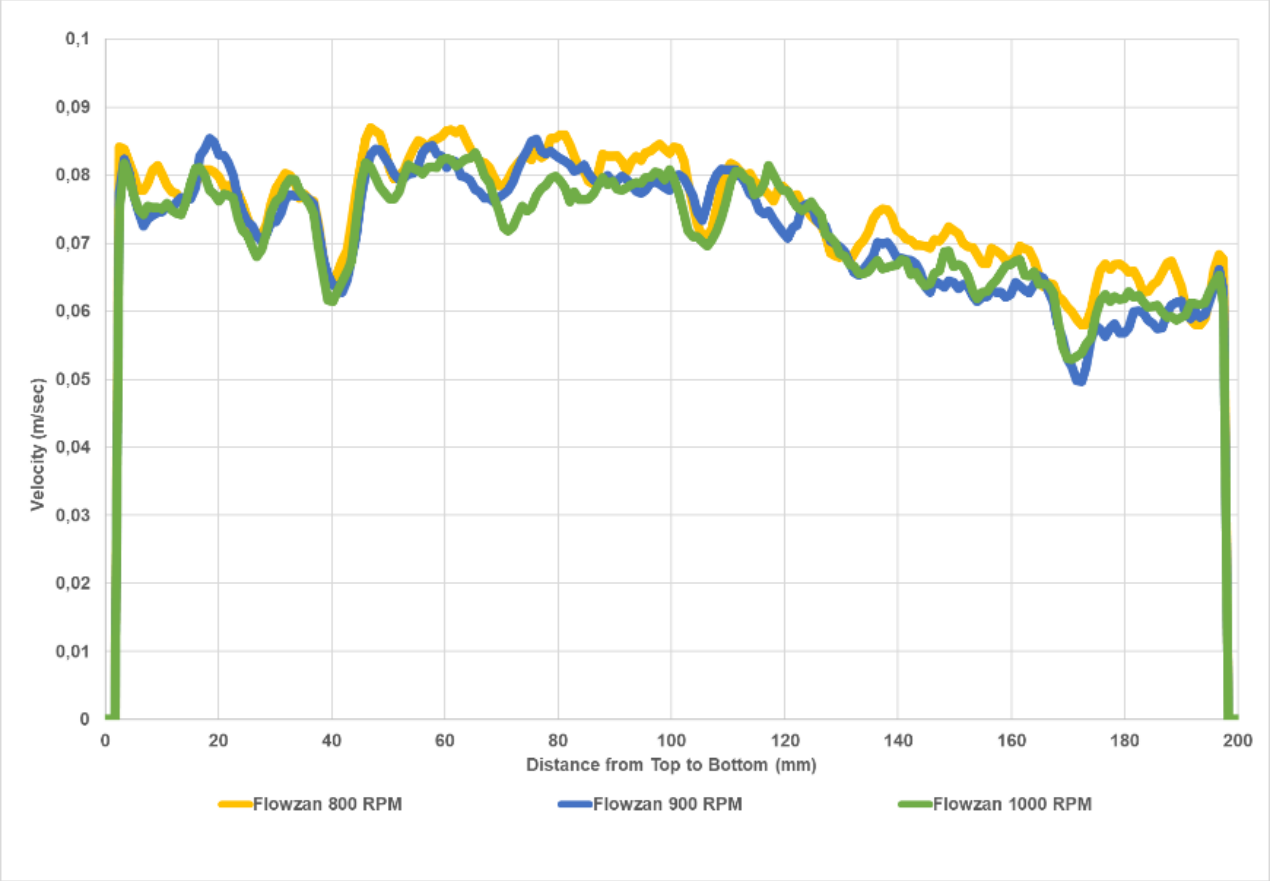

Figure 4-14: Non-Newtonian (Flowzan) fluid velocity profile on different RPMs in horizontal annulus in 60% eccentric condition

4.2.2.4 Toe-up 2.5˚ Annulus with Concentric Condition

The graph reported in Figure 4-15 illustrates the velocity profile of a non-Newtonian fluid measured utilizing the PIV technique on different pump RPMs from 800-1000 RPM. The velocity profile reported is for 2.5˚ toe-up annulus in concentric condition, and no solids were injected. The plot shows the asymmetric flow.

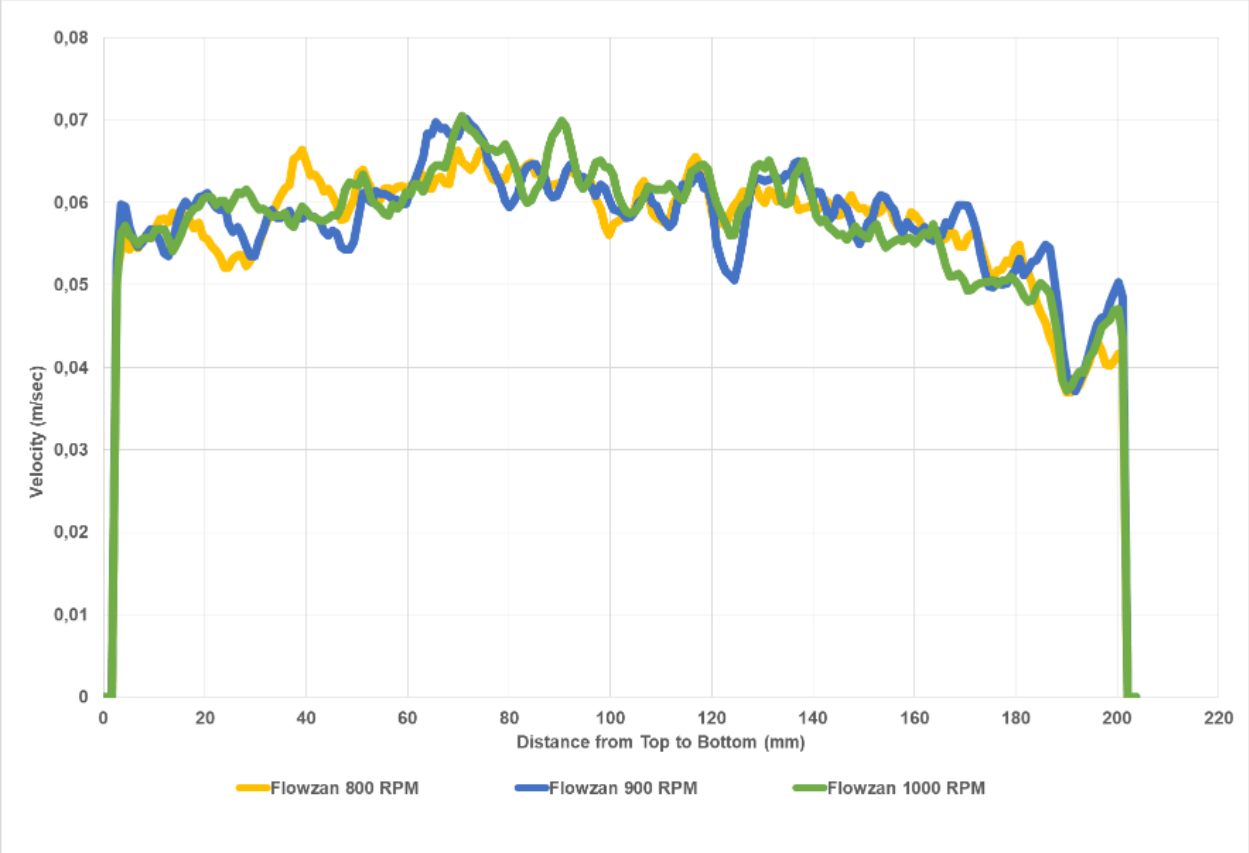

Figure 4-15: Non-Newtonian (Flowzan) fluid velocity profile on different RPMs in 2.5˚ toe-up annulus in concentric condition

4.2.2.5 Toe-up 2.5˚ Annulus with 30% Eccentric Condition

The graph reported in Figure 4-16 illustrates the velocity profile of a non-Newtonian fluid measured utilizing the PIV technique on different pump RPMs from 800-1000 RPM. The velocity profile reported is for 2.5˚ toe-up annulus in 30% eccentric condition, and no solids were injected. The plot shows the asymmetric flow.

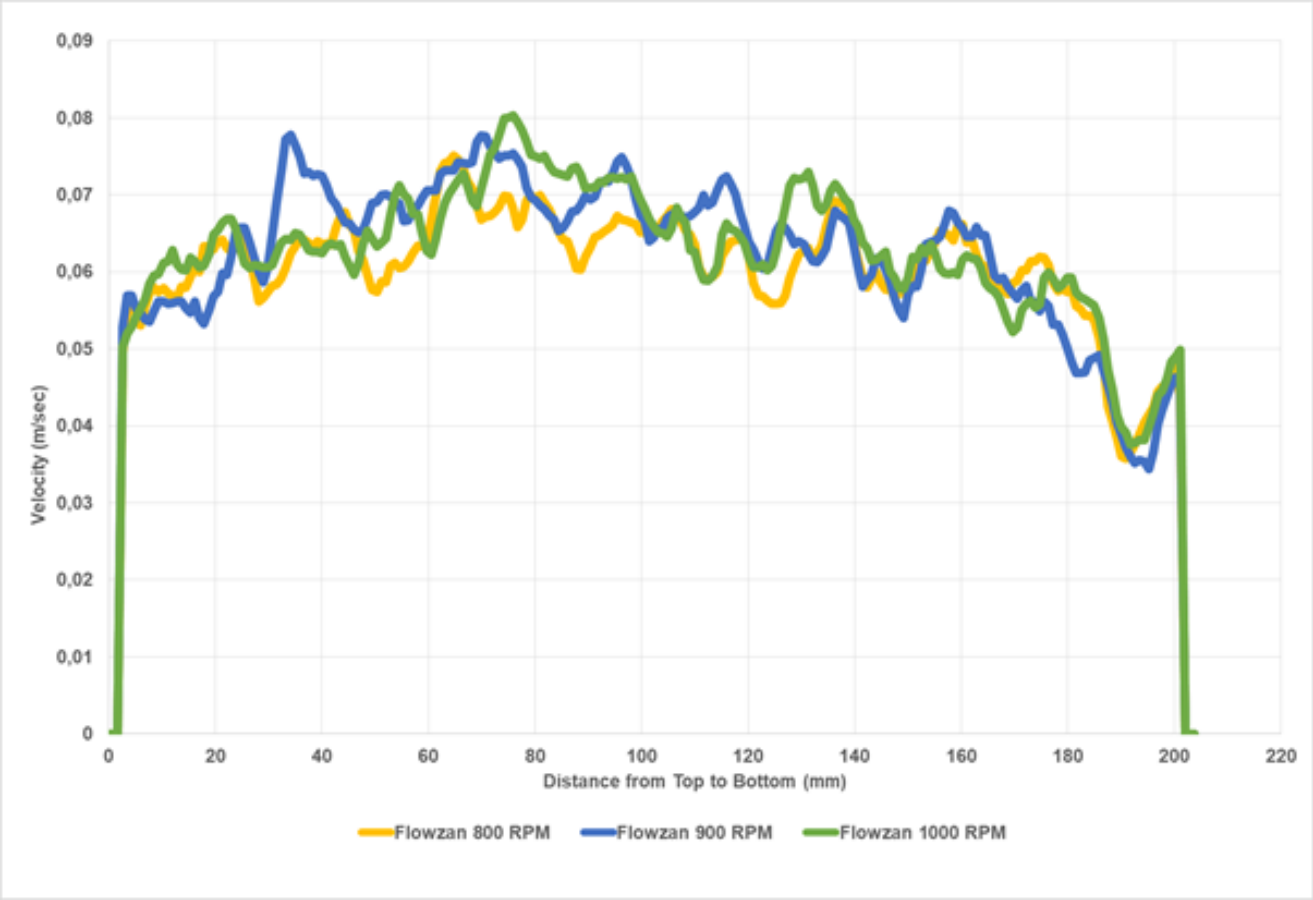

Figure 4-16: Non-Newtonian (Flowzan) fluid velocity profile on different RPMs in 2.5˚ toe-up annulus in 30% eccentric condition

4.2.2.6 Toe-up 2.5˚ Annulus with 60% Eccentric Condition

The graph reported in Figure 4-16 illustrates the velocity profile of a non-Newtonian fluid measured utilizing the PIV technique on different pump RPMs from 800-1000RPM. The velocity profile reported is for horizontal annulus in 30% eccentric condition and no solids were injected. The plot shows the asymmetric flow. Still, the inner pipe effect can be observed in all previous velocity profiles mentioned. However, the pump RPM shows a very low impact on fluid velocity. However, the eccentricity effect on velocity can be observed on the right side of the graph. Velocity tends to decrease as it moves on the right.

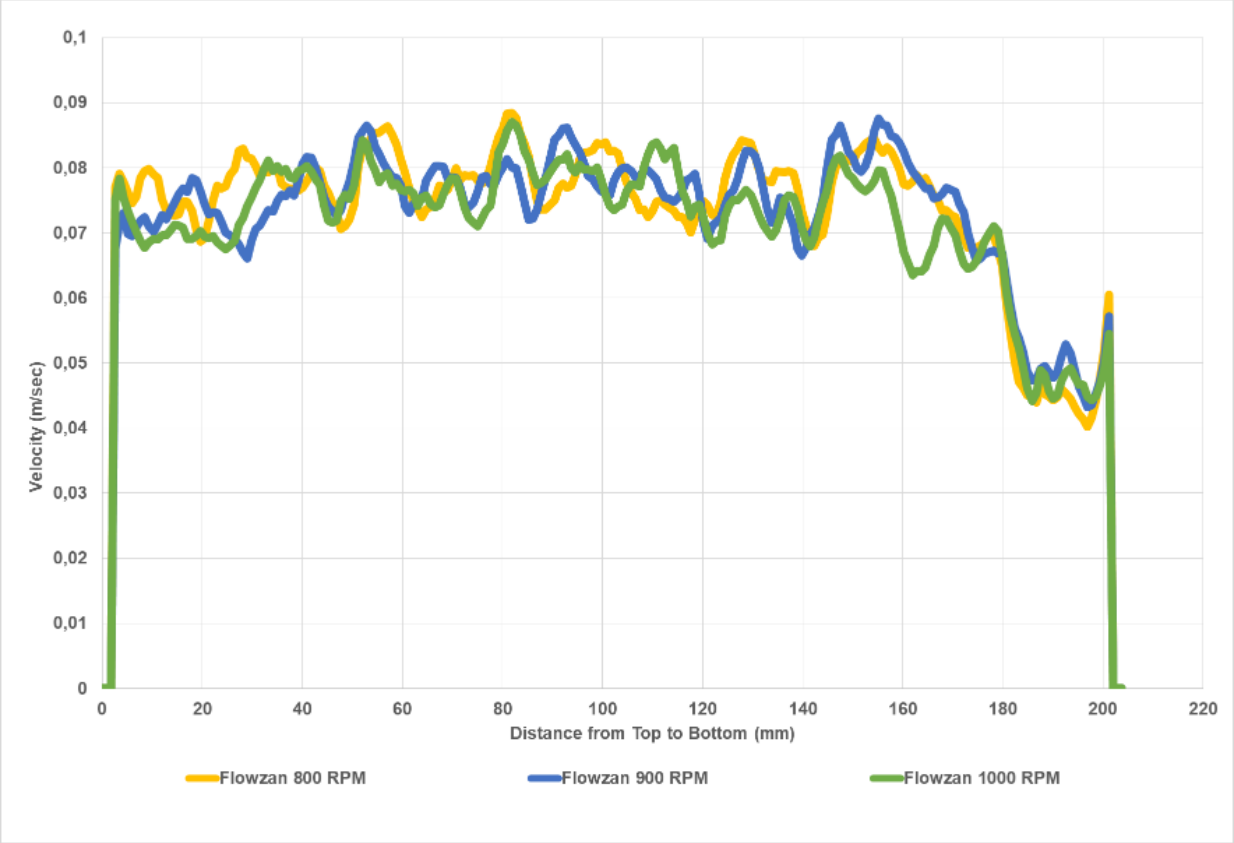

Figure 4-17: Non-Newtonian (Fowzan) fluid velocity profile in 60% eccentric condition

4.2.2.7 Toe-down 2.5˚ Annulus with Concentric Condition

Toe-down shows smooth velocity profile due to the action of gravitational force on the top of our interrogating window. As the liquid tends to move forward more quickly from the top, Figure 4-18 exhibits the same pattern while velocity reduces near the inner pipe.

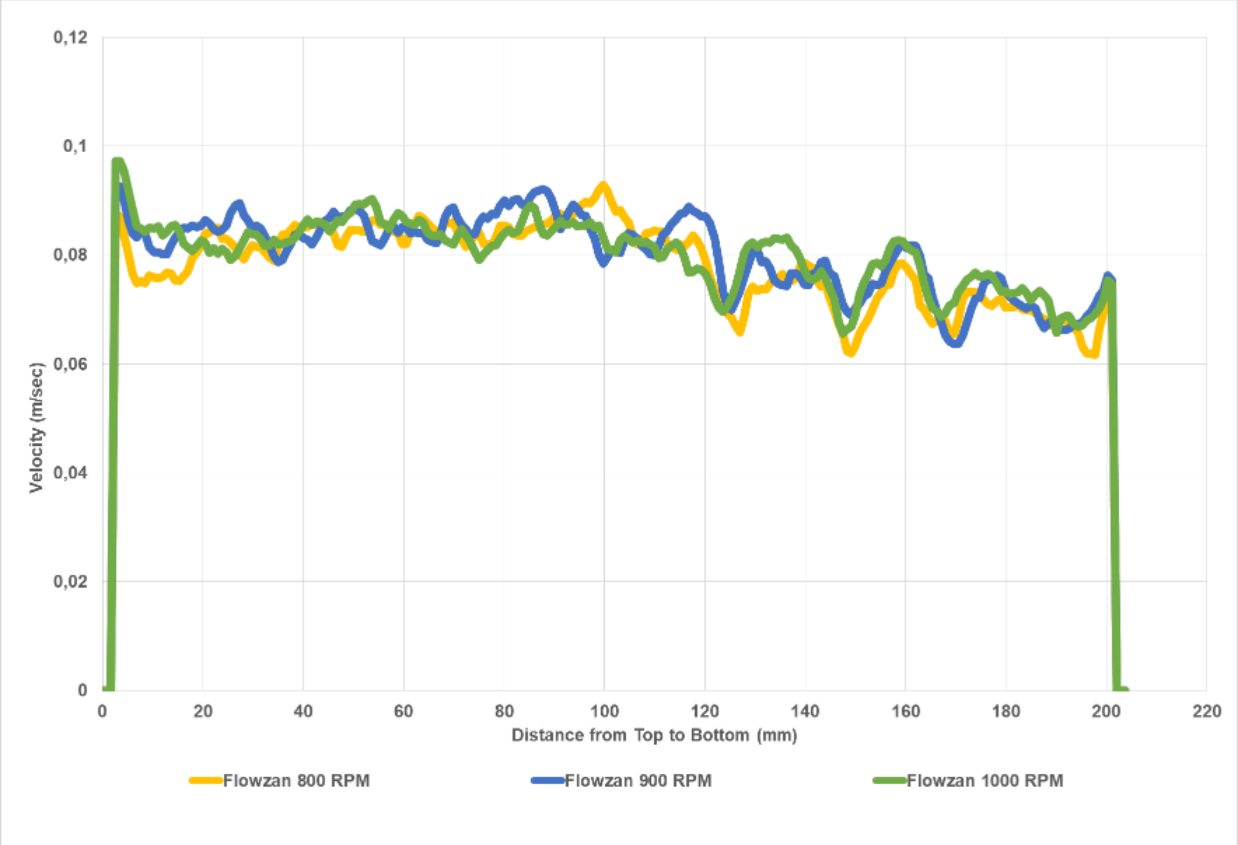

Figure 4-18: Non-Newtonian (Flowzan) fluid velocity profile on different RPMs in 2.5˚ toe-down annulus in concentric condition

4.2.2.8 Toe-down 2.5˚ Annulus with 30% Eccentric Condition

Toe-down condition and increasing the eccentricity shows the velocity drop near the drill pipe Figure 4-19, as seen in previous results as well. In Toe-down scenario, the fluorescent particle moves quickly, so the top position have less fluctuated profile.

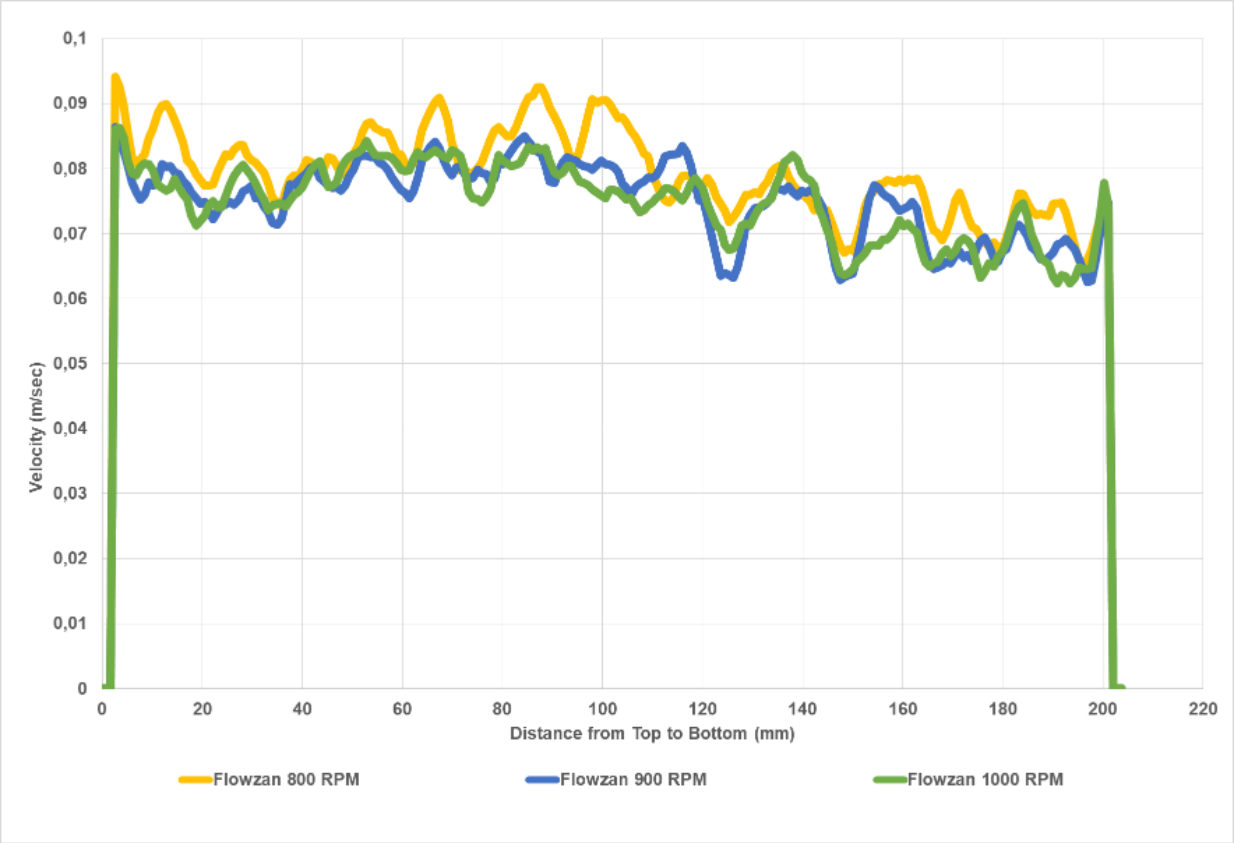

Figure 4-19: Non-Newtonian (Flowzan) fluid velocity profile on different RPMs in 2.5˚ toe-down annulus in concentric condition

4.2.2.9 Toe-down 2.5˚ Annulus with 60% Eccentric Condition

Toe-down increasing the eccentricity to 0.06 shows the velocity drop near the drill pipe Figure 4-20, as seen in previous results as well. In Toe-down scenario, the fluorescent particle moves quickly, so the top position have less fluctuated profile. We can also see the high velocity drop at the top of our inner pipe.

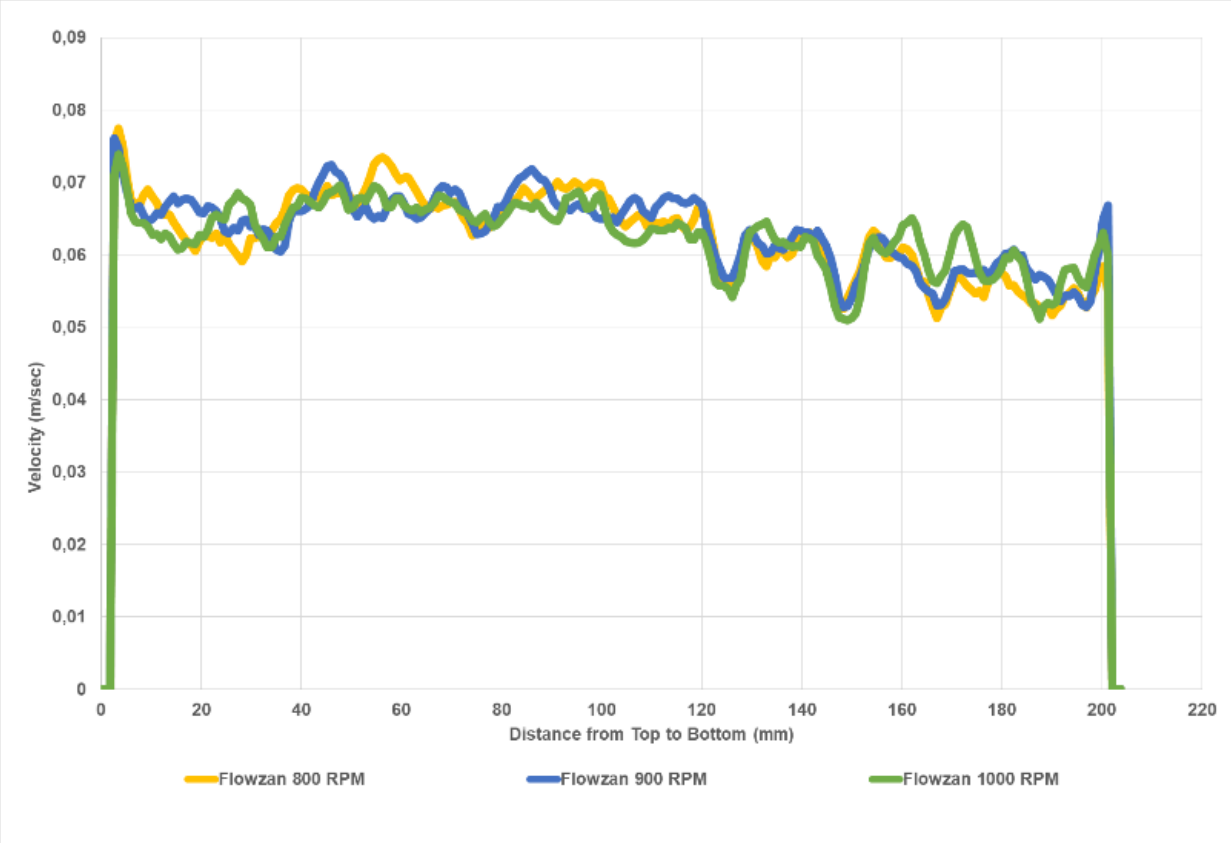

Figure 4-20: Non-Newtonian (Flowzan) fluid velocity profile on different RPMs in 2.5˚ toe-down annulus in concentric condition

4.2.3 Velocity Profiles – Comparision between Newtonian (Water) and non-Newtonian Fluid (Flowzan) in Horizontal Annulus

As reported in the core outline, our main goal was to compare both Newtonian and non-Newtonian results. This section of the chapter reports the analysis based on the observation.

4.2.3.1 Concentric Condition Comparision Only Fluids

In concentric condition, as shown in Figure 4-21 displays the significant velocity boost with less concentration of a non-Newtonian fluid. As observed the velocity drop for Newtonianv fluid near inner pipe is overcome with the non-Newtonian fluid due to its high-viscous behaviour.

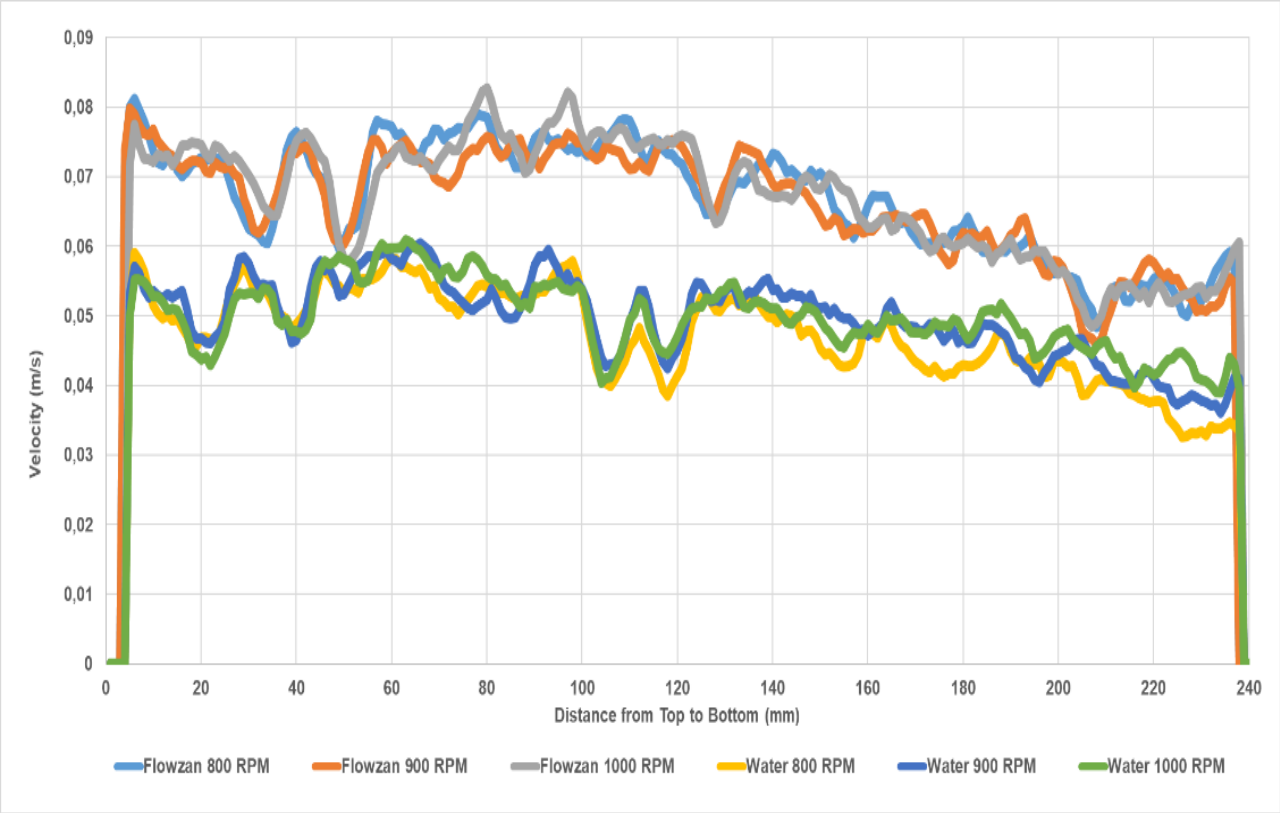

Figure 4-21: Newtonian and Non-newtonian Comparison in concentric condition

4.2.3.2 30% Eccentric Condition Comparision only Fluids

In 30% eccentric condition, as shown in Figure 4-22 displays the same significant velocity boost as in concentric position. As observed from the velocity drop for Newtonian fluid near the inner pipe is overcome with the non-Newtonian fluid due to its high-viscous behaviour.

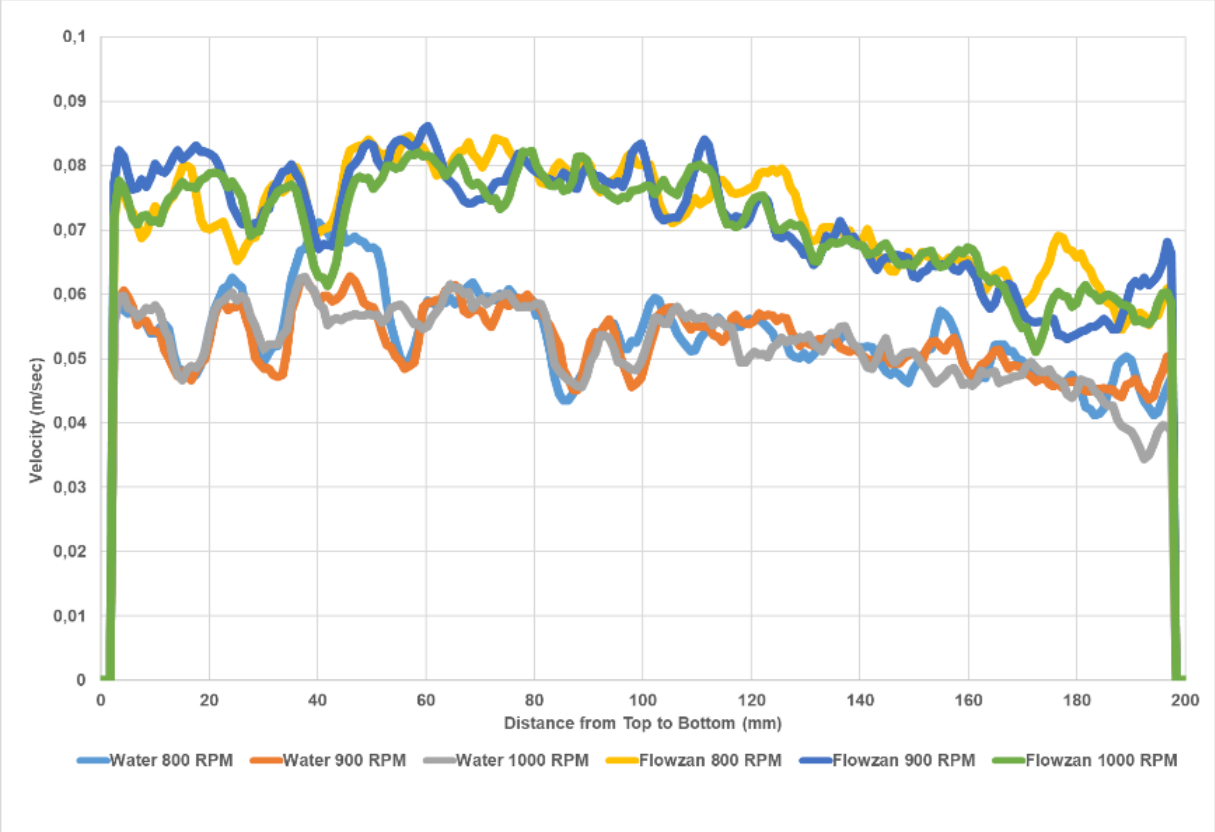

Figure 4-22: Newtonian and Non-newtonian Comparison in 30% eccentric condtion

4.2.3.3 60% Eccentric Condition Comparision only fluids

In 60% eccentric condition, as shown in Figure 4-23 displays the same significant velocity boost as in concentric and 30% eccentric position. As observed from the velocity drop for Newtonian fluid near the inner pipe is overcome with the non-Newtonian fluid due to its high-viscous behaviour.

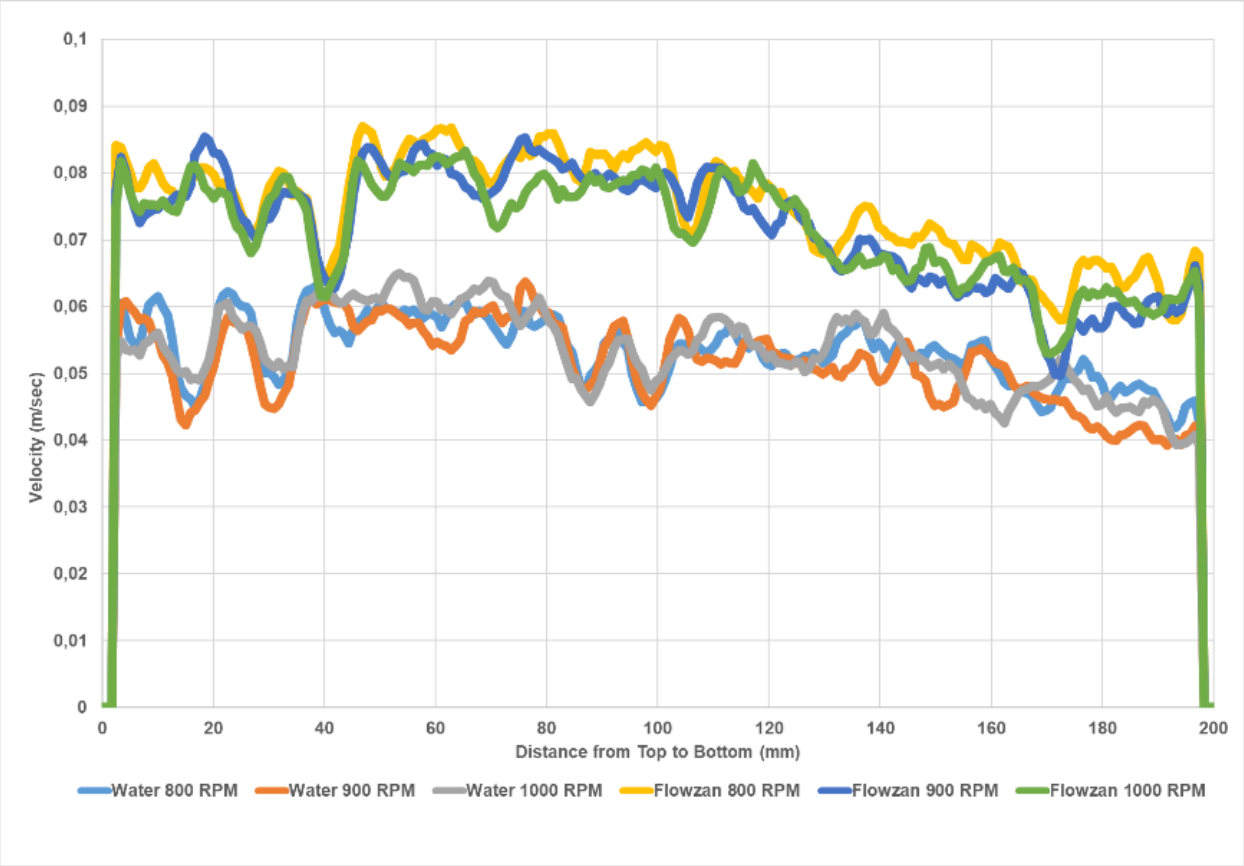

Figure 4-23: Newtonian and Non-newtonian Comparison in 60% eccentric condition

4.2.4 Velocity Profiles – Comparision between Newtonian (Water) and non-Newtonian Fluid (Flowzan) in 2.5˚ Toe-up Annulus

The comparison of both fluids in toe-up 2.5˚ annulus has been reported in this section on different drilling parameters.

4.2.4.1 Concentric Condition Comparision Only Fluids

In concentric condition, as shown in Figure 4-24: Newtonian and Non-newtonian Comparison in concentric condition displays the same significant velocity boost with the use of non-Newtonian fluid. Due to high-viscous nature of Flowzan it tends to increase the velocity of the flow in same RPM.

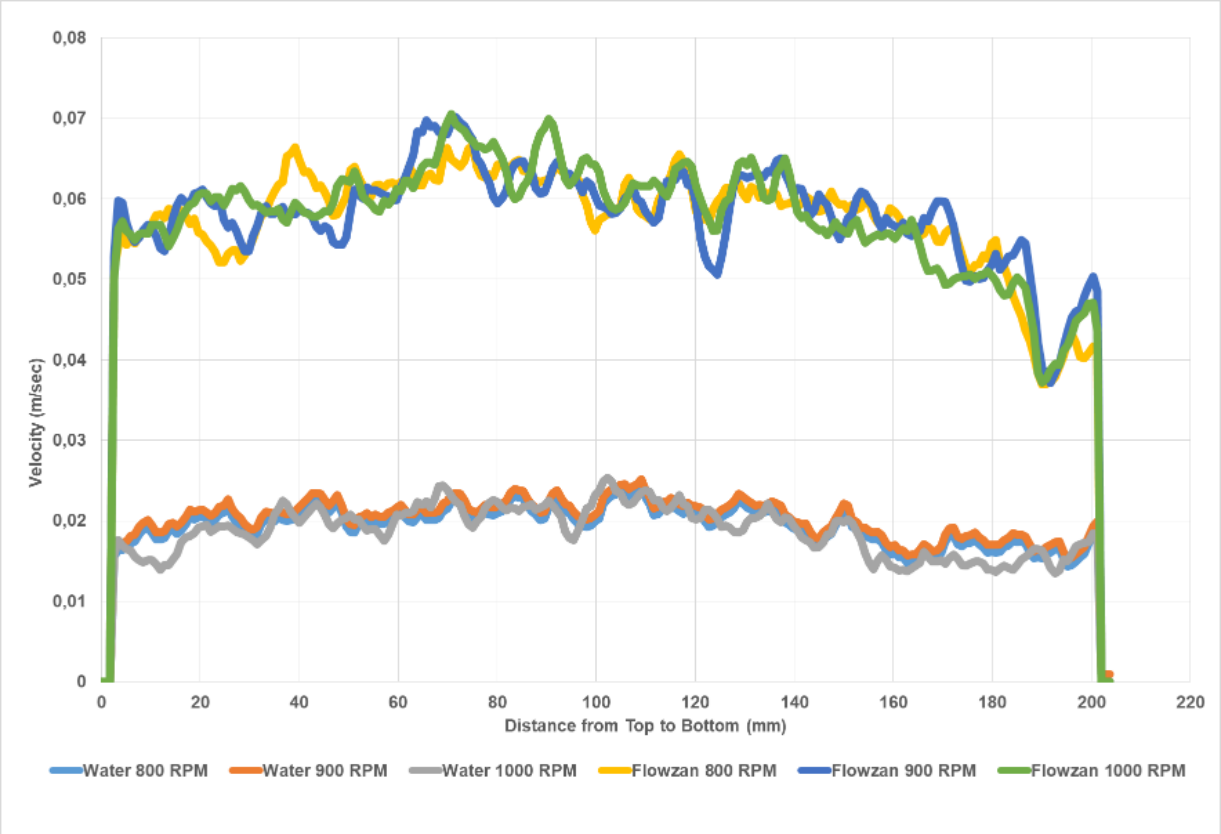

Figure 4-24: Newtonian and Non-newtonian Comparison in concentric condition

4.2.4.2 30% Eccentric Condition Comparision only Fluids

In 30% eccentric condition, as shown in Figure 4-25: Newtonian and Non-newtonian Comparison in 30% eccentric condition did not display the same significant velocity boost as in concentric position. We can observe an increase in velocity profile but it not as much as in concentric condition.

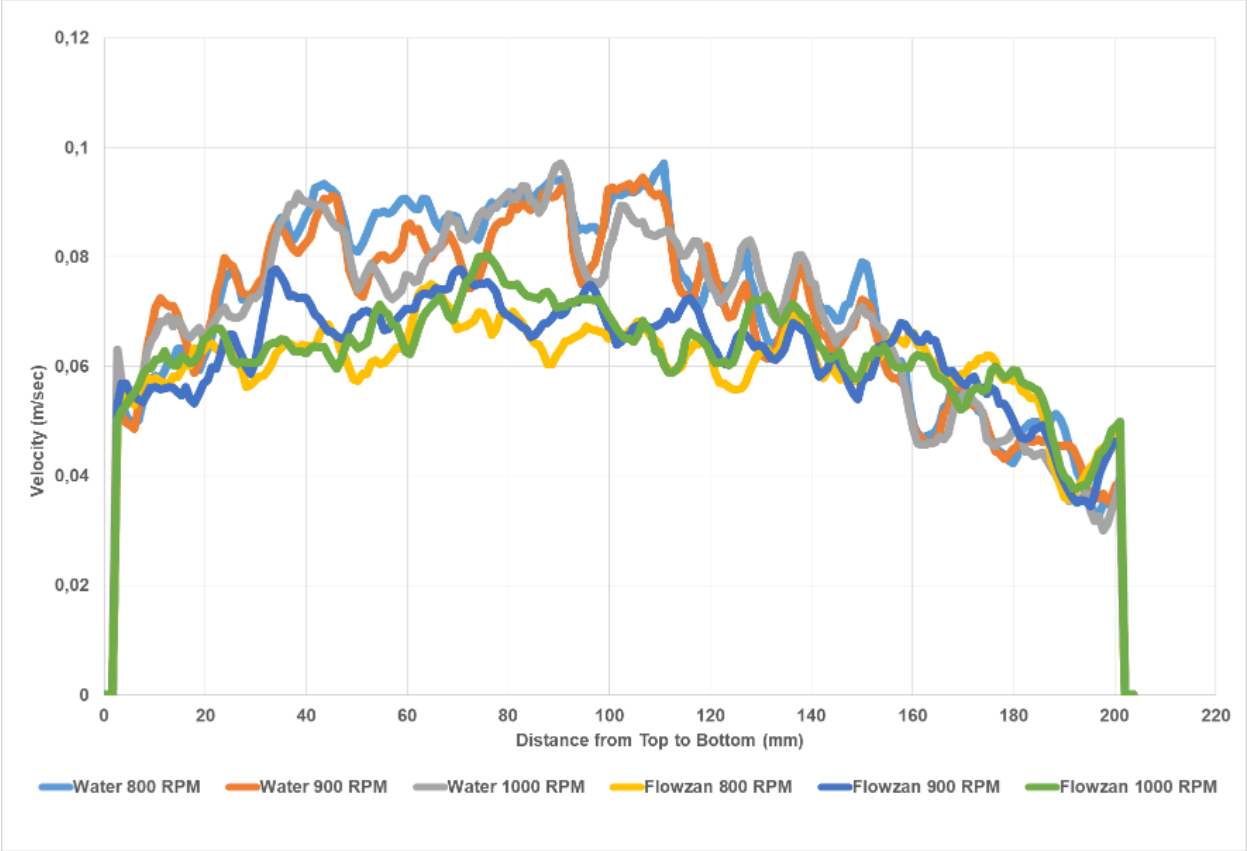

Figure 4-25: Newtonian and Non-newtonian Comparison in 30% eccentric condition

4.2.4.3 60% Eccentric Condition Comparision

In 60 % eccentric condition, as shown in Figure 4-26 displays the velocity boost as in concentric and 30% eccentric position. Non-Newtonian fluid has proved to increase the velocity profile regarding of the drilling parameters.

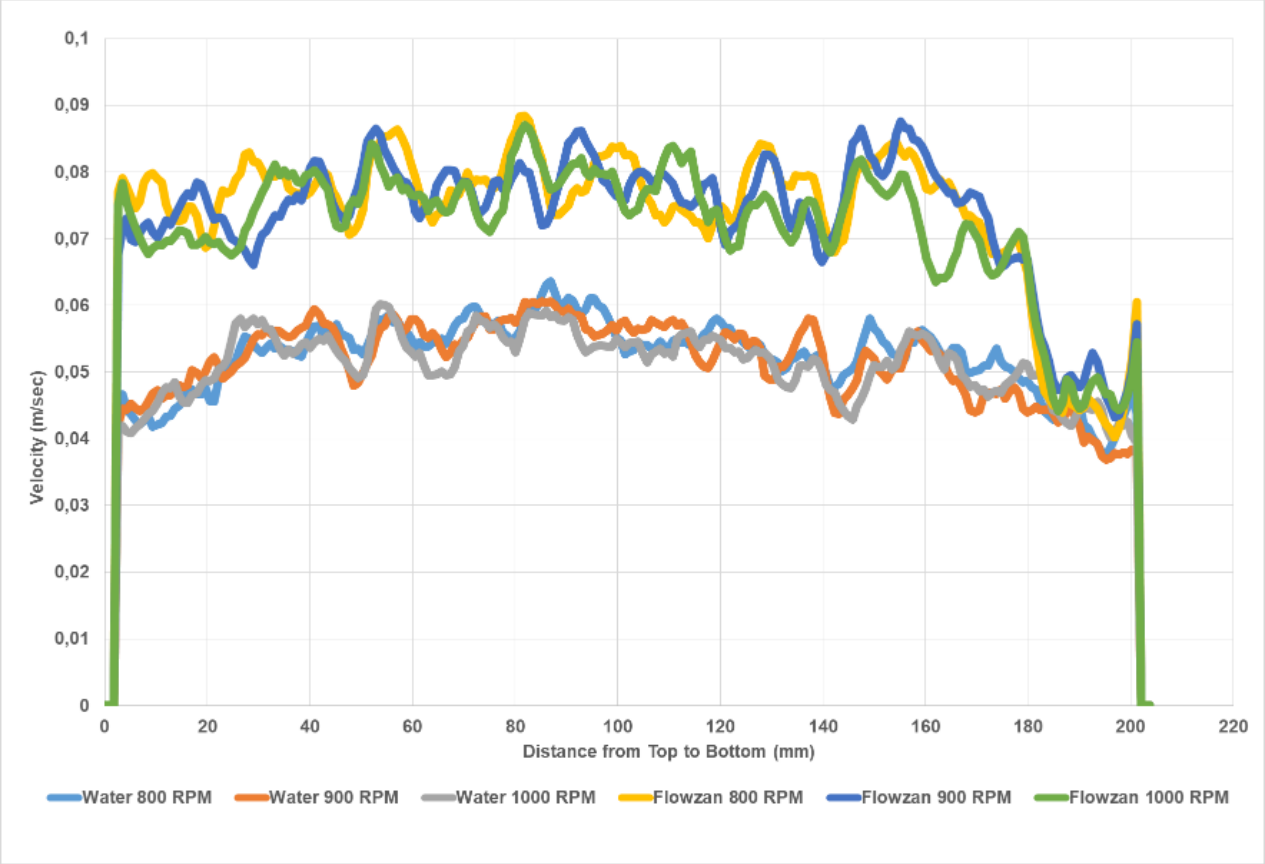

Figure 4-26: Newtonian and Non-newtonian Comparison in 60% eccentric condition

4.2.5 Velocity Profiles – Comparision between Newtonian (Water) and non-Newtonian Fluid (Flowzan) in 2.5˚ Toe-down Annulus

The comparison of both fluids in toe-up 2.5˚ annulus has been reported in this section with different drilling parameters.

4.2.5.1 Concentric Condition Comparision Only Fluids

In concentric condition, as shown in Figure 4-27 displays the reverse effect with the use of non-Newtonian fluid. The main reason was the viscous force was overcoming the gravitational flow in case of non-Newtonian fluid. Due to the high-viscous nature of Flowzan it tends to decrease the velocity of the flow in toe-down condition.

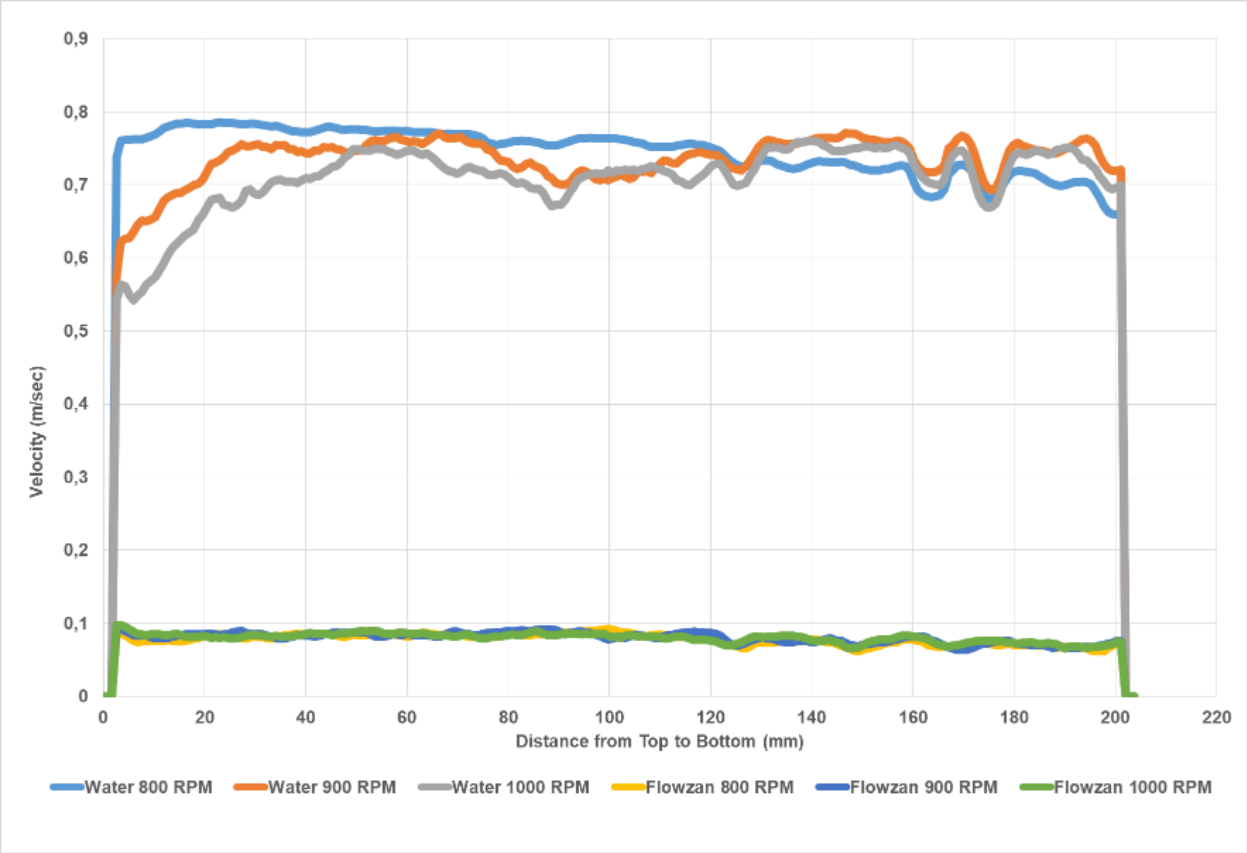

Figure 4-27: Newtonian and Non-newtonian Comparison in concentric condition

4.2.5.2 30% Eccentric Condition Comparision only Fluids

In 30% eccentric condition, as shown in Figure 4-28 displays the reverse effect with the use of non-Newtonian fluid the same as observed in concentric condition. The main reason was the viscous force was overcoming the gravitational flow in case of non-Newtonian fluid. Due to the high-viscous nature of Flowzan it tends to decrease the velocity of the flow in toe-down condition.

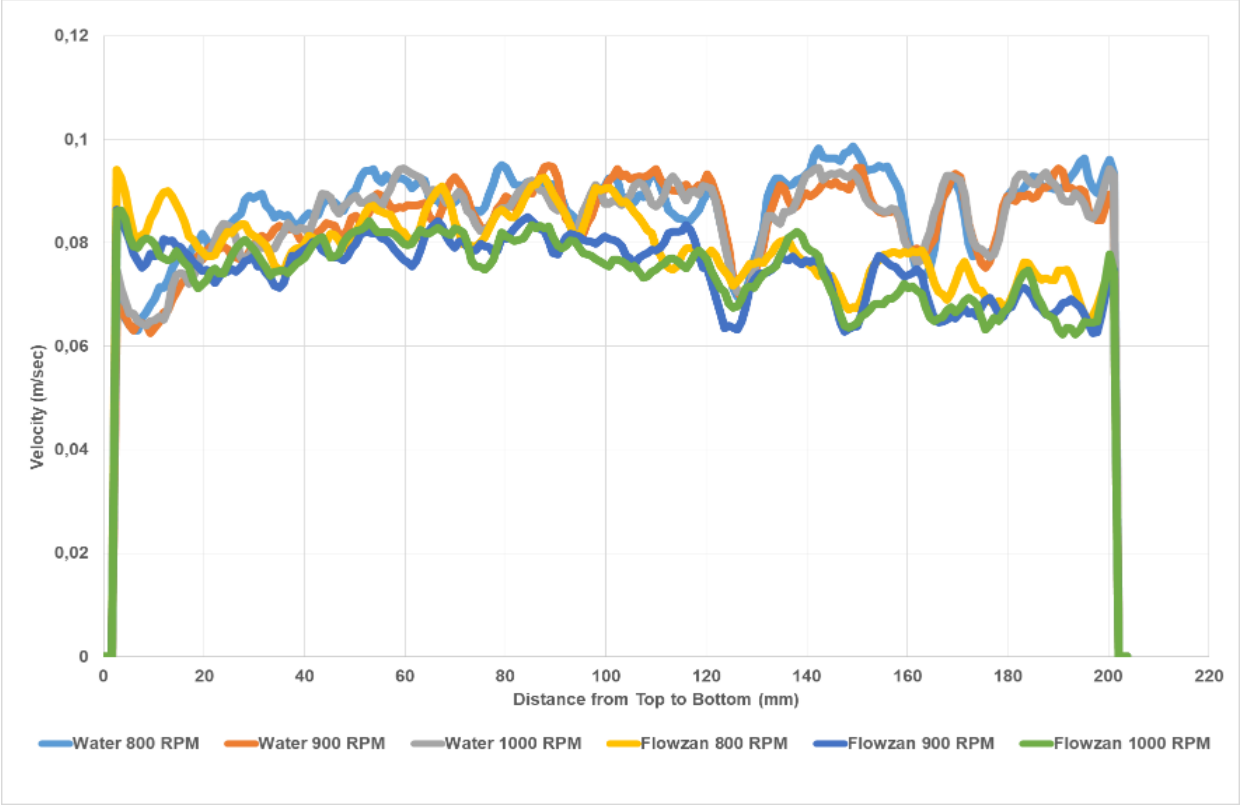

Figure 4-28: Newtonian and Non-newtonian Comparison in 30% eccentric condition

4.2.5.3 60% Eccentric Condition Comparision only Fluids

In 60% eccentric condition, as shown in Figure 4-29 displays the reverse effect with the use of non-Newtonian fluid the same as observed in concentric and 30% eccentric condition. The main reason was the viscous force was overcoming the gravitational flow in case of non-Newtonian fluid. Due to the high-viscous nature of Flowzan it tends to decrease the velocity of the flow in toe-down condition.

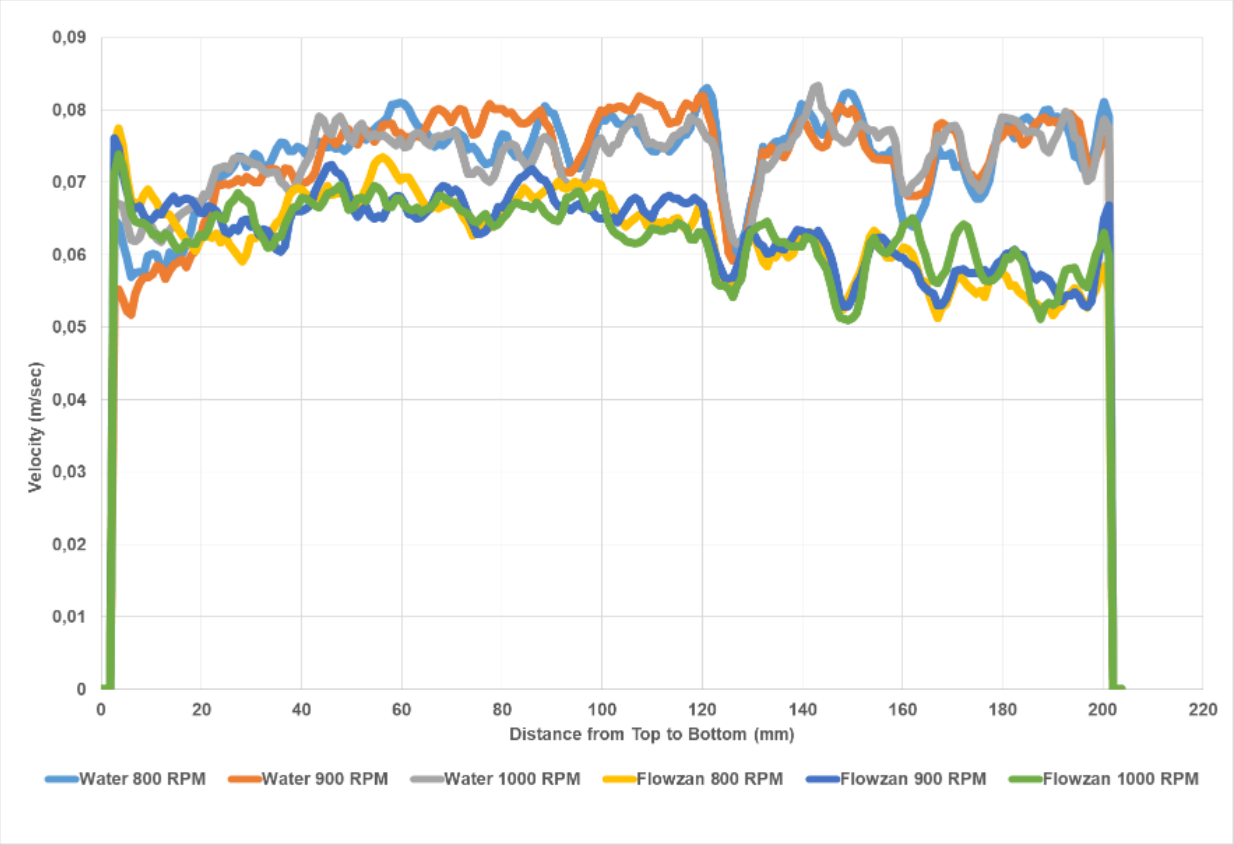

Figure 4-29: Newtonian and Non-newtonian Comparison in 60% eccentric condition

4.3 Velocity Profiles Non-Newtonian Fluid (Flowzan) + Solid Comparision – Horizontal and Inclination

The flow of solid with liquid refers to two-phase fluid flow. The observation was carried out through the PIV system. The plotted figure represents the impact of the solid cutting transport on the fluid.

4.3.1 Concentric Condition - 800 RPM

The critical velocity of our system was at 500 RPM. Running flow loop system on 500 RPM results in the stationary bed formation. The graph Figure 4-30 shows that at 2.5˚ and 5˚ velocity seems to be increased. This can be due to the uplift force and rolling of the particles.

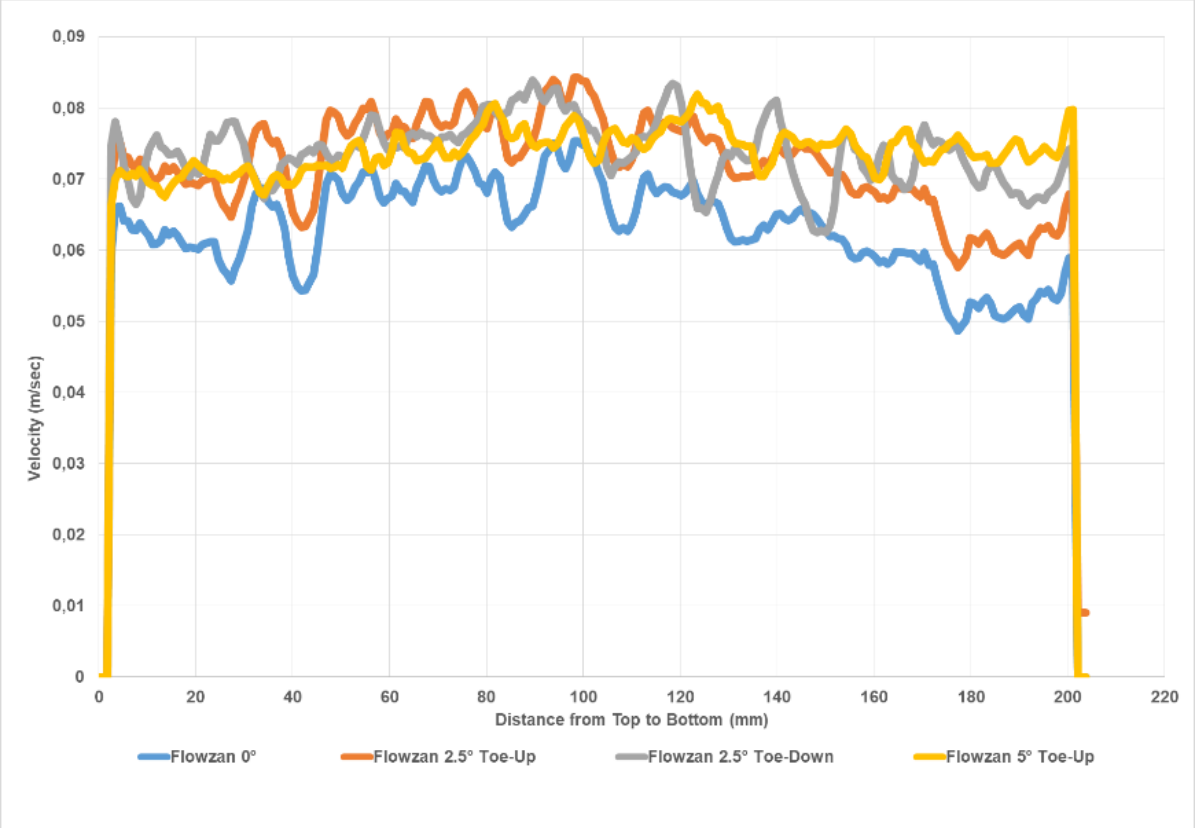

Figure 4-30: Newtonian and Non-newtonian Comparison in concentric condition

4.3.2 30% Eccentric Condition - 800 RPM

The critical velocity of our system was at 500 RPM. Running flow loop system on 500 RPM results in the stationary bed formation. The graph Figure 4-31 shows that at 5˚ velocity seems to be high. In eccentric condition, the beds tend to straighten and providing uplift of the particle from the back, and as result velocity is increased.

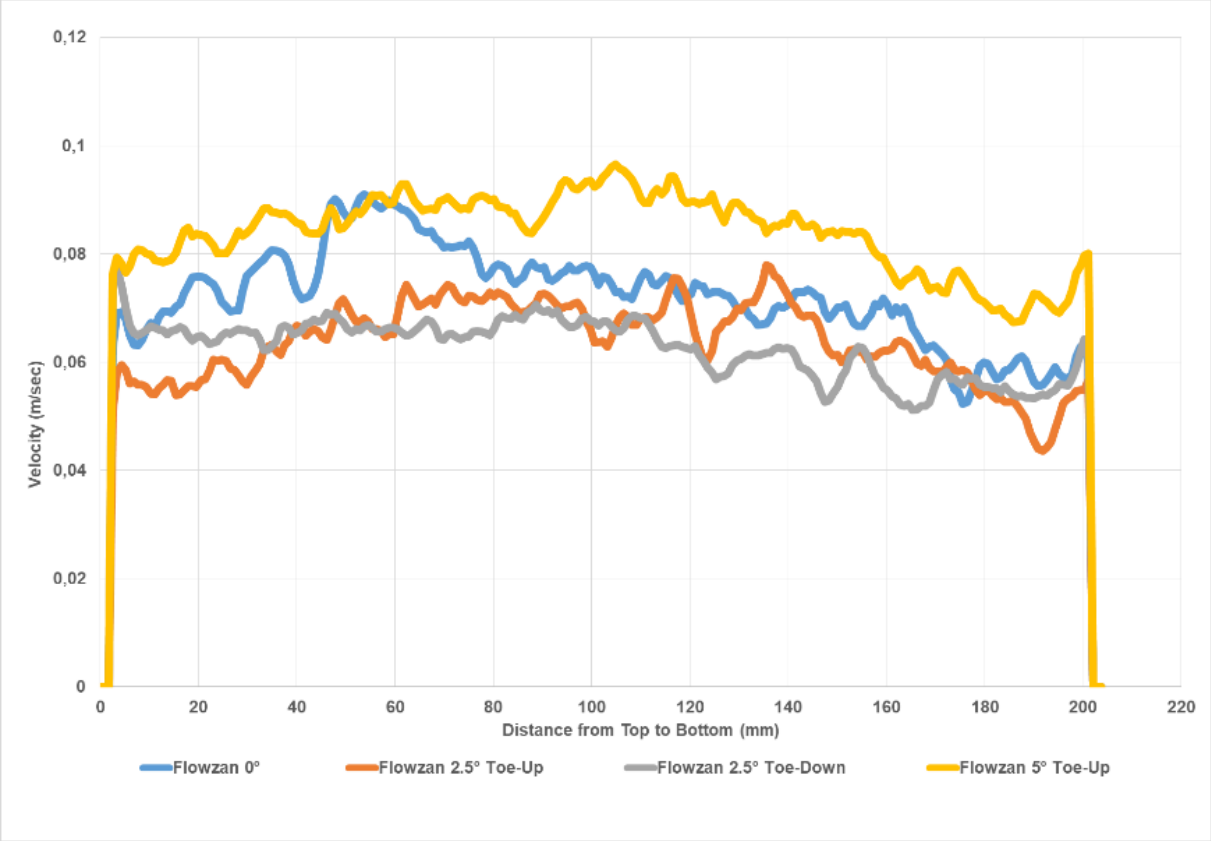

Figure 4-31: Newtonian and Non-newtonian Comparison in 30% eccentric condition

4.3.3 60% Eccentric Condition - 800 RPM

The graph Figure 4-32 shows that with the increase in angle in toe-up condition from the horizontal the velocity tends to increase in 60% eccentric condition. The more the eccentric condition, the beds tend to straighten and providing uplift of the particle from the back, and as result velocity is increased.

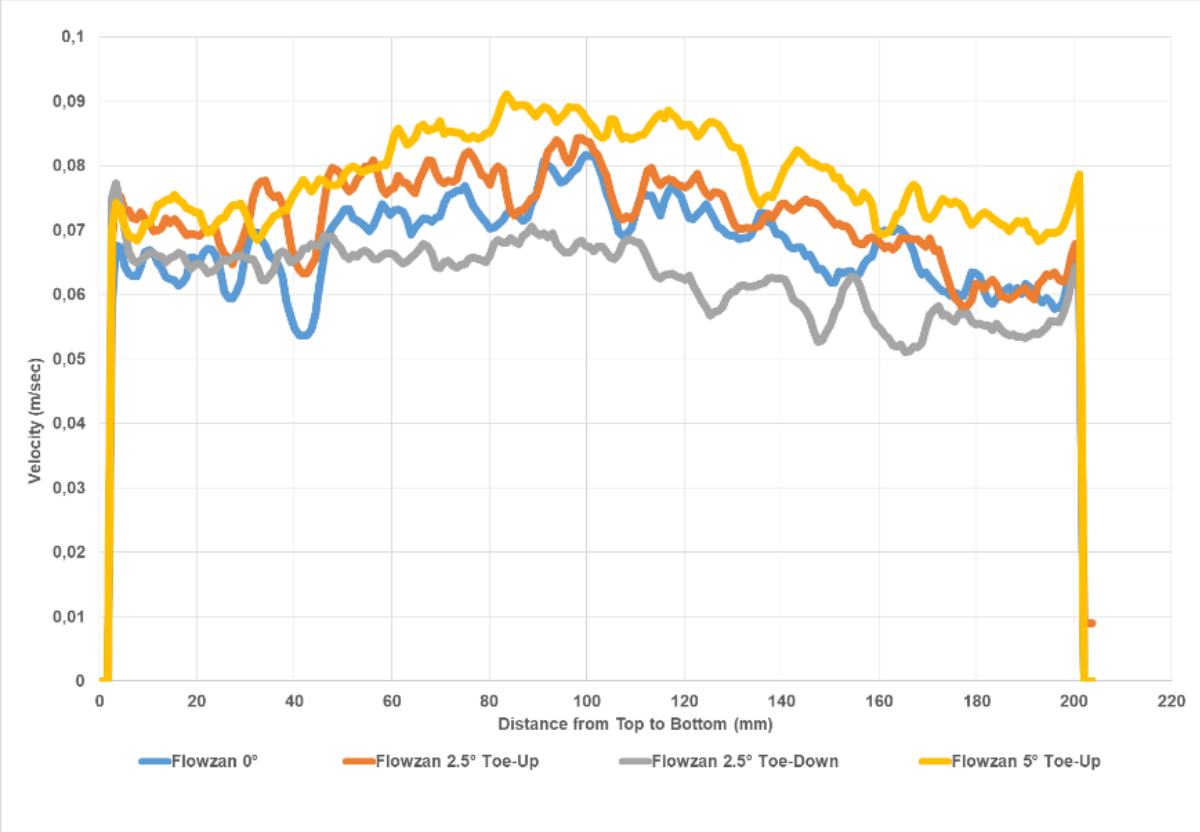

Figure 4-32: Newtonian and Non-newtonian Comparison in 60% eccentric condition

4.3.4 Concentric Condition - 900 RPM

For 900 RPM and concentric condition, the flow of solid cuttings is faster as compared to 800 RPM. With the increase in RPM, the solids movement from in the direction flow tends to increase. With the increase in toe-down inclination, the solid beds move fast due to gravitational force, and we observe high velocities. However, as compared to toe-up inclination, the viscous force overcomes the gravitation flow. It tends the flow of solid beds slower, and as a result, velocity decline is observed as illustrated in Figure 4-33.

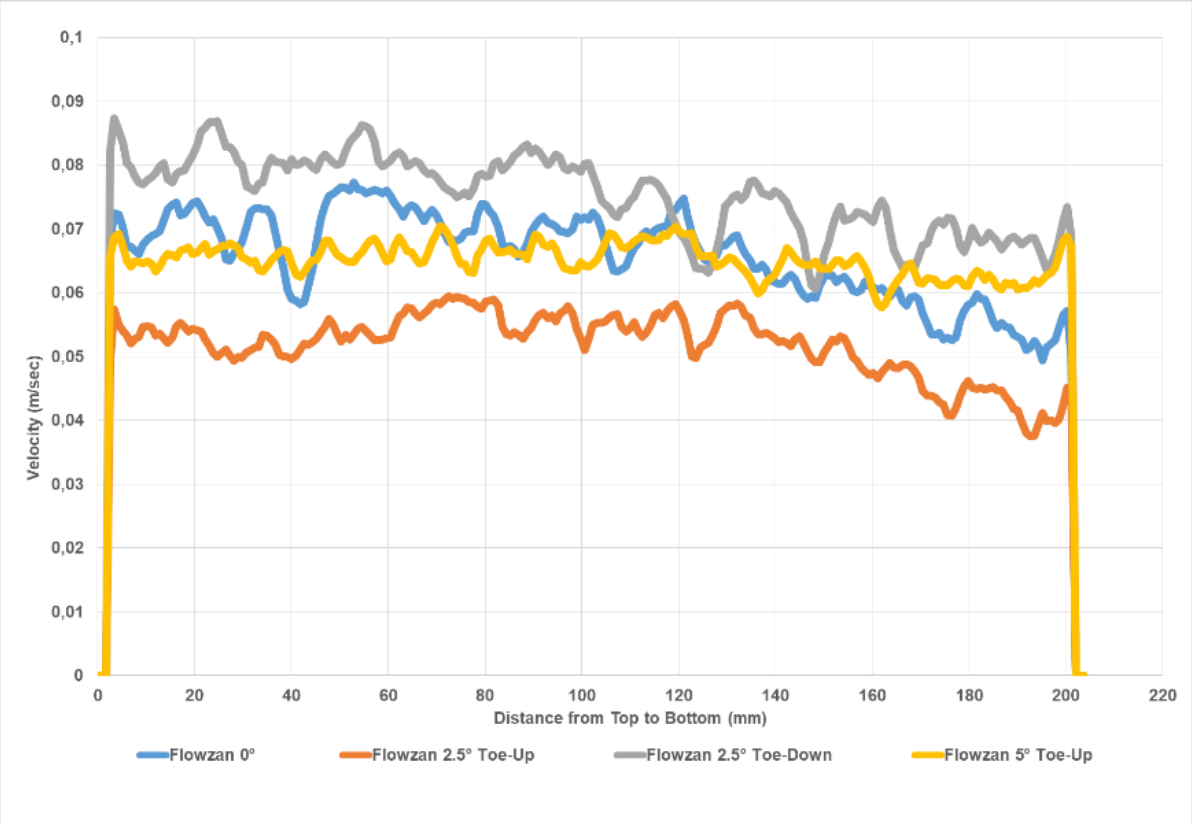

Figure 4-33: Newtonian and Non-newtonian Comparison in concentric condition

4.3.5 30% Eccentric Condition - 900 RPM

For 900 RPM and 30% eccentric condition, the flow of solid cuttings is faster as compared to 800 RPM. With the increase in RPM, the movement of the solid in the direction flow tends to increase. With the increase in toe-down inclination, the solid beds move fast due to gravitational force, and we observe high velocities. However, as compared to toe-up inclination, the viscous force overcomes the gravitation flow. It tends the flow of solid beds slower, and as a result, velocity decline is observed as illustrated in Figure 4-34. The more inclination in toe-up condition with eccentricity, the more straight bed will form and it requires more velocity to uplift the solid particles. As a consequence, the backflow of fluid will start to occur, and high velocity was observed in the 5˚ inclination.

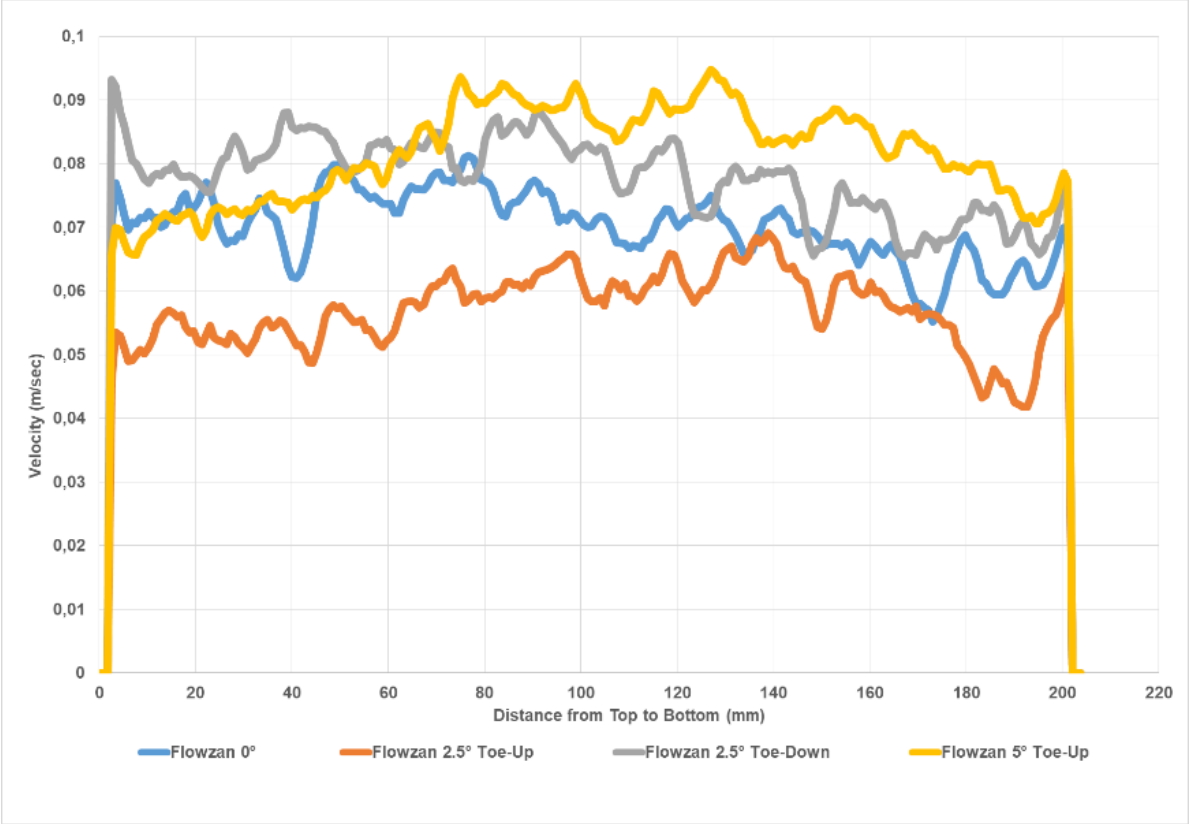

Figure 4-34: Newtonian and Non-newtonian Comparison in 30% eccentric condition

4.3.6 60% Eccentric Condition - 900 RPM

For 900 RPM and 60% eccentric condition, the flow of solid cuttings is faster as compared to 800 RPM in 60% eccentric condition. With the increase in RPM, the movement of the solid in the direction flow tends to increase, but at the same time, straight bed tends to form. The more inclination we increase, the more solid beds will form. We can observe in Figure 4-35 at 5˚ toe-up inclination, due to solid bed formation, we see a decrease in velocity on the bottom of the annulus. With the increase in toe-down inclination, the solid beds move fast due to gravitational force, and we observe high velocities.

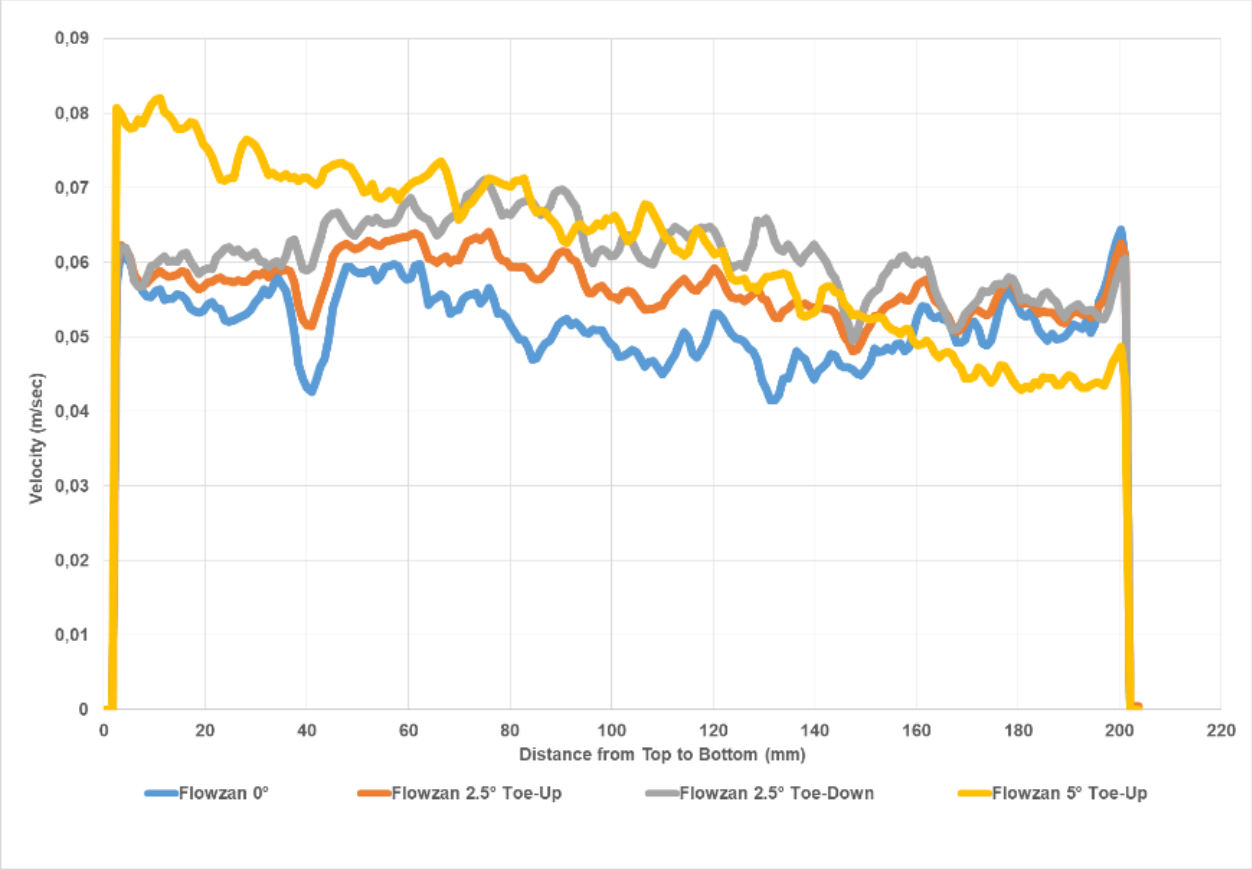

Figure 4-35: Newtonian and Non-newtonian Comparison in 60% eccentric condition

4.3.7 Concentric Condition - 1000 RPM

The solid cutting behaviour, as shown in Figure 4-36 shows the higher velocities in toe-down condition because of the gravitational force. However, in toe-up condition, we see high velocities in 5˚ as compared to 2.5˚ due to the little backflow of particles.

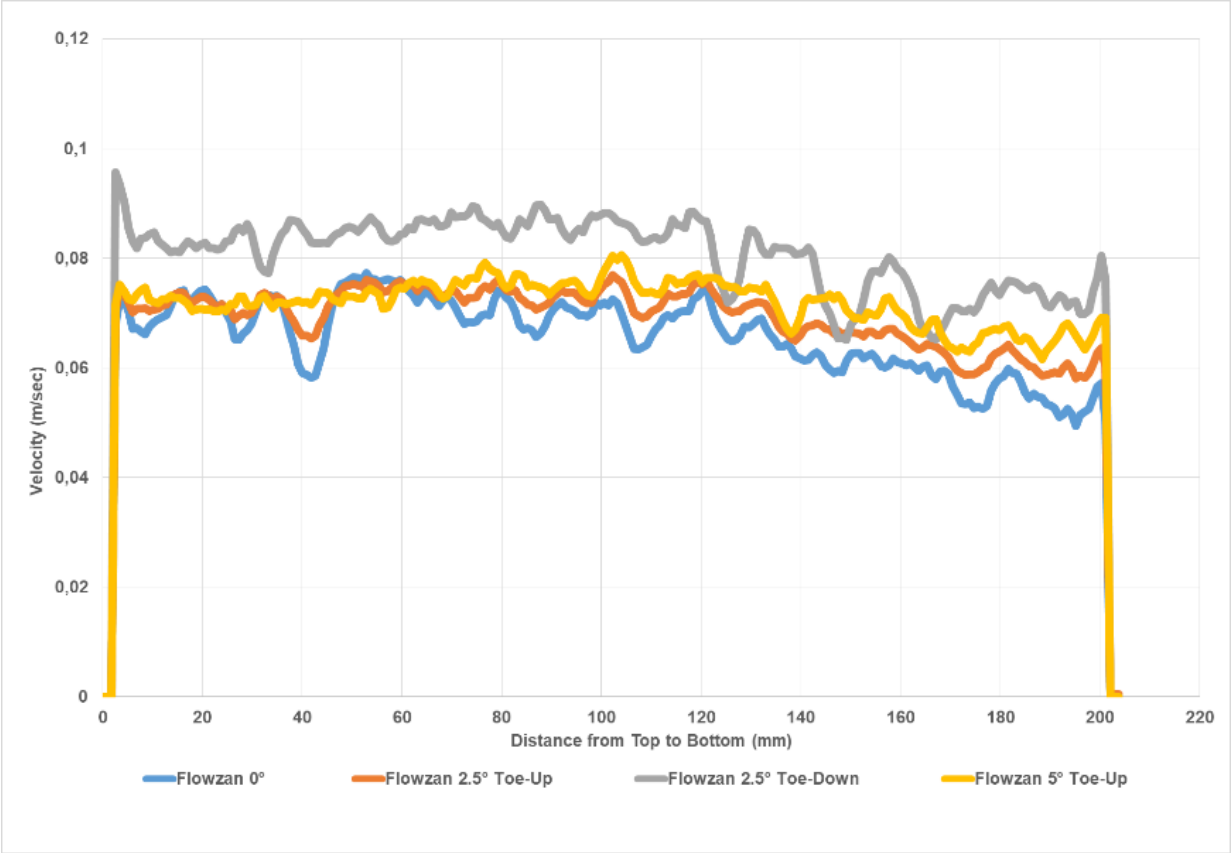

Figure 4-36: Newtonian and Non-newtonian Comparison in concentric condition

4.3.8 30% Eccentric Condition - 1000 RPM

As investigated in Figure 4-37 in 30% eccentric condition, we see a solid bed formation. However, due to high RPM, solid bed accumulation does not produce much effect on the velocity profile. Although, we can see a velocity decline as compared to the concentric condition as compared with the eccentric condition because the eccentricity produced a bed accumulation with less effect on velocities.

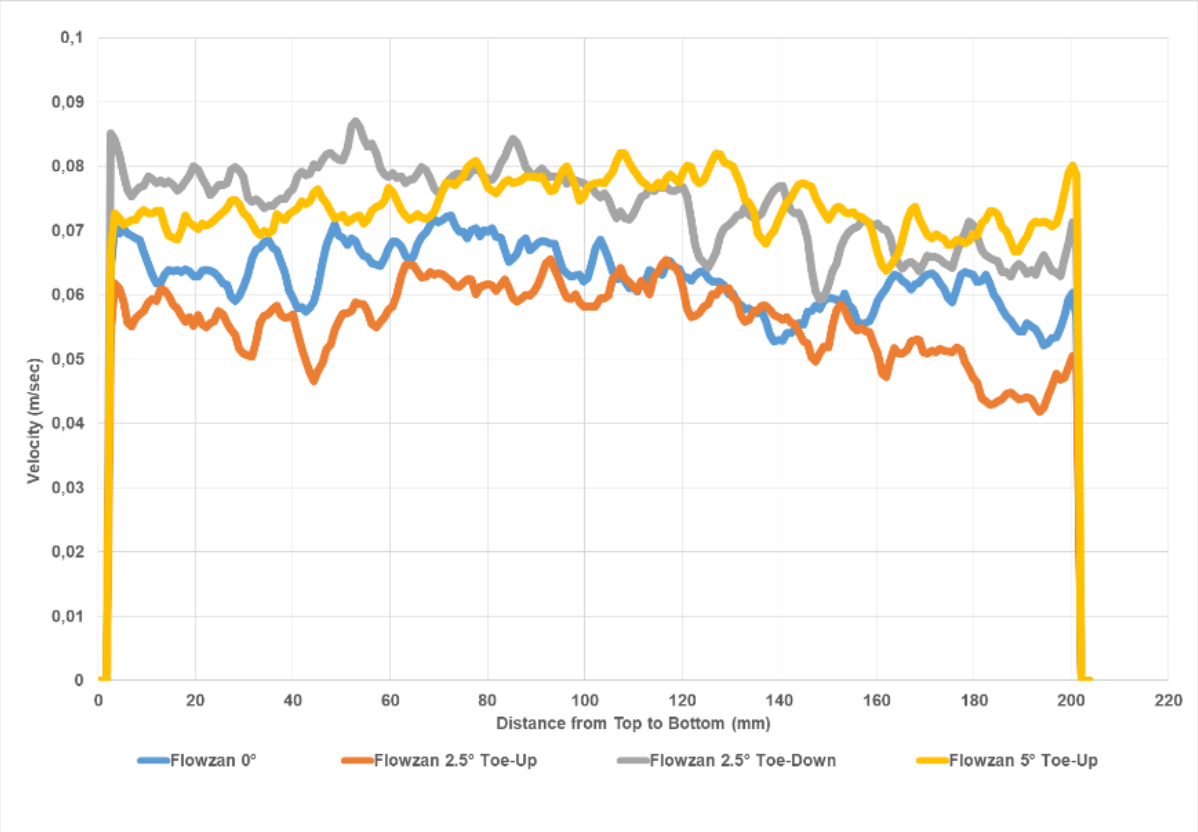

Figure 4-37: Newtonian and Non-newtonian Comparison in 30% eccentric condition

4.3.9 60% Eccentric Condition - 1000 RPM

For 1000 RPM and 60% eccentric condition, the flow of solid cuttings is faster as compared in 60% eccentric condition on the bottom of the annulus. With the increase in RPM, the movement of the solids in the direction of the flow tends to increase. The solid movement tends to increase from the back of the dune, and as a result at the bottom of the annulus, high velocities are observed in the case of toe-up inclination. The case is vice versa in toe-up inclination since the additional gravitational force acts, so the solid bed movement is fast. At the same time, the velocities on the top of the annulus are faster than the velocity at the solid cuttings area as displayed in Figure 4-38.

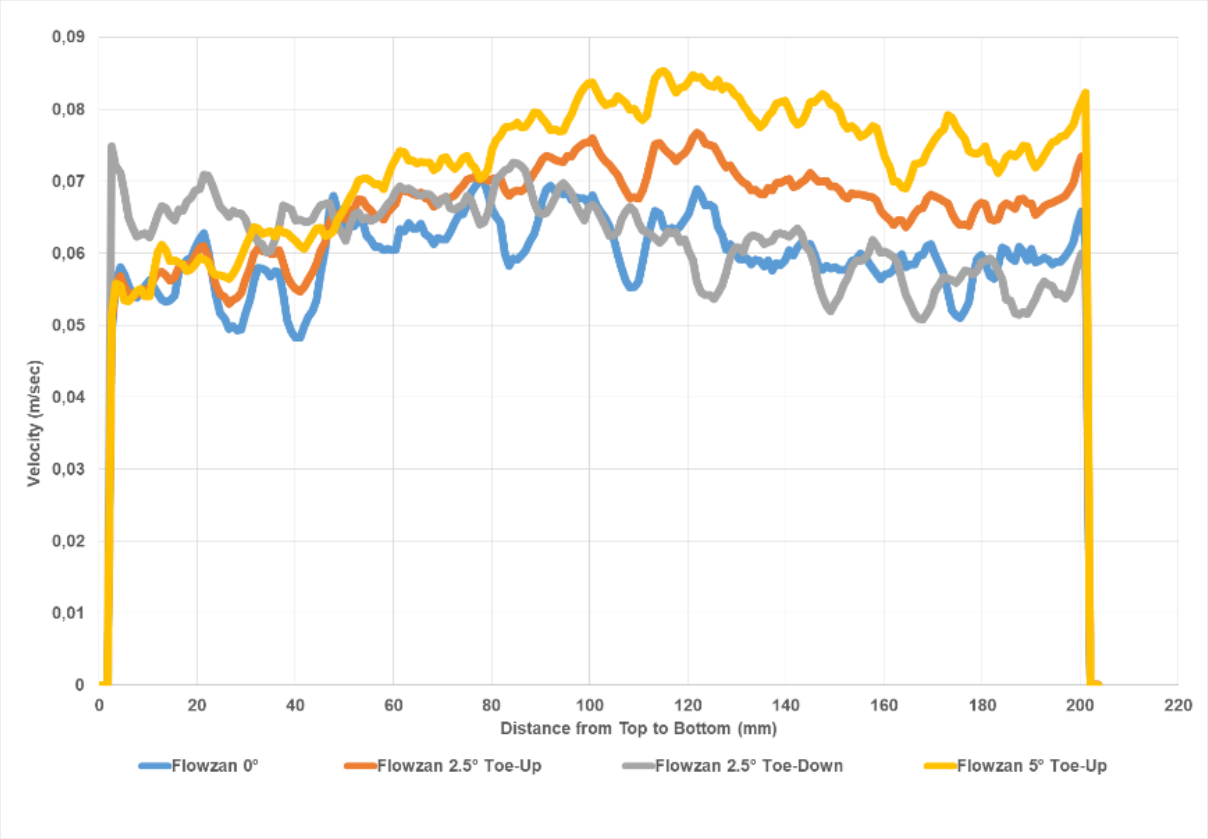

Figure 4-38: Newtonian and Non-newtonian Comparison in 60% eccentric condition

Chapter 5 Conclusion and Recommendations

5.1 Conclusion

The main aim of this research thesis was to find the velocity profiles of Newtonian and non-Newtonian fluids and their impact on solid cutting transport with different drilling parameters with the help of Particle Image Velocimetry technique. A set of experiments were carried out, and a vast collection of data was collected with varying parameters, for example, change in flow rates, inclination angle and inner pipe position. During this investigation, the results were significant:

- Varying flow rate, eccentricity, inclination, and comparing them with the same fluid does not possess considerable velocity change.
- Varying flow rate and comparison of Newtonian fluid and non-Newtonian possess considerable velocity change. The velocity of non-Newtonian velocity was found to be higher than Newtonian fluid due to its shear-thinning behaviour.
- Different eccentricity and comparison of Newtonian fluid and non-Newtonian possess considerable velocity change. In both, 30% and 60% eccentricity the cutting transport was faster than Newtonian fluid. The reason for the fast transport was the high-viscous behaviour of the polymer.
- Gravitational forces possess an important role in the transport of solid cuttings concerning inclination. The solid cuttings transport was fast in toe-down condition as compared to toe-up because of the drag forces, viscous forces and gravitational forces.
- PIV provided enough information about fluid flow in the annulus and a better option to describe the single-phase and dual-phase fluid flow.
- The flow pattern factors reported were on behalf of personal visualisation and recorded images during the experiment.
- In this particular flow loop system, the critical velocity was found to be at 500 RPM. This is the point at which the flowrate was not supporting the bed movement, and a stationary bed was forming.

5.2 Recommendations

To better understand the solid cutting behaviour, the change of non-Newtonian fluid or by changing the concentration of the same polymer may provide additional help to study the behaviour.

This thesis was based one property of solid bead. Changing the diameter and its properties would give more indication on the cutting transport behaviour and its effect.

The inner pipe rotation was not observed due to the malfunctioning of the inner pipe motor. However, analysing the inner pipe rotation effect will provide more scope of the investigation.

These studies are based on experimental work. It would be interesting to compare them with the CFD or modelling.

References

[1] S. K. Arnipally, M. M. Hirpa, M. Bizhani, and E. Kuru, "Effect of particle size on the near wall turbulence characteristics and the critical velocity required for the particle removal from the sand bed deposited in horizontal pipelines," presented at the 11th North American Conference on Multiphase Production Technology, Banff, Canada, 2018/12/10/, 2018. [Online].

[2] T. Nazari, G. Hareland, and J. J. Azar, "Review of Cuttings Transport in Directional Well Drilling: Systematic Approach," presented at the SPE Western Regional Meeting, Anaheim, California, USA, 2010/1/1/, 2010. [Online]. Available: https://doi.org/10.2118/132372-MS.

[3] J. Li and B. Luft, "Overview of Solids Transport Studies and Applications in Oil and Gas Industry - Experimental Work," presented at the SPE Russian Oil and Gas Exploration & Production Technical Conference and Exhibition, Moscow, Russia, 2014/10/14/, 2014. [Online]. Available: https://doi.org/10.2118/171285-MS.

[4] J. Li and B. Luft, "Overview Solids Transport Study and Application in Oil-Gas Industry-Theoretical Work," presented at the International Petroleum Technology Conference, Kuala Lumpur, Malaysia, 2014/12/10/, 2014. [Online]. Available: https://doi.org/10.2523/IPTC-17832-MS.

[5] M. Naegel, E. Pradie, T. Delahaye, C. Mabile, and G. Roussiaux, "Cuttings Flow Meters Monitor Hole Cleaning in Extended Reach Wells," presented at the European Petroleum Conference, The Hague, Netherlands, 1998/1/1/, 1998. [Online]. Available: https://doi.org/10.2118/50677-MS.

[6] P. H. Tomren, A. W. Iyoho, and J. J. Azar, "Experimental Study of Cuttings Transport in Directional Wells," *SPE-12123-PA,* vol. 1, no. 01, pp. 43-56, 1986/2/1/ 1986, doi: 10.2118/12123-PA.

[7] S. Okrajni and J. J. Azar, "The Effects of Mud Rheology on Annular Hole Cleaning in Directional Wells," *SPE-12123-PA,* vol. 1, no. 04, pp. 297-308, 1986/8/1/ 1986, doi: 10.2118/14178-PA.

[8] D. Nguyen and S. S. Rahman, "A Three-Layer Hydraulic Program for Effective Cuttings Transport and Hole Cleaning in Highly Deviated and Horizontal Wells,"

presented at the SPE/IADC Asia Pacific Drilling Technology, Kuala Lumpur, Malaysia, 1996/1/1/, 1996. [Online]. Available: https://doi.org/10.2118/36383-MS.

[9] M. M. Hirpa, S. K. Arnipally, M. Bizhani, E. Kuru, G. Gelves, and I. Al-Rafia, "Effect of Particle Size and Surface Properties on the Sandbed Erosion with Water Flow in a Horizontal Pipe," *SPE-199875-PA,* vol. Preprint, no. Preprint, p. 17, 2020/1/1/ 2020, doi: 10.2118/199875-PA.

[10] M. Duan, S. Z. Miska, M. Yu, N. E. Takach, R. M. Ahmed, and C. M. Zettner, "Transport of Small Cuttings in Extended-Reach Drilling," *SPE-104192-PA,* vol. 23, no. 03, pp. 258-265, 2008/9/1/ 2008, doi: 10.2118/104192-PA.

[11] F. T. Pinho and J. H. Whitelaw, "Flow of non-newtonian fluids in a pipe," *Journal of Non-Newtonian Fluid Mechanics,* vol. 34, no. 2, pp. 129-144, 1990/01/01/ 1990, doi: https://doi.org/10.1016/0377-0257(90)80015-R.

[12] A. Japper-Jaafar, M. P. Escudier, and R. J. Poole, "Laminar, transitional and turbulent annular flow of drag-reducing polymer solutions," *Journal of Non-Newtonian Fluid Mechanics,* vol. 165, no. 19, pp. 1357-1372, 2010/10/01/ 2010, doi: https://doi.org/10.1016/j.jnnfm.2010.07.001.

[13] B. Aadnøy, "Technology Focus: Multilateral/Extended-Reach Wells," *SPE-0516-0079-JPT,* vol. 68, no. 05, pp. 79-79, 2016/5/1/ 2016, doi: 10.2118/0516-0079-JPT.

[14] "Extended reach wells." https://petrowiki.org/Extended_reach_wells (accessed.

[15] G. J. Guild, I. M. Wallace, and M. J. Wassenborg, "Hole Cleaning Program for Extended Reach Wells," presented at the SPE/IADC Drilling Conference, Amsterdam, Netherlands, 1995/1/1/, 1995. [Online]. Available: https://doi.org/10.2118/29381-MS.

[16] A. A. Zahid *et al.*, "The Effect of Multiphase Flow Behaviour on a Horizontal Annulus by Integrating High-Speed Imaging Technique," 2019: Begel House Inc.

[17] S. M. Willson *et al.*, "Assuring Stability in Extended Reach Wells - Analyses, Practices and Mitigations," presented at the SPE/IADC Drilling Conference, Amsterdam, The Netherlands, 2007/1/1/, 2007. [Online]. Available: https://doi.org/10.2118/105405-MS.

[18] G. Heisig and M. Neubert, "Lateral Drillstring Vibrations in Extended-Reach Wells," presented at the IADC/SPE Drilling Conference, New Orleans, Louisiana, 2000/1/1/, 2000. [Online]. Available: https://doi.org/10.2118/59235-MS.

[19] L. Quintero, M. Azari, and F. Hamza, "Dynamics of Multiphase Flow Regimes in Toe-Up and Toe-Down Horizontal Wells," presented at the SPWLA 23rd Formation Evaluation Symposium of Japan, Chiba, Japan, 2017/11/1/, 2017. [Online]. Available: https://doi.org/.

[20] S. Browning* and R. Jayakumar, "Effects of Toe-Up Vs Toe-Down Wellbore Trajectories on Production Performance in the Cana Woodford," 2016: Society of Exploration Geophysicists, American Association of Petroleum …, pp. 2671-2679.

[21] R. Brito, E. Pereyra, and C. Sarica, "Experimental Study To Characterize Slug Flow for Medium Oil Viscosities in Horizontal Pipes," presented at the 9th North American Conference on Multiphase Technology, Banff, Canada, 2014/7/9/, 2014. [Online]. Available: https://doi.org/.

[22] "Well Types." AAPG. https://wiki.aapg.org/Well_types#Horizontal_wells (accessed 2020).

[23] J. M. Peden, J. T. Ford, and M. B. Oyeneyin, "Comprehensive Experimental Investigation of Drilled Cuttings Transport in Inclined Wells Including the Effects of Rotation and Eccentricity," presented at the European Petroleum Conference, The Hague, Netherlands, 1990/1/1/, 1990. [Online]. Available: https://doi.org/10.2118/20925-MS.

[24] M. A. Silva and S. N. Shah, "Friction Pressure Correlations of Newtonian and Non-Newtonian Fluids through Concentric and Eccentric Annuli," presented at the SPE/ICoTA Coiled Tubing Roundtable, Houston, Texas, 2000/1/1/, 2000. [Online]. Available: https://doi.org/10.2118/60720-MS.

[25] O. C. Jones Jr and J. C. M. Leung, "An improvement in the calculation of turbulent friction in smooth concentric annuli," 1981.

[26] S. B. Pope, *Turbulent Flows*. Cambridge: Cambridge University Press, 2000.

[27] T. J. Napier-Munn, "The Effect of Dense Medium Viscosity on Separation Efficiency," *Coal Preparation,* vol. 8, no. 3-4, pp. 145-165, 1990/01/01 1990, doi: 10.1080/07349349008905182.

[28] B. K. Menge, "Analysis of turbulent flow in a pipe at constant reynolds number using computational fluid dynamics," 2015.

[29] R. R. Rothfus, W. K. Sartory, and R. I. Kermode, "Flow in concentric annuli at high Reynolds numbers," *AIChE Journal,* vol. 12, no. 6, pp. 1086-1091, 1966.

[30] J. A. Brighton and J. B. Jones, "Fully Developed Turbulent Flow in Annuli," *Journal of Basic Engineering,* vol. 86, no. 4, pp. 835-842, 1964, doi: 10.1115/1.3655966.

[31] D. W. Dodge and A. B. Metzner, "Turbulent flow of non-Newtonian systems," *AIChE Journal,* vol. 5, no. 2, pp. 189-204, 1959.

[32] P. K. Kundu, I. M. Cohen, and D. Dowling, "Fluid Mechanics 4th," ed: Elsevier, 2008.

[33] S. K. Robinson, "Coherent motions in the turbulent boundary layer," *Annual Review of Fluid Mechanics,* vol. 23, no. 1, pp. 601-639, 1991.

[34] F. E. Rodriguez Corredor, M. Bizhani, and E. Kuru, "Experimental investigation of cuttings bed erosion in horizontal wells using water and drag reducing fluids," *Journal of Petroleum Science and Engineering,* vol. 147, pp. 129-142, 2016/11/01/ 2016, doi: https://doi.org/10.1016/j.petrol.2016.05.013.

[35] "Flowzan." Flowzan. http://www.cpchem.com/bl/drilling/en-us/Pages/FlowzanBiopolymer.aspx (accessed.

[36] R. M. Turian and T. F. Yuan, "Flow of slurries in pipelines," *AIChE Journal,* vol. 23, no. 3, pp. 232-243, 1977.

[37] A. A. Zahid, S. R. ur Rehman, S. Rushd, A. Hasan, and M. A. Rahman, "Experimental investigation of multiphase flow behavior in drilling annuli using high speed visualization technique," *Frontiers in Energy,* 2018/09/10 2018, doi: 10.1007/s11708-018-0582-y.

[38] *8.4 Imaging tools for DaVis*, LaVision, 2017. [Online]. Available: https://www.lavision.de/en/downloads/manuals/index.php.

[39] I. Nezu and M. Sanjou, "PIV and PTV measurements in hydro-sciences with focus on turbulent open-channel flows," *Journal of Hydro-environment Research,* vol. 5, pp. 215-230, 12/01 2011, doi: 10.1016/j.jher.2011.05.004.